Novel Methods of Targeting Protein Cytotoxins to Metastatic Prostate Tumors:

Teaching “Old Proteins” “New Tricks”

by
Oliver C Rogers

A dissertation submitted to Johns Hopkins University in conformity with the requirements for the degree of Doctor of Philosophy.

Baltimore, Maryland

March, 2017

Abstract

Prostate cancer is among the leading causes of cancer-related death in the United States with 30,000 people succumbing to the disease every year. A vast majority of these men, at the time of diagnosis, presented with distal prostate cancer as opposed to cancer that was contained within the primary organ. Currently, there is no cure for metastatic prostate cancer despite novel therapeutic advances which have been made over the last 15 years. Our lab is interested in molecular engineering strategies that selectively poison cancer cells but do not affect normal cells. Because a majority of prostate-derived tumors grow very slowly, traditional anti-proliferative cytotoxic chemotherapies are largely ineffective. Therefore, we have selected an array of cytotoxic agents that kill cells regardless of their stage in the cell cycle. These agents, Pro-aerolysin, Granzyme B, and Pseudomonas Exotoxin A, are all protein weapons found in nature that have evolved millions of years to efficiently kill eukaryotic cells. Because these weapons all must be regulated to prevent off-target toxicity, we propose to modify the regulatory steps involved in these toxins' mechanisms in order to selectively kill prostate cancer cells. We aim to do this in a myriad of different ways using previously discovered modifications and mutations made to these agents which have been shown to modulate their activity. Specifically, we intend to engineer these toxins' ability to bind to cells more selectively or to be activated by enzymes selective for the prostate cancer micro-environment. This work will specifically discuss the rationale behind each modification, demonstrate the synthesis and purification of each protein, and assess the biological activity of each in respect to prostate cancer. Ultimately, we hope that the lessons learned from this study will serve as a useful case study in biochemical engineering principles that can lead to novel therapeutic discoveries for the treatment of human disease.

Thesis Advisor:

Dr. Samuel R Denmeade, M.D. (Designated Reader)

Thesis Committee Members:

Dr. Richard F. Ambinder,, M.D. Ph.D.

Dr. Phillip A. Cole, M.D. Ph.D.

Dr. Shawn E. Lupold, Ph.D. (Designated Reader)

Dr. Ronnie C. Mease, Ph.D.

Table of Contents

Abstract ii

Preface/Acknowledgments viii

Introduction

Prostate Cancer 1

Currently Approved MPC Therapies 2

Attractive Markers for Novel MPC Therapeutic 4

Biologics in Cancer 9

Pro-Aerolysin, Granzyme B, and Pseudomonas Exotoxin A Overview 10

References 15

Chapter 1: A Potent IL-2R Targeting Pro-drug as a Novel Anti-tumor Vaccine Adjuvant

Abstract 22

Introduction 23

Materials & Methods 26

Results 28

Discussion 34

References 38

Chapter 2: PLGA Microparticle Encapsulation of a Novel Prostate-Targeted Biologic For Tumor Delivery: Characterization of Release and Functionality

Abstract 41

Introduction 43

Materials & Methods 45
Results 50
Discussion 55
References 60

Chapter 3: PSA-Activated Serine Proteases as a Novel Therapeutic Strategy to Target Prostate Cancer

Abstract 62
Introduction 64
Materials & Methods 67
Results 75
Discussion 85
References 91

Chapter 4: Targeted Delivery of Cytotoxic Proteins via Small Molecule Peptidase Inhibitors

Abstract 94
Introduction 96
Materials & Methods 99
Results 109
Discussion 118
References 124

Curriculum Vitae 128

List of Figures

Chapter 1: Chapter 1: A Potent IL-2R Targeting Pro-drug as a Novel Anti-tumor Vaccine Adjuvant

Figure 1: Cartoon depicting the mechanism of cell death induced by PA 25

Figure 2: Comparison of WT PA vs. IL2-R336A PA 28

Figure 3: IL2-R336A depletes Tregs in tumor bearing mice 30

Figure 4: IL2-R336A improves response in combination with GVAX therapy 31

Figure 5: IL2-R336A reduces immune tolerance of HA-expressing splenocytes 33

Chapter 2: PLGA Microparticle Encapsulation of a Novel Prostate-Targeted Biologic For Tumor Delivery: Characterization of Release and Functionality

Figure 1: PRX302 Sandwich ELISA Development 51

Figure 2: PRX302 Sandwich ELISA Validation 52

Figure 3: Characterization of PRX302 PLGA MPs 54

Chapter 3: PSA-Activated Serine Proteases as a Novel Therapeutic Strategy to Target Prostate Cancer

Figure 1: Schematic of EK-PSA-GZMB and EK-PSA-TRP pro-drugs 67

Figure 2: Cloning and Expression of PSA-Activated TRP and GZMB 75

Figure 3: EK-PSA-TRP is a PSA-activated Trypsin mutant 77

Figure 4: EK-PSA-GZMB is a PSA-activated Granzyme B mutant 78

Figure 5: The N-terminal EK piece both stabilizes and inhibits EK-PSA-TRP and EK-PSA-GZMB 79

Figure 6: EK-PSA-TRP inhibits LNCaP cell growth selectively in the presence of PSA 80

Figure 7: EK-PSA-GZMB inhibits prostate cell growth selectively in the presence of PSA 81

Figure 8: GZMB induces prostate cancer cell growth inhibition via damage to the ECM 84

Chapter 4: Targeted Delivery of Cytotoxic Proteins via Small Molecule Peptidase Inhibitors

Figure 1: Synthesis and production of protein-urea drug conjugates 110

Figure 2: Protein-urea conjugates bind and inhibit PSMA 111

Figure 3: GZMB-MU2 internalizes into PIP cells but does not induce cell death 113

Figure 4: PE35-MU2 is selectively toxic to PSMA producing cells 114

Figure 5: PE35-MU2 is selectively internalized by PSMA expressing cells 115

Figure 6: PE35-MU2 regresses PSMA expressing xenografts when injected 117

Preface/Acknowledgements

If I was to accurately and wholly thank every person who helped me achieve what I have in the past few years, I would need a document longer than this manuscript. Science is a team effort, and I would have accomplished very little on my own. Therefore, this dissertation is more of a reflection and documentation of the immense amount of work that was done by not only me and my immediate colleagues but the 'giants' whose shoulders we have stood on as we delved into the unknown. I, merely, am the person who is formally recording the methods, data, and rationale behind each experiment. Before I spend the rest of this section directly thanking various individuals, I must, first, formally acknowledge those who are not explicitly mentioned including, but certainly not limited to, the JHMI community and the related scientists, administrators, and other members of various institutions who guided me through this journey.

First, I would like to thank my scientific family at Hopkins. It would be difficult to have worked with a kinder, more supportive group of people, all of which are brilliant and committed to our greater cause. Their collective decades of experience made a large portion of this work much more straight forward and easy to navigate. Their technical 'know-how' was the proverbial flashlight that guided me through the unknown abyss and without it, I would be undoubtedly still be lost in the dark somewhere. I also am exceptionally grateful for our comradery and the supportive work environment I was so fortunate to walk into every morning. Between our endless conversations about the world, daily communal crossword puzzles, and lab happy hours and lunches, I rarely ever felt that I was surrounded by co-workers. Rather, every day, I felt that I always surrounded by friends. I would also like to thank my three mentors, Sam, John, and Nate. I've been told that mentor selection is the most important decision a graduate student will make. I, personally, feel that choosing to work with you three was the best

decision I made while at Hopkins. If the technical help I received was a flashlight, than your discussions and overall guidance was the map that helped me understand the 'big picture' aspects of my work and helped mold what felt was a series of random experiments into a cohesive story. I hope that, someday, when I mentor young scientists, I guide them as well as you all have guided me. Next, I would like to thank Drs. Ambinder, Cole, Lupold, Mease, and Pomper, for their support and input regarding my work and for taking the time to sit on my thesis committee. Finally, I'd like to acknowledge the Departments of Pharmacology and Oncology staff for their support, and the United States Department of Defense for funding this work.

As much as I joked about never leaving the laboratory and never ceasing to think about science, I actually had quite the active life outside of Hopkins. Thus, I must acknowledge the personal guidance, support, and love that I received from my family and friends. I'd like to first thank my immediate nuclear family. Most notably, I must thank my father and sister who I cannot begin to express my gratitude for. Despite living hundreds of miles away from them, they were always a phone call or text message away. I would also like to acknowledge my late family members, whom this work is personally dedicated to. While I cannot begin to express my longing and sadness that you all are no longer with me, I am comforted in the fact that you all directly inspired me to pursue science so I could help improve the lives of mothers, fathers, friends, and family everywhere. I would also like to thank my married family, the Drummers. Despite being somewhat clichéd, you all have exemplified the notion that true family is not limited to those who you share DNA with. As far as helping me keep my day to day sanity, I would like to acknowledge my friends, both far and near. Between our daily bantering, various outings and social events, and the occasional adventures, you all have been invaluable to my life and, at times, were the major driving force which kept me optimistic and motivated. I would like

to especially thank my closest friends Nathan, Taylor, Chris, Nick, Matt & Nicole, Emily, and my closest and dearest friend Luke. The last two of which were in STEM PhD programs and who also shared this crazy and unforgettable experience with me. Finally, the last group of mammals I would like to thank are perhaps the most responsible for my personal well-being. I would like to thank my wife Ashley and our two feline children Artemis and Sophie. The endless supply of love I received from you three every single day of this experience is indescribable in words. Because of you, I was able to get out of bed every morning and slept comfortably at night and for that, I am eternally grateful. Like science, life is undoubtedly a team sport and after going through some of the most challenging moments of my life, I can safely say that my team came out on top.

Introduction: Current Status of Prostate Cancer Therapeutics and Biologic-based Targeted Agents

Prostate Cancer Overview

In the year 2016, over one hundred and fifty thousand men were diagnosed with prostate cancer in the United States (1). Prostate cancer cases represent almost a third of all cancer diagnoses in men and roughly one tenth of all total cases in human beings. The average number of cases diagnosed each year has steadily declined over the past decade (1), likely due to changes in practice by physicians who feel that the disease is currently being over-diagnosed and unnecessarily treated. Despite this, the overall prevalence of this malignancy in the Western population is a public health concern that will continue to challenge healthcare providers and researchers for decades to come due to the subset of patients with aggressive, therapy resistant, and ultimately , fatal disease.

Perhaps the most astonishing statistic associated with prostate cancer is the survival rate when compared with other solid tumors. It is estimated that the overall 5-year survival rate for men with prostate cancer is approximately 99% (1). Perhaps even more astonishing is that an overwhelmingly vast majority of patients who succumb to prostate cancer are diagnosed with metastatic tumors as opposed to localized or regional disease. This is clearly estimated in the survival rates within these patients. Men presenting with local or regional disease at time of diagnosis are almost always are alive after 5 years, with the respective survival rate for these tumors approaching 100%. Given this statistic, it is unprecedented that twenty six thousand men died of prostate cancer in 2016 (1). Because men with non-metastatic disease have disproportionately high survival rates when compared to those that do, the primary focus in the fields of diagnostics, therapeutics, and tumor biology is on metastatic prostate cancer (MPC).

MPC is the number two leading cause of cancer death in the United States in men. Unlike other stages of prostate cancer, the five year survival rate for this disease is 25%. Unfortunately, while some advancements have been made in the realm of therapeutics, there has been little improvement in overall survival of MPC over time. This is primarily due to the nature of MPC tumors, as they seem to be inherently resistant to most genres of therapy. Currently, most therapeutic strategies approved to treat MPC are primarily palliative and improve survival in patients only marginally. If we are to make substantial advancements in prostate cancer therapy, new, innovative, and comprehensive strategies must be developed based on lessons learned from currently approved therapies and insights into normal and malignant biology.

Currently Approved MPC Therapies

While there is currently no approved curative therapy for MPC, there exists a slowly growing range of therapeutic options that can effectively improve patient health, optimize quality of life, and reduce overall tumor burden. Probably the most studied and most utilized arms of MPC therapy is hormone therapy. MPC tumor cells, like localized cancers, are biochemically addicted to Androgen-dependent growth, pro-survival, and anti-apoptotic signals via Androgen Receptor (AR)-driven transcriptional programs. Current, there are two methods of targeting this pathway using chemical means. The first is Androgen Depravation Therapy (ADT) (2) in which a LHRH agonist is administered to the patient thus augmenting their testosterone signaling axis and thus decreasing systemic concentrations of testosterone over time. The other, anti-androgen therapy, which is usually reserved for castration resistant prostate cancer, involves chemically targeting AR with molecules that bind directly to the protein and inhibit its ability to bind testosterone and undergo the molecular changes necessary to affect gene transcription (3,4). It has also been shown that blocking the synthesis of androgens can

also generate similar effects via inhibitors of Cyp17 (5). Both modes of therapies inhibit cell growth and arrest the tumor in the G_0 phase of the cell cycle. Like ADT, anti-androgens are most effective when combined with another mode of therapy.

Recently, it has been shown that the cytotoxic chemotherapeutic agent, docetaxel, substantially improves survival and quality of life in men with MPC when combined with enzalutamide(6,7), (a second generation anti-androgen) and prednisone (for pain management). Docetaxel is a classical anti-cancer chemotherapeutic which kills rapidly replicating cells via stabilization of microtubule structures in cells thus arresting mitosis and leading to cell death (8). It is, therefore, paradoxical that prostate cancer cells are among the slowest of human tumors and hardly respond to other chemotherapeutic agents. Therefore, it is likely that docetaxel and other microtubule-targeting agents affect prostate cancer cells via a mechanism independent of proliferation. This problem was resolved by Zhu et al in 2010 when they showed that docetaxel directly inhibited the trafficking of AR to the nucleus of prostate cancer cells (9). This rendered ligand-bound AR unable to access its chromatin binding partners which allows the receptor to facilitate transcription of target genes and promote tumor cell survival. It is, therefore, to be expected that Taxol-based compounds would synergize with anti-androgens, as they both offer unique and effective methods of inhibiting AR signaling, on which MPC cells are dependent. Clearly then, MPC cell targeting cannot be successfully implemented using strategies that involve inhibiting proliferation or DNA replication directly due to MPC cell growth rates, tendency to remain in the G_0 stage of the cell cycle, and resistance to classical chemotherapeutics.

Another arm of anti-cancer treatment that has arisen in very recent years is immunotherapy. Specifically for MPC, the currently approved Sipuleucel-T has been

shown to significantly extend the lifespans of patients with advanced prostate cancer (10). Sipuleucel-T is administered by removing a patient's own dendrocytes and incubating them with a fusion protein containing two factors. The first is the prostatic acid phosphatase (PAP) which is a membrane-bound enzyme present on a majority of prostate cancer cells. This portion of the fusion exposes the immune cells to a cancer-selective antigen which should induce an immune response upon presentation *in vivo*. The second component of the fusion protein is GM-CSF, a protein which has been well characterized to stimulate the differentiation of dendrocytes into monocytes, neutrophils, basophils, and other pro-inflammatory cells. The, now matured, cocktail of immune cells is then re-administered to the patient and will go on to target the tumor. Sipuleucel-T can also be combined with the aforementioned strategies to further perturb tumor function and improve therapeutic responses (11). One major obstacle of Sipuleucel-T and other immunotherapies for MPC is the immunosuppressive micro-environment created by the tumor cells. While not fully understood, it is clear that tumor cells and –reprogrammed stromal cells are capable of recruiting other cell types that directly inhibit migration and function of various subtypes of inflammatory cells. Most notably, the MPC microenvironment has been shown to be rich in mesenchymal stem cells, myeloid derived suppressor cells, and T-regulatory cells, all of which have been shown to locally inhibit anti-tumor immune responses (12, 13). This not only limits the efficacy of most immunotherapies but also inhibits the utility of immune checkpoint inhibitors, as anti-tumor lymphocytes cannot effectively localize in the prostate cancer microenvironment. In order to improve the functionality of immunotherapies for MPC, we must first overcome this obstacle and aim to re-program anti-inflammatory signaling present in the tumor.

Attractive Markers for Novel MPC Therapeutics

In this work, our lab aims to utilize a diverse set of protein agents to generate new strategies to combat MPC. These agents all have been well characterized to kill mammalian cells of all types using robust mechanisms of inducing cell death. We aim to engineer these agents to either selectively kill anti-inflammatory immune cells thus improving immunotherapy efficacy or to directly target tumor and pro-tumor stromal cells based on the unique expression of prostate-selective enzymes. Because these proteins are all highly toxic to normal cells and do not greatly discriminate to which cell types they kill, we must use protein engineering approaches to re-target these agents to kill only cells in the tumor microenvironment and limit systemic toxicity which would otherwise minimize the usefulness of these drugs.

Of all markers of interest that have been used to hone a cytotoxic payload to a human tumor, the Prostate Specific Antigen (PSA) is among the most selective. PSA is a secreted serine protease with chymotrypsin-like activity (14). It is expressed by both normal and malignant prostate epithelial cells at amounts much higher than any other tissue in the body. Function wise, it is not completely clear what PSA's physiological biological role is, however, it does seem to contribute to semen liquefication following ejaculation in order to promote sperm motility (15). There is also evidence that PSA can cleave members of the complement system in order to regulate toxicity associated with chronic inflammation (16). Regardless, PSA has been shown to be overproduced by prostate derived tumors and is a well characterized biomarker of disease burden in men with both localized and advanced cancer. In men with MPC, it is likely that the patient has had a radical prostatectomy as an early therapeutic approach to maintain his disease. Because the two major sinks of PSA production are the prostate and prostate-derived tumors, men who have had surgery almost exclusively express PSA in their

tumor relative to the rest of the body. Thus, drugs requiring activation by PSA cleavage would be selective if not specific for the tumor in a man with MPC.

Due to the fact that PSA is both overproduced by MPC tumors and is lowly expressed in any other tissue, our lab has become interested in its enzymatic activity. Because PSA is found systemically throughout the body due to leaky tissue architecture in a man with prostatic disease, a PSA-activated pro-drug may be systemically activated by PSA that has leached into the bloodstream. To address this issue, our lab designed a highly selective PSA peptide substrate containing the amino acid sequence HSSKLQ and conjugated a fluorescent amino-methyl-coumarin reporter to it which is quenched upon conjugation. Upon PSA or PSA-like hydrolysis after the glutamine residue, the free fluorophore is released. To quantify PSA's enzymatic activity, our lab immuno-precipitated PSA from the extracellular fluid of MPC tumors and from serum from patients with MPC. To our surprise, we found that PSA's unique enzymatic activity was completely inhibited in serum from these patients as opposed to being almost 100% active in the extracellular fluid from the tumor (17). Later, it was found that PSA is rapidly inhibited by covalent protease inhibitor proteins present in abundance in the bloodstream. These proteins, alpha-1-antichymotrypsin and alpha-2-macroglobulin form irreversible adducts with PSA which can be detected in serum of patients with MPC (18). Because PSA is abundant in the extracellular space of tumors compared to other tissues, inactive in the bloodstream, and capable of cleaving highly sophisticated substrates selectively, it is an ideal candidate to target cytotoxic proteins to MPC cells via pro-drugs strategies. These pro-drugs, in theory, will be cytotoxic agents that are rendered inactive with an inhibitory peptide attached. This peptide will be linked to the agent of interest using a peptide substrate of PSA. For more potent cytotoxins, the substrate HSSKLQ was found to be a less efficient yet more specific substrate for PSA.

For less cytotoxic agents, the substrate KGISSQY is more robustly cleaved but also processed by other proteases (19). Previously characterized PSA-activated pro-drug cytotoxic agents include the plant toxin thapsigargin (20), an N-(2-hydroxypropyl) methacrylamide copolymer (21), phosphoramide mustards (22), and the bacterial toxin pro-aerolysin (23). All of which were shown to be toxic selectively to cells in the presence of enzymatically active PSA in various tissue culture and animal models.

Another attractive prostate cancer marker is the Prostate Specific Membrane Antigen (PSMA). PSMA is a carboxy-peptidase enzyme also expressed robustly by prostate epithelium (24). Its function in normal prostate biology is not well characterized but PSMA has been shown to process the neurotransmitter N-acetyl-aspartyl-glutamate (NAAG) into NAA and free glutamate via cleavage of the conjoining amide bond linking the two amino acids (25). PSMA is highly up-regulated in castrate resistant prostate cancer due to its negative regulation by AR. In the context of prostate cancer, PSMA's role in oncogenesis is not clear. It has been suggested that PSMA acts as a folate scavenger via internalization folate substrates under low folate conditions but this mechanism is still somewhat controversial (26). PSMA, recently, has been suggested as a predictive biomarker for aggressive prostate cancer. This is because PSMA has been shown to be overexpressed in patients who eventually have recurrent, more aggressive disease. In patients whose tumor cells were approximately 85% positive for PSMA, it was shown that they were not only more likely to relapse but were also more likely to relapse faster than patients who did not (27, 28). PSMA has also been shown to be extensively recycled on the cell membrane in that it is constantly being enveloped into the cell and re-shuttled back to the cell membrane. PSMA's enzymatic activity, strong correlation with aggressive cancer, and high turnover rate have made it an attractive marker for tumor-targeted therapeutic and imaging agents.

There are several reports by various groups developing PSMA-targeted therapeutic and diagnostic molecules for MPC. Most notably, two antibody conjugates are currently in clinical trials for the treatment of MPC. The first, J591, is a monoclonal antibody against PSMA which was successfully conjugated to ^{177}Lu (29). This radio-immunotherapy was shown in Phase II clinical trials to be tolerated by patients with a reasonable toxicity profile while generating partial responses in patients and lowering PSA levels. Another monoclonal antibody, MLN2704, was successfully fused to maytansinoid 1, a cytotoxin with Taxol-like functionality, and has shown some clinical benefit in a Phase I/II trial in which several patients observed some benefit of the drug when dosed (29).

Other, less conventional strategies, have also had clinical success. Recently, the lab of Dr. Martin Pomper has developed a class of urea-linked dipeptide inhibitors of PSMA. These molecules display remarkable potency and specificity for PSMA despite having an extremely simple chemical structure. It has been recently shown that these agents can successfully deliver imaging agents to MPC tumors as well as radiopharmaceuticals (30, 31). Currently, a 'urea' molecule linked to ^{18}F, known asF-18 DCFPyL is in clinical trials for the detection of MPC tumors on PET scans (32) and a ^{99m}Tc-linked urea is also being evaluated as a diagnostic agent for MPC (33). Rather than targeting PSMA as a means to internalize agents of interest, there are also efforts to target cytotoxic molecules to MPC tumors via PSMA's enzymatic activity. Currently, a molecule known as G202, is in clinical trials for the treatment of liver cancer. G202 is a poly-glutamated analog of the potent plant-based toxin thapsigargin (34). G202 can be given safely systemically due to being in an inactive conformation. Once in the MPC environment, PSMA can cleave these glutamate residues selectively and release the free toxin. It should be noted that PSMA is also expressed on neo-vasculature in tumors which explains why it can be utilized for other tumor types that don't inherently express PSMA (35). It is evident that

conjugating agents with therapeutic and diagnostic potential to PSMA antibodies, scFvs, inhibitors, and substrates is a well-studied and growing field in MPC research and is likely so successful due to PSMA's previously discussed biological and biochemical properties.

Biologics in Cancer

The primary goal of this work is to characterize the biochemical and pharmacological properties of various engineered biologic-based toxic proteins for their use as systemic MPC therapeutics. Our lab is very interested in the utilization of novel protein agents to treat MPC. One major reason for this interest is the natural tendency for proteins to accumulate in the microenvironment of tumors via the enhanced permeability and retention (EPR) effect. The EPR effect is a phenomenon in tumor biology in which large macro-molecules have a greatly increased retention time in tumors than in normal tissue (36). This is due primarily to two different physiological properties of tumors. The first is that neo-vasculature formed in the cancer stroma tends to be compromised which causes material from the bloodstream to leak into the tumor at rates higher than normal tissue. The second is that most tumors do not have well established lymphatic drainage in and around the stroma. Thus, an increase in material flowing in and little to no sufficient drainage from the tumor yields a net accumulation of molecules above ten thousand Daltons. This makes utilizing large macromolecules naturally advantageous for cancer therapy, as the tumor's own physiology can be used against it as a means to selectively concentrate cytotoxic agents in the adjacent space to the tumor cells.

Naturally, due to our understanding of the EPR effect, a large increase in molecular details with respect to tumor biology and biochemistry, and a spike in recombinant technologies, protein-based cancer therapeutics have become immensely popular in the

past two decades. Since the year 2013 alone, there have been dozens of monoclonal antibodies and other biologic-based therapies to treat human cancers. These agents provide remarkable selectivity for their respective antigen and can efficiently deliver some of the most lethal cytotoxins known to human biology to cancer cells while minimizing toxicity (37). These agents can also be used to 'tag' tumor cells for destruction by the immune system and the antibody-dependent cell cytotoxicity pathway as well as interfere with extracellular pro-tumor signaling pathways such as the immunosuppressive PD1-PDL1 signaling system (38). As the demand for new therapies for MPC grows, thus does the need for new strategies to target tumors with these agents. Despite an overwhelming amount of success from a biochemical and molecular standpoint, there are currently no approved biologics for either local or distal prostate cancer. In order to develop such an agent, potent cytotoxins must be engineered appropriately to target prostate cancer cells selectively. In this work, we discuss new methods to regulate the toxicity of 4 different human and bacterial toxic proteins into 4 novel therapeutic strategies each with its own advantages and pitfalls.

Pro-Aerolysin, Granzyme B, and Pseudomonas Exotoxin A Overview

In order to develop novel, targeted protein toxins for the treatment of MPC, we selected three protein 'toxins' due to their unique mechanisms of action as well as their ability to be regulated via biochemical switches and conditions. Pro-aerolysin (PA) perhaps exemplifies this principle the most. PA is a bacterial pro-toxin produced by the infectious prokaryote *Aeromonas Hydrophila* (39). Secreted as an inactive dimer, PA binds to GPI-anchored proteins on target cell surfaces and is proteolytically processed by the trypsin-like protease furin near the C-terminus of the toxin (40, 41). Proteolysis of the toxin releases an inhibitory peptide which, upon removal, stabilizes a conformational change which allows the protein to oligomerize from the inactive dimer to a pore-forming

heptamer (42). This structure internalizes into the cell membrane inducing rampant cell lysis and subsequent cell death. This mechanism of targeted cell lysis is an attractive power to harness for therapeutic purposes, as it is very difficult for tumor cells and neighboring stromal cells to become resistant to plasma membrane damage.

PA has two steps in its mechanism in which it can be regulated. The first is the cell binding step which allows the protein to concentrate on the plasma membrane allowing for hepatmerization to occur. It was shown that a simple point mutation, R336A, obliterates binding to GPI-anchored proteins in the cell, thus making the protein several orders of magnitude less toxic. It was also shown that attaching ligands and/or binding moieties to the N-terminus transforms the protein from an inactive mutant into a selective immunotoxin. Specifically, the cytokine IL2 was fused to R336A and was shown to selectively kill IL2 producing tumor cells both *in vitro* and *in vivo* (43). The other critical step that is exploitable for therapeutic engineering purposes is the proteolytic activation step. Recently, our lab mutated the furin activation sequence near PA's C-terminus and inserted the HSSKLQ PSA substrate thus generating a mutant PA, deemed PRX302, which was selectively activated by functional PSA (23). PRX302 was shown to be selectively toxic to cells in culture in the presence of PSA and had anti-tumor activity against PSA producing lines *in vivo* when injected intratumorly. Unfortunately, this agent cannot be given systemically due to the non-discriminant GPI-binding properties of the toxin. In this work, we explore the utilization of both engineered mutants of PA. First, we explore the capacity of IL2-R336A to target IL2-expressing immune cells *in vivo* and augment efficacy of anti-tumor immunotherapies. Second, we assess the feasibility of bypassing the limited systemic availability of PRX302 using controlled release methods via PLGA microparticles.

Because unique bacterial toxins are likely to induce immune responses which would decrease the efficacy of the drug and increase systemic toxicity, our lab has become interested in the utilization of protein agents that do not illicit an immune response. The most straightforward approach to this problem is to, simply, use toxins that are of human origin. Granzyme B (GZMB) is a secreted, caspase-like serine protease produced by cytotoxic $CD8^+$ T-lymphocytes upon activation by an antigenic cell (44). Once the cell secretes GZMB, it is delivered into the endosome of the target cell via a calcium-induced membrane repair response (45) induced by the pore forming protein perforin, a co-secreted factor with homology to members of the complement pathway. Once in the endosome, GZMB can translocate to the cytoplasm via perforin pores in the vesicle membrane (46). Once liberated, GZMB will proteolytically process a vast array of intracellular substrates such as members of the caspase family, Bcl2, and the apoptosis inhibiting ICAD protein (47). This causes a global apoptotic response in the cell leading to cell death. Like PA, we are interested in regulating GZMB's activity to prostate cancer cells. This can be done in two different ways. The first is by regulating its proteolytic activation. While GZMB, at low concentrations, is harmless to cells in an extracellular context, at high concentrations it has been shown that GZMB can cleave substrates in the extracellular matrix and disrupt tumor cell growth and viability (48). This is an attractive 'field effect' therapy that could induce large scale damage to the tumor integrity and structure. However, this activity must be specific to the MPC tumor. In order to avoid inducing auto-apoptosis, $CD8^+$ T-cells express GZMB as an inactive zymogen. The pro-form of this protein contains an N-terminal inhibitory dipeptide with the sequence G-E. Upon store in the granule compartment of the cell, pro-GZMB is activated by Cathepsin C between the glutamate residue and isoleucine 3 releasing the active enzyme (49). Compartmentalization and pH of the cytotoxic granule minimizes the effects of GZMB on T-cell viability. Because PRX302 mutagenesis was rather easy when converting the

wildtype protein into a PSA-activated pro-drug, we aim to do the same with GZMB. This mutant will be catalytically inactive until encountering functional PSA in the tumor microenvironment and be able to affect tumor cells, stromal cells, and other adjacent pro-tumor cells via re-modeling of the extracellular protein content.

Another method of engineering GZMB to target MPC tumors is regulating internalization of the protein by attaching a targeting moiety to its C-terminus, similar to other immunotoxins developed utilizing monoclonal antibodies and scFv fragments delivered GZMB as a payload (50). This is an attractive strategy, as GZMB requires the presence of perforin in order to be functional which should render the drug very safe at reasonable doses. To assess GZMB's use as a MPC-targeting cytotoxin, we aim to make protein drug conjugates using the catalytic domain of this enzyme fused to inhibitors of PSMA. These inhibitors will, in theory, bind PSMA, and facilitate the intracellular delivery of GZMB allowing it to induce apoptosis on the target cell thus killing it. Because GZMB activates several, independent, arms of the apoptosis pathway, we would expect tumor cells to be unable to develop a resistance to this therapy. The major pitfall of this therapy is whether or not the GZMB cargo would be able to translocate into the cytoplasm and access its substrates. To explore and rectify this problem, we also intend on evaluating and characterizing the activity of the potent bacterial toxin fragment, Pseudomonas Exotoxin (PE) A, called PE35 (51, 52). This toxin has been shown to internalize into cells when conjugated to a cell binding moiety such as a growth factor or monoclonal antibody, translocate into the cytoplasm, and inhibit protein synthesis thus arresting the cell growth and killing it. We chose this toxin due to its well characterized mechanism of cell targeting, its ability to escape the endosomal compartments, and its success as a cytotoxic payload in various immunotoxin platforms. In fact, one such agent, Moxetumomab-pasudotox which contains an anti-CD22 monoclonal antibody fused to a

fragment of PE is currently in Phase III trials for the treatment of Hairy Cell Leukemia (53). This protein is especially exciting, as it has been shown to be engineered to lack antigens that would lead to decreased tolerance by the immune system thus making the toxin ‘humanized’ (54). PE35 is a nice alternative to GZMB due to its drastically different mechanism of action and success as an anti-cancer pharmaceutical. The two diverse agents will paint an informative picture regarding the types of protein-based cytotoxins that can be successfully delivered into MPC cells via PSMA targeting.

This study exhibits a multi-strategy approach to evaluate targeting protein toxins to the prostate cancer microenvironment using protein engineering and drug delivery principles. We intend to evaluate the biochemical and pharmacological principles of each method and evaluate their potential as novel cancer therapies. Lessons learned from this study will elucidate the limitations of each approach and provide insight into which strategies and protein-based agents have the most potential to move forward into more advanced pre-clinical studies and beyond. Ultimately, we hope that this will contribute to the greater understanding of the roll that biologic based agents can play in treating prostate cancer and other solid tumors which will help yield more effective treatments thus improving and extending patients’ lives.

References

1. Howlader N, Noone AM, Krapcho M, Miller D, Bishop K, Altekruse SF, Kosary CL, Yu M, Ruhl J, Tatalovich Z, Mariotto A, Lewis DR, Chen HS, Feuer EJ, Cronin KA (eds). SEER Cancer Statistics Review, 1975-2013, National Cancer Institute. Bethesda, MD.
2. Sharifi N, Gulley JL, Dahut WL. Androgen Deprivation Therapy for Prostate Cancer. JAMA. 2005;294(2):238-244.
3. Goa KL, Spencer CM. Bicalutamide in advanced prostate cancer. A review. Drugs Aging. 1998;12(5):401-22.
4. Tran C, Ouk S, Clegg NJ, et al. Development of a Second-Generation Antiandrogen for Treatment of Advanced Prostate Cancer. Science (New York, NY). 2009;324(5928):787-790.
5. Alex AB, Pal SK, Agarwal N. CYP17 inhibitors in prostate cancer: latest evidence and clinical potential. Therapeutic Advances in Medical Oncology. 2016;8(4):267-275.
6. IF Tannock, R de Wit, WR Berry , etal : Docetaxel plus prednisone or mitoxantrone plus prednisone for advanced prostate cancer N Engl J Med 351: 1502– 1512,2004.
7. Ceresoli GL, De vincenzo F, Sauta MG, Bonomi M, Zucali PA. Role of chemotherapy in combination with hormonal therapy in first-line treatment of metastatic hormone-sensitive prostate cancer. Q J Nucl Med Mol Imaging. 2015;59(4):374-80.
8. Morse DL, Gray H, Payne CM, Gillies RJ. Docetaxel induces cell death through mitotic catastrophe in human breast cancer cells. Mol Cancer Ther. 2005;4(10):1495-504.

9. Zhu ML, Horbinski CM, Garzotto M, Qian DZ, Beer TM, Kyprianou N. Tubulin-targeting chemotherapy impairs androgen receptor activity in prostate cancer. Cancer Res. 2010;70(20):7992-8002.
10. Small EJ, Schellhammer PF, Higano CS, et al. Placebo-controlled phase III trial of immunologic therapy with Sipuleucel-T (APC8015) in patients with metastatic, asymptomatic hormone refractory prostate cancer. J Clin Oncol. 2006;24(19):3089-94.
11. Olson BM, McNeel DG. Sipuleucel-T: immunotherapy for advanced prostate cancer. Open Access Journal of Urology. 2011;3:49-60.
12. Ida Silvestri, Susanna Cattarino, Anna Maria Aglianò, Giulia Collalti, and Alessandro Sciarra, “Beyond the Immune Suppression: The Immunotherapy in Prostate Cancer,” BioMed Research International, vol. 2015, Article ID 794968, 9 pages, 2015.
13. Han Z, Jing Y, Zhang S, Liu Y, Shi Y, Wei L. The role of immunosuppression of mesenchymal stem cells in tissue repair and tumor growth. Cell & Bioscience. 2012;2:8.
14. Lebeau AM, Singh P, Isaacs JT, Denmeade SR. Prostate-specific antigen is a "chymotrypsin-like" serine protease with unique P1 substrate specificity. Biochemistry. 2009;48(15):3490-6.
15. Lee C, Keefer M, Zhao ZW, et al. Demonstration of the role of prostate-specific antigen in semen liquefaction by two-dimensional electrophoresis. J Androl. 1989;10(6):432-8.
16. Manning ML, Williams SA, Jelinek CA, Kostova MB, Denmeade SR. Proteolysis of complement factors iC3b and C5 by the serine protease prostate-specific antigen in prostatic fluid and seminal plasma. J Immunol. 2013;190(6):2567-74.

17. Denmeade SR, Sokoll LJ, Chan DW, Khan SR, Isaacs JT. Concentration of enzymatically active prostate-specific antigen (PSA) in the extracellular fluid of primary human prostate cancers and human prostate cancer xenograft models. Prostate. 2001;48(1):1-6.
18. Stenman UH, Leinonen J, Alfthan H, Rannikko S, Tuhkanen K, Alfthan O. A complex between prostate-specific antigen and alpha 1-antichymotrypsin is the major form of prostate-specific antigen in serum of patients with prostatic cancer: assay of the complex improves clinical sensitivity for cancer. Cancer Res. 1991;51(1):222-6.
19. Denmeade SR, Lou W, Lövgren J, Malm J, Lilja H, Isaacs JT. Specific and efficient peptide substrates for assaying the proteolytic activity of prostate-specific antigen. Cancer Res. 1997;57(21):4924-30.
20. Denmeade SR, Jakobsen CM, Janssen S, et al. Prostate-specific antigen-activated thapsigargin prodrug as targeted therapy for prostate cancer. J Natl Cancer Inst. 2003;95(13):990-1000.
21. Chandran SS, Nan A, Rosen DM, Ghandehari H, Denmeade SR. A prostate-specific antigen activated N-(2-hydroxypropyl) methacrylamide copolymer prodrug as dual-targeted therapy for prostate cancer. Mol Cancer Ther. 2007;6(11):2928-37.
22. Wu X, Hu L. Design and synthesis of peptide conjugates of phosphoramide mustard as prodrugs activated by prostate-specific antigen. Bioorg Med Chem. 2016;24(12):2697-706.
23. Williams SA, Merchant RF, Garrett-mayer E, Isaacs JT, Buckley JT, Denmeade SR. A prostate-specific antigen-activated channel-forming toxin as therapy for prostatic disease. J Natl Cancer Inst. 2007;99(5):376-85.

24. Lapidus RG, Tiffany CW, Isaacs JT, Slusher BS. Prostate-specific membrane antigen (PSMA) enzyme activity is elevated in prostate cancer cells. Prostate. 2000;45(4):350-4.
25. Carter RE, Feldman AR, Coyle JT. Prostate-specific membrane antigen is a hydrolase with substrate and pharmacologic characteristics of a neuropeptidase. Proc Natl Acad Sci USA. 1996;93(2):749-53.
26. Yao V, Berkman CE, Choi JK, O'keefe DS, Bacich DJ. Expression of prostate-specific membrane antigen (PSMA), increases cell folate uptake and proliferation and suggests a novel role for PSMA in the uptake of the non-poly-glutamated folate, folic acid. Prostate. 2010;70(3):305-16.
27. Ross JS, Sheehan CE, Fisher HAG, Kaufaman RP, Jr., Kaur P, et al. (2003) Correlation of primary tumor prostate-specific membrane antigen expression with disease recurrence in prostate cancer. Clin Cancer Res 9: 6357–462.
28. Sweat SD, Pacelli A, Murphy GP, Bostwick DG. Prostate-specific membrane antigen expression is greatest in prostate adenocarcinoma and lymph node metastases. Urology. 1998;52(4):637-40.
29. Naveed H. Akhtar, Orrin Pail, Ankeeta Saran, Lauren Tyrell, and Scott T. Tagawa, “Prostate-Specific Membrane Antigen-Based Therapeutics,” Advances in Urology, vol. 2012, Article ID 973820, 9 pages, 2012.
30. Chen Y, Dhara S, Banerjee SR, et al. A Low Molecular Weight PSMA-Based Fluorescent Imaging Agent for Cancer. Biochemical and biophysical research communications. 2009;390(3):624-629.
31. Will L, Sonni I, Kopka K, Kratochwil C, Giesel FL, Haberkorn U. Radiolabeled PSMA small molecule inhibitors. Q J Nucl Med Mol Imaging. 2017;48 (supplement 2):25P.

32. Szabo Z, Mena E, Rowe SP, et al. Initial Evaluation of [(18)F]DCFPyL for Prostate-Specific Membrane Antigen (PSMA)-Targeted PET Imaging of Prostate Cancer. Mol Imaging Biol. 2015;17(4):565-74.
33. Hillier SM, Maresca KP, Lu G, et al. 99mTc-labeled small-molecule inhibitors of prostate-specific membrane antigen for molecular imaging of prostate cancer. J Nucl Med. 2013;54(8):1369-76.
34. Denmeade SR, Mhaka AM, Rosen DM, et al. Engineering a prostate-specific membrane antigen-activated tumor endothelial cell prodrug for cancer therapy. Sci Transl Med. 2012;4(140):140ra86.
35. Haffner MC, Kronberger IE, Ross JS, et al. Prostate-specific membrane antigen expression in the neovasculature of gastric and colorectal cancers. Hum Pathol. 2009;40(12):1754-61.
36. Greish K. Enhanced permeability and retention (EPR) effect for anticancer nanomedicine drug targeting. Methods Mol Biol. 2010;624:25-37.
37. Antibody therapy of cancer. Nature Reviews Cancer. 2012;12(4):278.
38. Philips GK, Atkins M. Therapeutic uses of anti-PD-1 and anti-PD-L1 antibodies. Int Immunol. 2015;27(1):39-46.
39. Buckley JT. The channel-forming toxin aerolysin. FEMS Microbiol Immunol. 1992;5(1-3):13-7.
40. Abrami L, Fivaz M, Decroly E, et al. The pore-forming toxin proaerolysin is activated by furin. J Biol Chem. 1998;273(49):32656-61.
41. Abrami L, Fivaz M, Glauser P-E, Parton RG, van der Goot F. A Pore-forming Toxin Interacts with a GPI-anchored Protein and Causes Vacuolation of the Endoplasmic Reticulum. The Journal of Cell Biology. 1998;140(3):525-540.

42. Lesieur C, Frutiger S, Hughes G, Kellner R, Pattus F, Van der goot FG. Increased stability upon heptamerization of the pore-forming toxin aerolysin. J Biol Chem. 1999;274(51):36722-8.
43. Osusky M, Teschke L, Wang X, Wong K, Buckley JT. A chimera of interleukin 2 and a binding variant of aerolysin is selectively toxic to cells displaying the interleukin 2 receptor. J Biol Chem. 2008;283(3):1572-9.
44. Hoves S, Trapani JA, Voskoboinik I. The battlefield of perforin/granzyme cell death pathways. J Leukoc Biol. 2010;87(2):237-43.
45. Keefe D, Shi L, Feske S, et al. Perforin triggers a plasma membrane-repair response that facilitates CTL induction of apoptosis. Immunity. 2005;23(3):249-62.
46. Thiery J, Keefe D, Boulant S, et al. Perforin pores in the endosomal membrane trigger release of endocytosed granzyme B to the cytosol of target cells. Nature immunology. 2011;12(8):770-777.
47. Cullen SP, Adrain C, Lüthi AU, Duriez PJ, Martin SJ. Human and murine granzyme B exhibit divergent substrate preferences. The Journal of Cell Biology. 2007;176(4):435-444.
48. Buzza MS, Zamurs L, Sun J, et al. Extracellular matrix remodeling by human granzyme B via cleavage of vitronectin, fibronectin, and laminin. J Biol Chem. 2005;280(25):23549-58.
49. Pham CT, Ley TJ. Dipeptidyl peptidase I is required for the processing and activation of granzymes A and B in vivo. Proc Natl Acad Sci USA. 1999;96(15):8627-32.
50. Kurschus FC, Jenne DE. Delivery and therapeutic potential of human granzyme B. Immunol Rev. 2010;235(1):159-71.

51. Weldon JE, Pastan I. A guide to taming a toxin: recombinant immunotoxins constructed from Pseudomonas exotoxin A for the treatment of cancer. The FEBS journal. 2011;278(23):4683-4700.
52. Wolf P, Elsässer-beile U. Pseudomonas exotoxin A: from virulence factor to anti-cancer agent. Int J Med Microbiol. 2009;299(3):161-76.
53. Kreitman RJ, Tallman MS, Robak T, et al. Phase I Trial of Anti-CD22 Recombinant Immunotoxin Moxetumomab Pasudotox (CAT-8015 or HA22) in Patients With Hairy Cell Leukemia. Journal of Clinical Oncology. 2012;30(15):1822-1828.
54. Mazor R, Eberle JA, Hu X, et al. Recombinant immunotoxin for cancer treatment with low immunogenicity by identification and silencing of human T-cell epitopes. Proceedings of the National Academy of Sciences of the United States of America. 2014;111(23):8571-8576.

Chapter 1: A Potent IL-2R Targeting Pro-drug as a Novel Anti-tumor Vaccine Adjuvant

Immuno-therapies offer an exciting approach to anti-cancer therapy. Unfortunately, there are currently only two anti-tumor vaccines approved for the treatment of human cancer. The immunosuppressive properties of the microenvironment is likely responsible for some of the failures observed by these anti-cancer vaccines. One strategy to improve vaccine efficacy is to target this microenvironment with a selectively toxic chemical adjuvant. To do this, we employ the usage of a chimeric protein containing IL-2 and a binding mutant of the bacterial toxin Pro-aerolysin in order to target and kill immunosuppressive T regulatory cells that express the IL-2 receptor gene. This protein pro-toxin was shown to kill cells expressing IL-2R at low doses while having little to no effect on cells negative for this target. This chimera, known as IL2-R336A, depleted Tregs in both tumor bearing and non-tumor bearing mice. Mice given a GMCSF expressing CT-26 vaccine had reduced tumor growth when given IL2-R336A as an adjuvant. IL2-R336A also decreased tolerance to splenocytes expressing HA in transgenic mice with HA producing prostates. This suggests that this toxin may be a useful tool in enhancing the immune response against tumor antigens that would otherwise be tolerated. We propose that the use of this chimeric toxin and other agents capable of targeting Tregs may be useful adjuvants for cancer vaccines and other immuno-therapies.

Introduction

Tumor targeting vaccines offer an attractive strategy as both a prophylactic in high risk patients and as a therapy to treat patients suffering from aggressive, therapy refractive cancer. Despite the large number of efforts to develop new immune based therapies, there are only two vaccines currently approved for the treatment of cancer and only one approved in the United States. This vaccine, Sipuleucel-T, is a protein vaccine using the prostate antigen Prostatic Acid Phosphatase and the patient's own dendritic cells to systemically target metastatic tumors (1,2). While this therapy has been clinically validated to improve patient outcomes, the number of approved therapies is disproportionate with the amount of research done in this field. This is likely due, at least in part, to the immuno-suppressive properties of the tumor microenvironment. Several groups have reported decreased T cell, dendritic cell, and Natural Killer cell activation in a variety of solid malignancies and that a higher immune cell count at time of diagnosis tends to correlate with better patient outcome (3,4). One mechanism of this inhibition is believed to be mediated through secretion of inhibitory cytokines by the tumor and stromal cells thus negatively regulated local immune cells (5). Another, more indirect mechanism, is the activation of regulatory immune cells in the tumor microenvironment that are able to potently suppress T cell activity thus promoting tolerance and overall tumor survival.

Multiple cell subtypes are capable of locally inhibiting an anti-tumor response. These subtypes include Myeloid-derived suppressor cells (MDSCs), Mesenchymal stem cells, and T regulatory cells (Tregs) (5). Tregs, in particular, are characterized by being $CD4^{+}CD25^{+}Foxp3^{+}$ and are potent regulators of local immune cell functionality (6). Modulation of T cell activity in the tumor microenvironment occurs through a plethora of mechanisms, many of which are not well understood. However, multiple cytokines

secreted by both tumor and stromal cells have been shown to be important for activating both of these subtypes including IL-6, IL-10, and TGF-β (7). It was shown by Hoelzinger et al. that disrupting IL-9 signaling inhibits Treg proliferation and Treg mediated immunosuppression (8) implicating the role of this pathway in promoting a tumor-tolerant phenotype by these cells. Recently, it has been shown that targeting immunosuppressive pathways can augment the immune system's tolerance of a tumor in a clinical setting via the success of anti PD1 and PDL-1 antibodies (9, 10). Thus, specific targeting and depletion of Tregs and other suppressive cells in the tumor microenvironment could improve the potency of an anti-cancer vaccine or other immune based therapy and may be a useful therapeutic tool.

Pro-aerolysin (PA) is an extremely potent protein toxin secreted by the pathogenic bacterium *Aeromonas Hydrophila* (IC_{50} < 100 pM against most cell-lines) (11). The toxin kills target cells via oligomeric pore formation in the target cell plasma membrane thus inducing osmotic lysis. PA is secreted in an inactive dimerized form that must be proteolytically activated on the C-terminus by the ubiquitously expressed enzyme furin or other trypsin like peptidases (12). In order to reach a sufficient concentration to oligomerize, the toxin must localize to the target cell membrane. PA accomplishes this by binding to GPI anchored membrane proteins via a membrane binding domain on the N-terminus of the toxin (13). The full mechanism of PA is depicted in Figure 1. Both properties of this toxin are crucial for its function, as perturbing either substantially raises the IC_{50} several orders of magnitude. Recently, we generated a mutant PA variant that was proteolytically activated specifically by the prostate specific protease PSA (14). This mutant killed PSA expressing cells both *in vitro* and *in vivo* and is currently in Phase III clinical trials for the treatment of Benign Prostate Hyperplasia. This work strongly suggests that PA mutants have the capability to be modified into cell specific targeting

agents despite having a relatively non-specific mechanism of activation. It also suggests that these PA variants have the capability of becoming useful therapeutics.

Re-targeting PA is not limited to just modification of the C-terminal proteolytic activation site. Osusky et al. reported that a simple point mutation (R336A) can completely impede

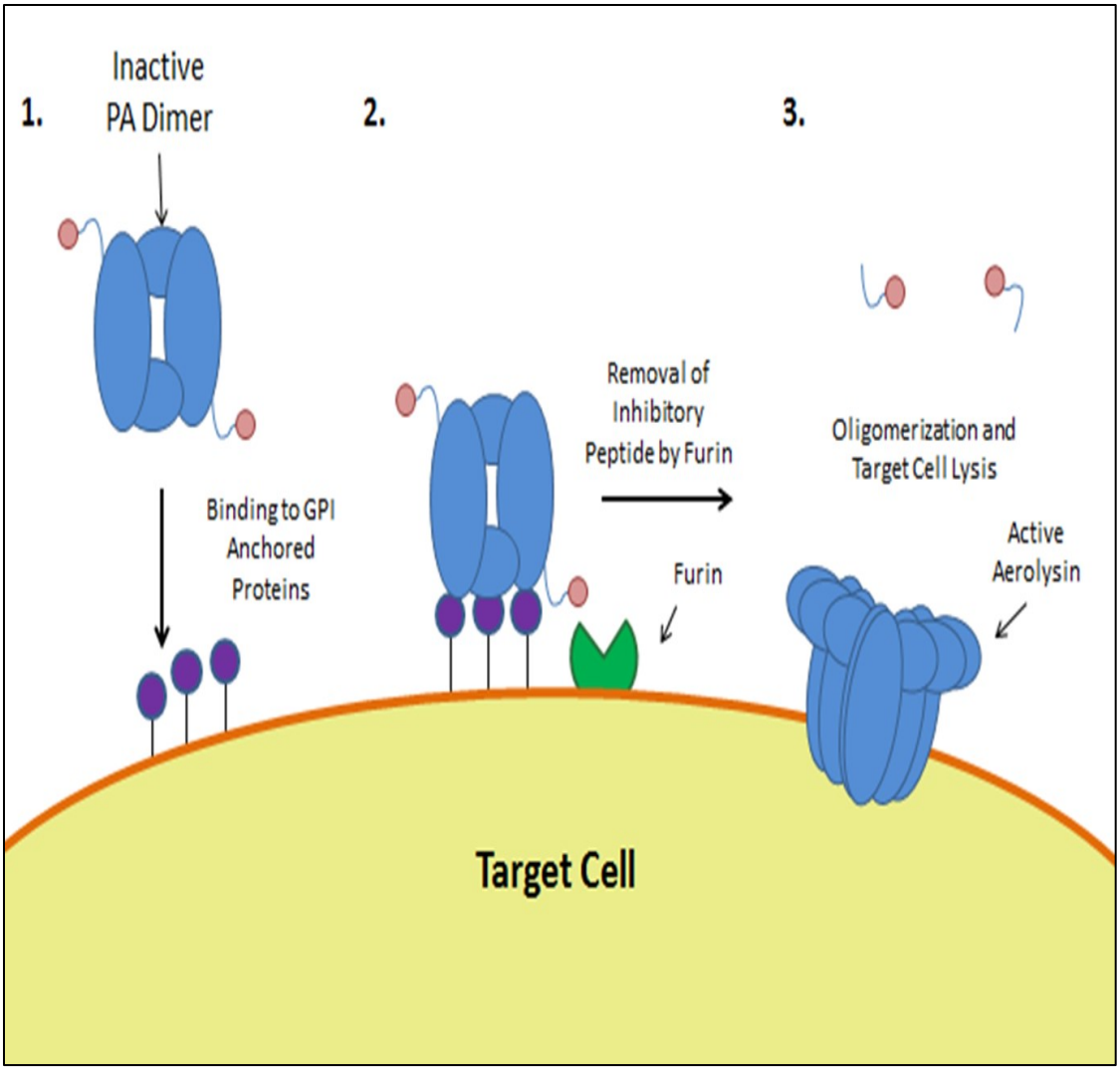

Figure 1: Cartoon depicting the mechanism of cell death induced by PA.

PA's ability to bind to GPI anchors and thus localize to target cells (15). They then show that adding the cytokine IL-2 to the N-terminus of PA can rescue this capability and make PA toxic to only cells expressing the IL2 receptor (IL2R). This mutant (IL2-R336A)

was not toxic to non-IL-2R expressing cells at any concentration tested. Therefore, it is reasonable to suggest that IL2-R336A could specifically and potently target IL-2R expressing cells *in vivo* and would have limited toxicity, if any, against all other cells. Because Tregs express IL-2R in reasonable quantities relative to other cells (16), we hypothesized that IL2-R336A could be used to deplete Tregs *in vivo* and potentially augment immune-based therapies in tumor bearing mice. In this study, we evaluate the potential of this strategy as an immuno-activator and vaccine adjuvant in mice.

Materials and Methods

Cell Lines

All cell lines were from the American Type Culture Collection (Manassas, VA). The CTLL-2 mouse cell line was maintained in RPMI 1640 medium supplemented with 10% fetal bovine serum and 10% T-STIM with concanavalin A or with 100 units/ml of human recombinant IL2. The EL-4 mouse cell line was maintained in Dulbecco's modified Eagle's medium supplemented with 1 mM sodium pyruvate and 10% fetal bovine serum. The HuT-78 human cell line was maintained in Iscove's modified Dulbecco's medium supplemented with 20% fetal bovine serum. The PC3 cells were maintained in RPMI 1640 medium supplemented with 10% fetal calf serum and 2 mm l-glutamine. Proaerolysin (PA) and IL2-R336A-PA proteins were provided by Dr. Buckley, University of Victoria and were generated as previously described (15). Unless otherwise specified all other reagents were from Sigma (St. Louis, MO).

Effects of IL2-R336A on response to GVAX cell vaccine

The mouse colorectal cancer cell line CT-26 cells were purchased from ATCC. CT-26 cells secreting murine GM-CSF (GVAX) were generated as previously described (17). To assess direct effects on growth Balb-c mice were inoculated subcutaneously with 5 x

105 CT-26 cells on day -7. On days -3, -2, and -1, mice received a single intravenous injection of 10μg/kg of IL2-R336A in sterile saline or saline vehicle. On day 0, Balb/c mice were immunized subcutaneously with vehicle or 106 irradiated (50Gy) CT26-GM-CSF cells. Tumor volumes were measured serially. For survival experiment, 40 mice were treated as described above with exception that mice received 2 injections of 5 x 105 irradiated CT-26-GMCSF cells with one injection near axial lymph nodes and the second injection near inguinal lymph nodes. Animals were sacrificed by CO2 overdose when tumors reached 2cc in size. All animal experiments were conducted according to protocols approved by the Johns Hopkins University School of Medicine Animal Care and Use Committee.

Treg Depletion

Balb/c mice were implanted subcutaneously with 106 4T1-HA cells. Mice received a 200μl intravenous injection with either 100 μg/ml (20 μg) PC61 anti-mouse CD25 antibody (BD Pharmingen) (n=6) or 68 μg/mL (13.6 μg) IL2-R336A-PA (n=6) or no treatment control (n=7). Blood was collected from the tail vein of each mouse 8 hours after injection. Draining lymph nodes, spleens and tumor tissue was also obtained. Staining for CD4, CDC25, and FoxP3 expression was performed by as previously described by Leao et al (18). Antibodies to CD4 (Allophycocyanin-conjugated, APC) and CD25 (Biotin-conjugated, pure) were purchased from BD Pharmingen (La Jolla, CA, USA). PE-labeled Ab to Foxp3 was purchased from eBiosciences (San Diego, CA, USA), and intracellular staining was carried out according to the manufacturer's instructions. The secondary Ab for CD25 was Streptavidin-Alexa Fluor® 488 (Invitrogen, Carlsbad, CA, USA). The cells were stained and analyzed by FACScan (Becton Dickinson, Mountain View, CA, USA) using the CellQuest software. The acquired data were reanalyzed using the Flowjo software (Treestar, Inc., Ashland, OR, USA).

Vaccination studies.

Transgenic mice expressing hemagglutinin antigen (HA) under the minimal rat Probasin promoter (−426 to +28 bp) in the prostate were provided by Dr. Drake and generated as previously described (19). Vaccinia virus and Listeria Monocytogenes expressing HA were provided by Dr. Drake and generated as previously described (20, 21). The recombinant vaccinia viruses were amplified in HuTK- cells, purified over 36% sucrose, and tittered using HuTK− cells.

Results

A

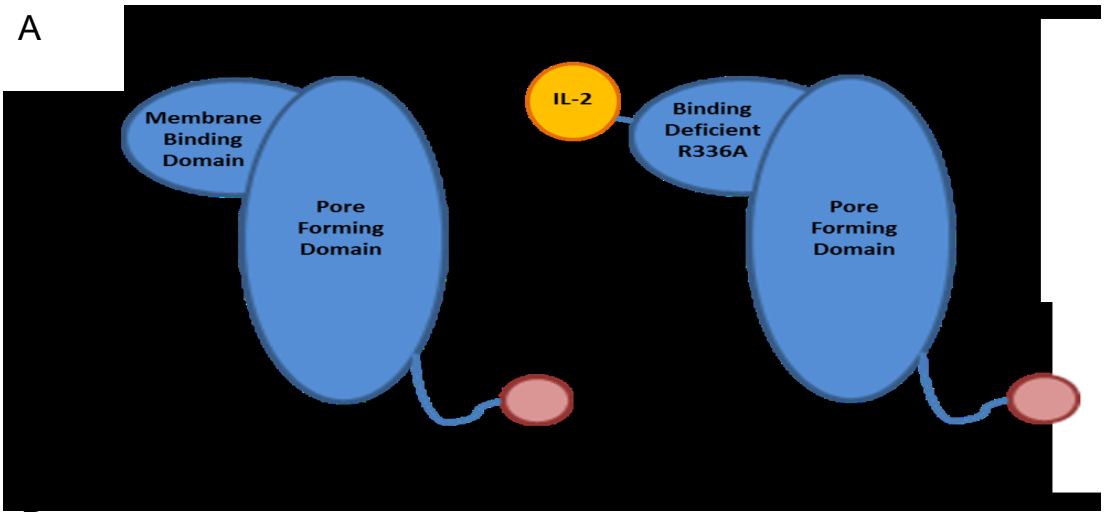

Cell line	Species	Cell Type	IL-2 Receptor	% Viability[a] PA	% Viability[a] IL2-R336A
EL4	Mouse	Lymphoma	No	20	100
HuT78	Human	T-cell Lymphoma	No	25	95
CT26	Mouse	Colon Cancer	No	8	95
PC-3	Human	Prostate Cancer	No	12	95
CTLL-2	Mouse	T cell	Yes	5	25

[a]Cells exposed for 1 hr to toxin at 1 nM and then viable cells assayed using Promega CellTiter cell proliferation assay. % Viability is percent of untreated controls. All assays done in triplicate.

Figure 2: Comparison of WT PA vs. IL2-R336A PA Schematic of WT PA (left) and the modified IL2-R336A (right) (A). Table depicting the cell killing capabilities of both toxins on cell lines. Some data adapted from Osusky et al. 2007 (B).

In order to specifically and potently target IL-2R positive Tregs, two modifications were made to WT PA (Figure 2A) as shown by Osusky et al. First, a single point mutation, R336A, was made in the membrane binding region of the protein in order to ablate GPI anchor binding and reduce toxicity against cells not expressing IL-2R. Second, recombinant IL-2 was fused to the N-terminus of PA in order rescue the toxin's ability to localize to plasma membranes (Figure 2A). All cell lines tested were very sensitive to lysis via WT PA as 1 nM of the toxin killed vast a majority of cells within an hour. However, the four cell lines not expressing the IL2 receptor were hardly affected with the same dose of IL2-R336A despite their inerrant PA sensitivity. The cell line, CTLL-2 was almost equally as sensitive to both pro-drugs with 1 nM of IL2-R336A killing 75% of the cells after only an hour (Figure 2B). It should be noted that CT26, the line used for GVAX experiments, was not particularly sensitive to IL2-R336A.

To assess the *in vivo* effect of IL2-R336A, we measured Treg depletion in mice dosed with the toxin. Specifically, the ratio of Treg cells to non Treg cells (determined by flow cytometry) was used to quantify this effect. One dose of 400 μg/kg of the toxin reduced the peripheral Treg to non Treg ratio by 50% and 75% in non-tumor bearing and tumor bearing mice respectively (Figure 3A). Somewhat surprisingly, there was no difference in this ratio between tumor bearing and non-tumor mice that received no treatment. We then determined the dosage required to see such a depletion in draining lymph nodes. We injected mice with 1 or 3 doses (once per day) of IL2-R336A and measured the Treg to non Treg ratio after 24 hours. The effect generated by the drug was compared to an IL2R antibody to determine whether or not this depletion was due to specific PA mediated lysis or via perturbation of IL2 signaling. IL2R antibody treatment had no effect in Treg count after 24 hours compared with the control group. A single 400 μg/mL dosage of IL2_R336A also had no effect on this ratio in draining lymph nodes. However,

3 daily doses of the toxin depleted Tregs by 50% after 24 hours of the final dose (Figure 3B). Based on this experiment, we used this dosing scheme for our GMCSF vaccine adjuvant studies.

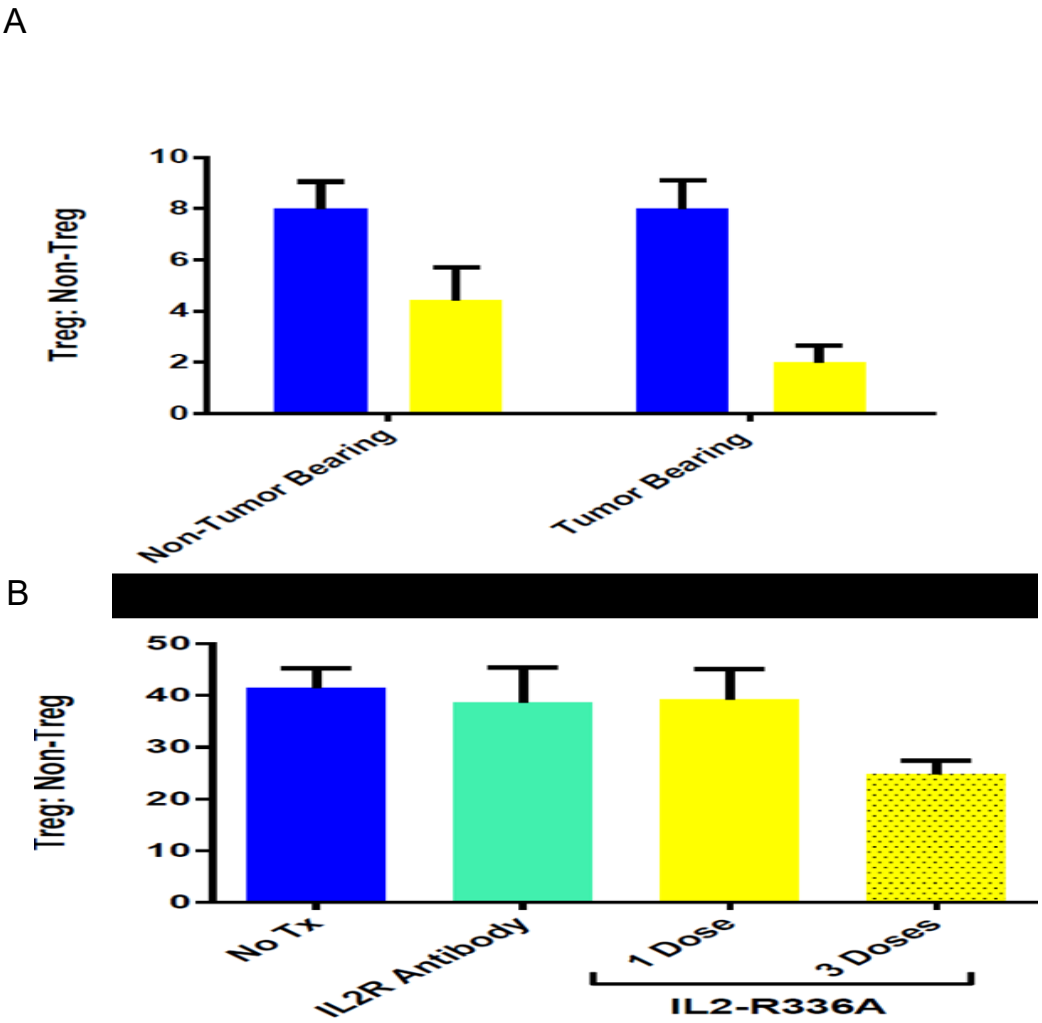

Figure 3: IL2-R336A depletes Tregs in tumor bearing mice. Peripheral Treg: Non Treg cell count of control animals (blue) or animals dosed with 400 ug/mL IL2-R336A (yellow) in tumor bearing vs non-tumor bearing mice (A)**.** The same dose was given either once or three times for three days. Treg counts were determined from draining lymph nodes after three days (B).

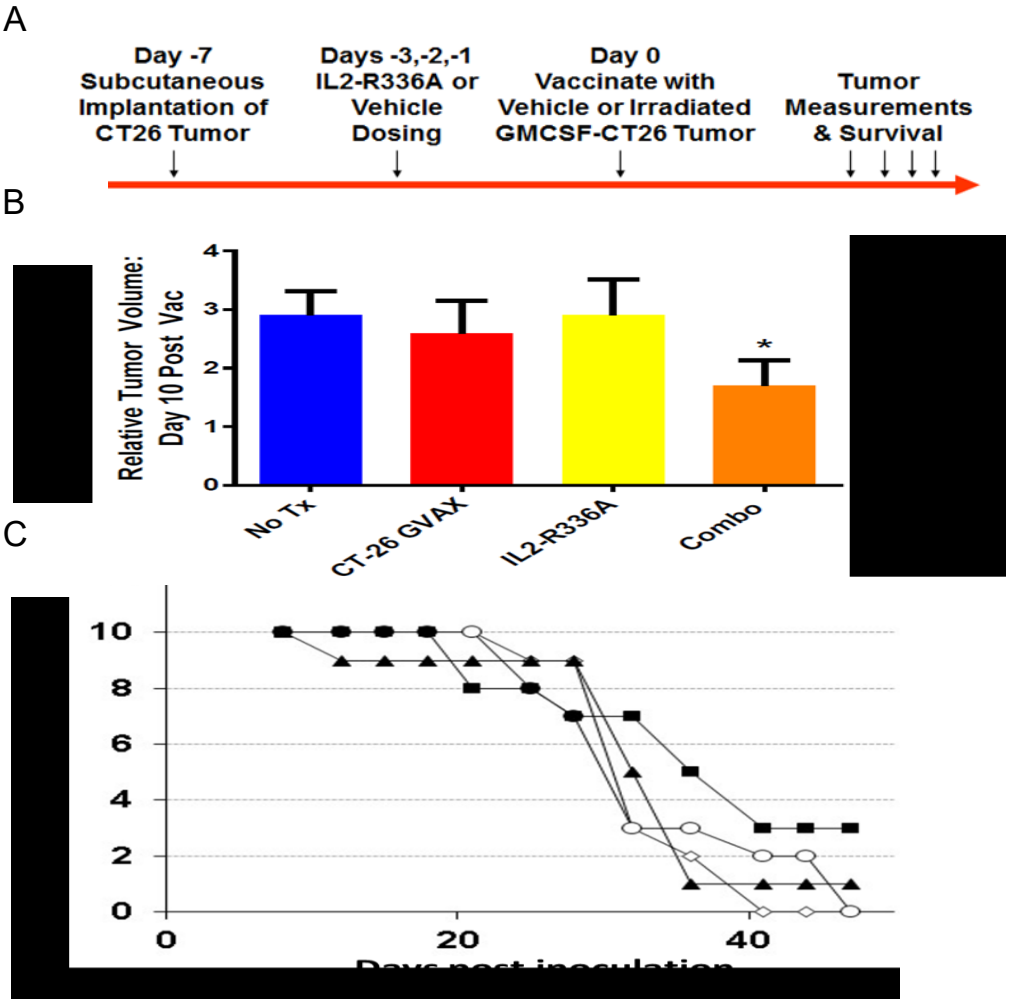

Figure 4: IL2-R336A improves response in combination with GVAX therapy. Balb-c mice implanted with a CT26 tumor were dosed with 400µg/kg IL2-R336A or Vehicle three times on three consecutive days. On day 4, mice were given a GMCSF expressing irradiated CT26 tumor vaccine or the vehicle (A). Tumor measurements were made 10 days post vaccination and compared to the day 0 starting volume (B). Survival of CT-26 xenograft mice dosed with CT-26 GVAX (black triangles), IL2-R336A (white circles), both agents (black squares) or neither (white diamonds) (C).

If IL2-R336A can be used as a potent vaccine adjuvant, it must be able to improve the therapeutic response in vaccine model systems. In order to do this, we gave three daily doses (400 µg/kg) of IL2-R336A to Balb-c mice that were implanted with a CT-26 tumor 4 days prior to the first injection. We then vaccinated the mice with a GMCSF expressing CT-26 tumor the day after the third injection of the toxin (Figure 4A). Relative tumor

volume (compared to the tumor volume the day of vaccination) was measured ten days afterwards. Mice given no treatment, the toxin itself, or the vaccine itself showed no significant change in relative tumor volume after ten days. Only mice given both the vaccine and the sequential doses of IL2-R336A showed a reduction in tumor growth. These mice had relative tumor volumes half that of the control mice after ten days. This difference was determined to be statistically significant with a p value less than 0.05 (Figure 4B). We also assessed the survival (tumors greater than 2 cubic cm) of these treated animals. We saw no difference in survival between control animals, and animals dosed with CT-26 GVAX or IL2-R336A alone. We did, however, find that mice treated with combination of the vaccine and the toxin adjuvant had a slight survival advantage (not statistically significant), consistent with the decreased tumor size observed in these animals (Figure 4C).

We then asked whether or not IL2-R336A could enhance the efficacy of a tumor vaccine against an antigen that was otherwise tolerated by T cells present in the tumor a common phenomenon in solid malignancies. We gave a single dose (400 μg/kg) of IL2-R336A to Balb-c transgenic mice expressing hemagglutinin (HA) on their prostate gland. Two days later, we gave either a vaccine against HA expressing *Vaccinia* or HA expressing *Listeria Monocytogenes*. We then injected HA producing mouse splenocytes loaded with dye. We measured T cell mediated cytolysis and release of the dye using flow cytometry and measured vaccine efficacy as specific lysis of these splenocytes (Figure 5). Mice given no treatment or the toxin alone showed no specific lysis after 24 hours. Mice given either the Vaccinia or *Listeria* vaccines alone showed modest amounts of specific lysis at this time point. When given in tandem with IL2-R336A, both groups receiving vaccines showed an increase in T cell mediated killing. Specifically, mice given the adjuvant and the Vaccinia vaccine had an approximate 10 fold increase

in specific lysis. Mice given the *Listeria* vaccine showed a more modest 50 % increase in specific lysis compared to the no adjuvant group. It should be noted that there was substantially more background lysis (roughly 25 fold) in mice that received the *Listeria* vaccine.

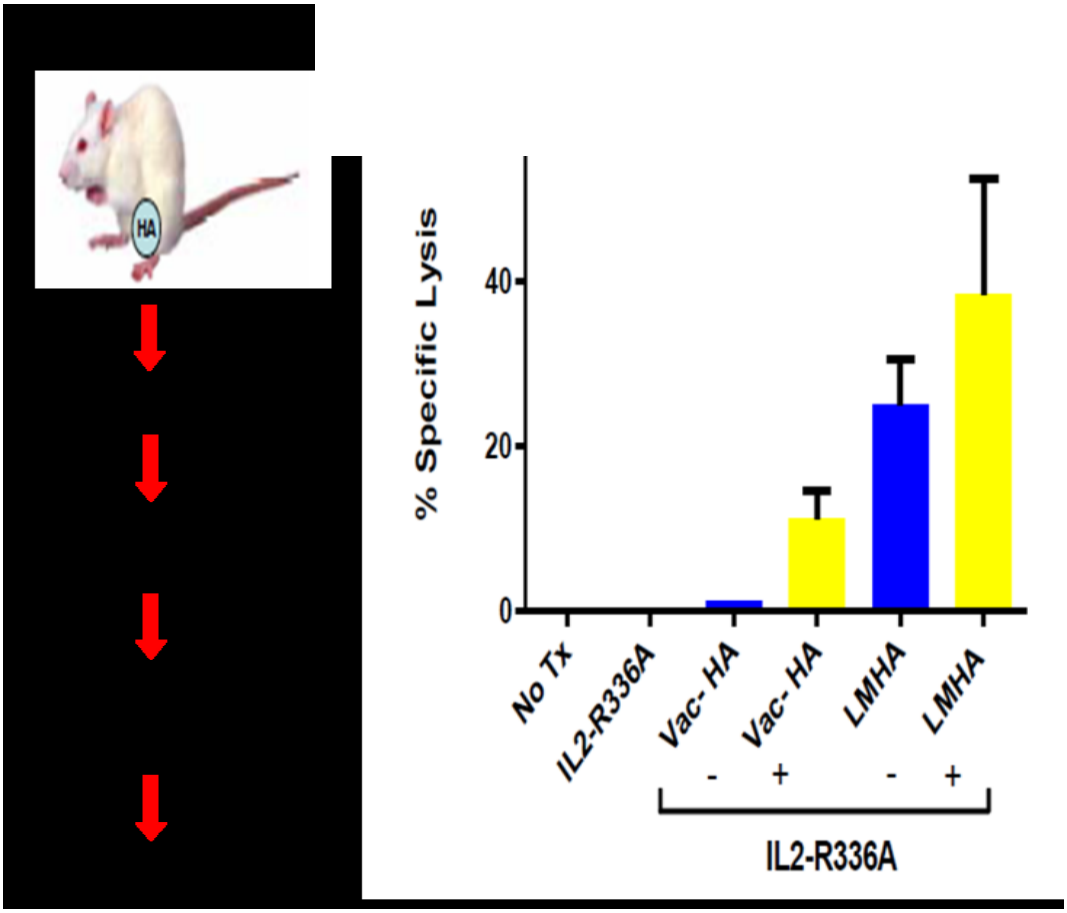

Figure 5: IL2-R336A reduces immune tolerance of HA-expressing splenocytes. A single 400 µg/kg dose of Il2-R336A was given to HA producing transgenic mice two days prior to administration of a Vaccinia (Vac) or *Listeria Monocytogenes* (LM) HA producing vaccine or the vehicle. On day 7, HA producing splenocytes loaded with dye were administered and specific T-cell mediated lysis was measured using flow cytometry.

Discussion

We used a previously generated, mutant, chimeric toxin in order to disturb Treg function in immuno-competent mice and assessed the protein's potential as a vaccine adjuvant. The protein, IL2-R336A, was shown by Osusky et al. to selectively and potently target IL-2R expressing cell lines while having no effect on IL-2R negative cell lines. We supplemented this finding by injecting R336A PA into mice and observed no toxicity at any dose tested (data not shown) despite using doses that are orders of magnitude higher than the therapeutic range of this protein. Both of these data suggest that R336A PA and mutants of this protein are safe to give at therapeutic doses without generating any acute toxicity and is suggestive that the R336A mutation substantially improved the therapeutic range of the protein.

IL2-R336A, *in vivo,* was shown to deplete Tregs in peripheral blood after 24 hours with a single 400 μg/kg dose by 50% in both tumor bearing and non- tumor bearing mice suggesting the toxin is both potent and fast acting as the cell based assays would indicate. Three daily consecutive doses of the toxin depleted Tregs in draining lymph nodes 24 hours after the third dose was administered. An antibody against mouse IL-2R did not generate the same depletion of Tregs strongly suggesting that the depletion is a result of specific PA mediated killing as compared to modification of IL-2 signaling. Both experiments show a significant decrease in Tregs supporting the idea that IL-2R based targeting is a viable strategy depleting these cells in both the circulatory and lymphatic system. We did not examine the dosing regimen necessary to completely ablate Tregs as this may generate more unwanted autoimmune side effects due to decreased tolerance by the immune system. The optimal dose and Treg depletion level will still need to be determined in order to maximize effect and minimize unwanted toxicity.

Regardless, we then assessed whether depletion of Tregs through both tested regiments was sufficient to enhance the response of an immune based therapy. Because three doses of IL2-R336A was enough to deplete Tregs by 50% in draining lymph nodes after a mere 24 hours, we used this dosing strategy to see if the toxin could enhance the effect of an anti-tumor vaccine in Balb-c mice. Neither GMCSF CT-26 vaccine given nor the toxin given by itself had any effect on tumor growth, however, when given together, a significant reduction in tumor volume was seen after 10 days. Because the vaccine had no effect by itself, this experiment suggests that the presence of immuno-suppressive Treg cells in the stroma alone was enough to suppress any anti-tumor T-cell activity. IL2-R336A was able to augment the GMCSF CT-26 vaccine, as tumor growth was slowed substantially 10 days post vaccination. This experiment, as a whole, demonstrates the large influence that Tregs play in the tumor microenvironment and that simply reducing the number of these cells is enough to reverse this effect and improve the efficacy of an immuno-therapy.

One major obstacle facing any anti-cancer immune based therapy is the issue of tolerance, that is, the immune system's inability to be activated by the presence of tumor antigens despite being exposed to them via a vaccination or by other means. To address this issue, we used a transgenic mouse line that has become tolerant to the HA antigen growing in the prostates of the animals. We then vaccinated the mice against HA and assessed whether or not IL2-R336A could augment the response to this antigen via injection of dye labeled, HA expressing splenocytes. Mice given both the toxin and an anti- HA Vaccinia vaccine had a staunch increase in HA specific targeting compared to mice only given the vaccine while mice given the toxin and a *Listeria* showed a modest increase in HA specific cell killing. The reason between this substantial difference is not entirely clear, however, it may be due to the natural difference in immunogenicity

between the two organisms used or the amount of HA produced by each vaccine. Again, because Tregs likely play a crucial role in promoting tolerance of host based antigens, it is unsurprising that selectively killing these cells would have a notable effect on vaccine efficacy. This experiment suggests that one dose of IL2-R336A can reduce the tolerance to an antigen of interest and help re-activate the local immune cells. This system, while artificial, demonstrates the therapeutic potential in targeting Treg cells for immunotherapy purposes and their overall influence in negatively regulating the immune system in the context of cancer. This finding has yet to be examined on tumor specific antigens *in vivo*.

It is clear through this study and others that the presence of Tregs in the tumor microenvironment is one of the most important factors that determines the immune system's ability to target neoplastic cells. Our IL-2R targeting pro-toxin IL2-R336A was able to both enhance the efficacy of a tumor-based vaccine and reduce tolerance to host derived antigen-based vaccines in immuno-competent mice. Further study must be done on how the quantity of the depletion of these cells correlates with the overall efficacy of a vaccine as well as the types of solid tumors that are most likely to benefit from a Treg targeting agent. Because IL2-R336A was able to augment vaccine efficacy *in vivo* and be given safely at therapeutic doses, we propose that the usage of this toxin as a tumor vaccine adjuvant warrants further study in other malignancies and animal models. We also advocate for the usage of other, similar strategies to target immuno-suppressive cell types in the tumor stroma. It is not unreasonable that given the success observed with IL2-R336A that other targeting moieties such as growth factors and scFv fragments could be fused to this mutant toxin in order to generate novel pro-drugs capable of targeting both tumor cells directly and pro-tumor stromal cells. We are optimistic about the therapeutic and biochemical power this protein offers and the possible ways it could

be utilized as a therapeutic or adjuvant therapeutic to treat and combat human malignancies.

References

1. Small EJ, Schellhammer PF, Higano CS, et al. Placebo-controlled phase III trial of immunologic therapy with Sipuleucel-T (APC8015) in patients with metastatic, asymptomatic hormone refractory prostate cancer. J Clin Oncol. 2006;24(19):3089-94.
2. Olson BM, McNeel DG. Sipuleucel-T: immunotherapy for advanced prostate cancer. Open Access Journal of Urology. 2011;3:49-60.
3. Hadrup S, Donia M, thor Straten P. Effector CD4 and CD8 T Cells and Their Role in the Tumor Microenvironment. Cancer Microenvironment. 2013;6(2):123-133.
4. García-Martínez E, Gil GL, Benito AC, et al. Tumor-infiltrating immune cell profiles and their change after neoadjuvant chemotherapy predict response and prognosis of breast cancer. Breast Cancer Research : BCR. 2014;16(6):488.
5. Lindau D, Gielen P, Kroesen M, Wesseling P, Adema GJ. The immunosuppressive tumour network: myeloid-derived suppressor cells, regulatory T cells and natural killer T cells. Immunology. 2013;138(2):105-15.
6. Pandiyan P, Zheng L, Lenardo MJ. The molecular mechanisms of regulatory T cell immunosuppression. Front Immunol. 2011;2:60.
7. Burkholder B, Huang RY, Burgess R, et al. Tumor-induced perturbations of cytokines and immune cell networks. Biochim Biophys Acta. 2014;1845(2):182-201.
8. Hoelzinger D, Dominguez A, Pollock K, Lustgarten J, Cohen P, Gendler S. IL-9 strategy to perturb Treg function and enhance anti-tumor immunity. The Journal of Immunology May 1, 2013, 190 (1 Supplement) 140.9.
9. Chen L, Han X. Anti-PD-1/PD-L1 therapy of human cancer: past, present, and future. J Clin Invest. 2015;125(9):3384-91.

10. Philips GK, Atkins M. Therapeutic uses of anti-PD-1 and anti-PD-L1 antibodies. Int Immunol. 2015;27(1):39-46.
11. Buckley JT. The channel-forming toxin aerolysin. FEMS Microbiol Immunol. 1992;5(1-3):13-7.
12. Abrami L, Fivaz M, Decroly E, et al. The pore-forming toxin proaerolysin is activated by furin. J Biol Chem. 1998;273(49):32656-61.
13. Abrami L, Fivaz M, Glauser P-E, Parton RG, van der Goot F. A Pore-forming Toxin Interacts with a GPI-anchored Protein and Causes Vacuolation of the Endoplasmic Reticulum. The Journal of Cell Biology. 1998;140(3):525-540.
14. Williams SA, Merchant RF, Garrett-mayer E, Isaacs JT, Buckley JT, Denmeade SR. A prostate-specific antigen-activated channel-forming toxin as therapy for prostatic disease. J Natl Cancer Inst. 2007;99(5):376-85.
15. Osusky M, Teschke L, Wang X, Wong K, Buckley JT. A chimera of interleukin 2 and a binding variant of aerolysin is selectively toxic to cells displaying the interleukin 2 receptor. J Biol Chem. 2008;283(3):1572-9.
16. Cheng G, Yu A, Malek TR. T cell tolerance and the multi-functional role of IL-2R signaling in T regulatory cells. Immunological reviews. 2011;241(1):63-76.
17. Dranoff G, Jaffee E, Lazenby A, et al. Vaccination with irradiated tumor cells engineered to secrete murine granulocyte-macrophage colony-stimulating factor stimulates potent, specific, and long-lasting anti-tumor immunity. Proc Natl Acad Sci USA. 1993;90(8):3539-43.
18. Leao, I. C., Ganesan, P., Armstrong, T. D. and Jaffee, E. M. (2008), Effective Depletion of Regulatory T Cells Allows the Recruitment of Mesothelin-Specific CD8+ T Cells to the Antitumor Immune Response Against a Mesothelin-Expressing Mouse Pancreatic Adenocarcinoma. Clinical and Translational Science, 1: 228–239.

19. Dranoff G, Jaffee E, Lazenby A, et al. Vaccination with irradiated tumor cells engineered to secrete murine granulocyte-macrophage colony-stimulating factor stimulates potent, specific, and long-lasting anti-tumor immunity. Proc Natl Acad Sci USA. 1993;90(8):3539-43.

20. Drake CG, Doody AD, Mihalyo MA, Huang CT, Kelleher E, Ravi S, Hipkiss EL, Flies DB, Kennedy EP, Long M, et al. Androgen ablation mitigates tolerance to a prostate/prostate cancer-restricted antigen. Cancer Cell. 2005;7:239–249

21. Keenan BP, Saenger Y, Kafrouni MI, et al. A Listeria vaccine and depletion of T-regulatory cells activate immunity against early stage pancreatic intraepithelial neoplasms and prolong survival of mice. Gastroenterology. 2014;146(7):1784-94.e6.

Chapter 2: PLGA Microparticle Encapsulation of a Novel Prostate-Targeted Biologic For Tumor Delivery: Characterization of Release and Functionality

As the fields of therapeutics, pharmacology, and biotechnology continue to advance, more and more biologic-based agents are evaluated pre-clinically for their potential as therapeutic and diagnostic agents. While many of these agents will see success in such studies, others will ultimately fail due to a plethora of reasons. Agents that do not effectively reach their target tissue in pre-clinical and clinical studies usually do not advance further despite highly targeted and specific mechanisms of action. Targeted delivery of the biologic agent in question, however, could possibly circumvent these problems and improve the agent's pharmacologic profile. In this study, we evaluate one such approach, PLGA micro-particle encapsulation, in order to improve the systemic administration of a promising prostate-selective pro-toxin known as PRX302. PRX302 is a mutant bacterial toxin selectively activated by the prostate-specific peptidase PSA. Due to specific interactions with cell surfaces, this toxin cannot be delivered systemically in a safe manner. Currently, PRX302 is being evaluated for its potential as a locally administered treatment for benign prostate hyperplasia, however, due to its highly specific and potent mechanism of action, its use as a systemic prostate cancer therapeutic is enticing. Because of its interesting mechanism of action, delivering PRX302 to a target tissue via PLGA microparticles may facilitate this protein as a useful anti-cancer therapeutic. In order to explore this hypothesis, we enveloped PRX302 in PLGA micro-particles and examined its release and functionality using a home-made sandwich ELISA and cell based-cytotoxicity assays. The mutant pro-toxin was successfully encapsulated in these micro-particles and released in an aqueous environment. Quantitative release kinetic studies indicated that, after 10 days at 37

degrees, roughly 90 ng (10% total PRX loaded) of detectable material was released. This material, when incubated with enzymatically active PSA or cells expressing functional PSA, was cytotoxic to human cells. These results suggest that PRX302 can be successfully loaded into PLGA micro-particles and released slowly into the local micro-environment, however, the kinetics of this release may not be ideal depending on the desired concentration. The assay and methods described will facilitate future studies examining the controlled release of this protein using other PLGA formulations or other delivery platforms and suggest that this method of drug encapsulation may help circumvent the pharmacokinetic challenges associated with its current use.

Introduction

The use of biologics for treating human disease has risen dramatically in the past two decades. These agents can offer unique mechanisms of action and selectively not possible with small molecule-based pharmacophores. In the field of oncology alone, there are currently over a dozen monoclonal antibodies approved to treat both solid and liquid malignancies (1). The selective toxicity induced by these antibodies can often combine synergistically with radiation therapy, chemotherapy, or immune-based therapy. Given the modest success of these agents and the plethora of tumor-selective targets available, it is reasonable to expect the surge in biologic-based therapy to continue.

Unfortunately, undesirable pharmacokinetic properties of many of these agents have resulted in poor clinical trial performances and failure of the drug to ever be utilized for clinical purposes. Rather than leave these candidates to anecdote, re-targeting them using an alternative delivery platform may salvage their potential. This can be done using a variety of methods including controlled release via poly-lactic-glycolic acid (PLGA) micro-particles, a hydrophilic polymer capable of ensnaring both small molecule drugs and biologics, which slowly degrade via acid-catalyzed hydrolysis (2,3). PLGA microparticle encapsulation has some success in the context of cancer. PLGA micro-particles loaded with nafarelin (a GnRH agnostic) were shown to slowly release the peptide systemically and suppress testosterone production via GnRH axis feedback inhibition (4). It is evident that the pharmacokinetic and pharmacodynamics properties of macromolecules can be augmented using controlled release-based approaches which can yield desired effects that would be otherwise impossible using standard systemic dosing protocols.

Biologics that interact with cell surfaces or that are taken up non-specially may benefit from encapsulation provided that the loaded microspheres can be delivered to the tumor microenvironment efficiently using an appropriate vector. It is evident that unique aspects of the tumor-microenvironment facilitate cell-specific migrations that can be used for therapeutic purposes. It has been well established that, as a mechanism for suppressing the local immune response, prostate cancer cells recruit mesenchymal stem cells (MSCs) to the surrounding stroma via paracrine signaling (5). MSC's are a multipotent stem cell lineage capable of differentiating into a variety of cell types including osteocytes and adipocytes. Several studies have associated MSCs with the tumor micro-environment and their role in creating a pro-tumor stromal environment (6,7). Interestingly, MSCs have been shown to efficiently phagocytize PLGA micro-particles while maintaining viability and cell function (8). For these reasons, it is rational to predict that PLGA-loaded MSCs could facilitate the selective delivery of biologic-loaded microparticles with robust cell-targeting potential. Ideally, such a biologic agent would already display the ability to potently kill cancer cells *in vitro* and in *vivo.*

Pro-aerolysin (PA) is an attractive target for such a strategy. PA is a secreted bacterial toxin from the species Aeromonas Hydrophila which induces cell lysis via oligomeric channels formed in the target cell membrane (9). To regulate this function, PA requires specific proteolysis on its C-terminus to remove a small inhibitory peptide via the protease furin (10). In order to target the protein to prostate cancer cells, Williams et al mutated the native furin activation sequence to a peptide capable of being selectively activated by the Prostate Specific Antigen (PSA), a chymotrypsin-like serine protease which has been shown to be only functional in the stroma of normal and malignant prostate epithelial cells (11, 12,13). The mutant, known as PRX302, was only functional in the presence of enzymatically active PSA (13). PRX302 was shown to be selectively

toxic at picomolar doses to cell lines that produced sufficient amounts of functional PSA. Intratumoral injections of PRX302 yielded a robust regression in tumor size in PSA expressing xenografts. Unfortunately, due to PRX302's capability of localizing to cell membranes via binding to GPI-anchored proteins (14), it has poor bioavailability and cannot be distributed systemically in the body. Because, PRX302 was able to induce rampant cell death when locally injected into tumors, it is currently being evaluated in Phase III clinical trials for the treatment of Benign Prostate Hyperplasia (BPH) (15). Thus, in order to harness the potent and selective power of PRX302 for systemic cancer therapy, PRX302 must be delivered selectively to the tumor micro-environment.

It is for these reasons that our lab proposes to load PLGA microspheres with PRX302 as a cargo for MSC-facilitated targeted delivery. We have successfully delivered prostate-targeted pro-drugs previously for similar purposes. The PSA-activated thapsigargin analog G114 has been shown to be efficiently loaded and released from this material (16). This platform would take advantage of PRX302's ability to potently and externally lyse cancer and stromal cells while being selective for cells expressing PSA as well as MSC's ability to selectively localize in this same micro-environment. In order to assess the potential of this multi-armed approach, it is best to characterize the pro-toxin's functionality and release from these PLGA microspheres independent of the cell-based uptake. In this study, we develop a sensitive and accurate assay using two PRX302 antibodies, HG6 (monoclonal) and MPC (polyclonal), to characterize the release of this pro-toxin from loaded PLGA-microspheres and assess the functional capacity of this drug once it has been released using cell-based methods.

Materials and Methods

Materials and reagents

All reagents were purchased from Sigma Aldrich unless stated otherwise. Recombinant PRX302 protein and polyclonal MPC antibody were a gift from the laboratory of Peter Howard. These reagents were generated as previously described. Materials utilized for MP generation are as previously described (15). Human erythrocytes were obtained from discarded clinical specimens in accordance with IRB-approved protocols. All prostate-cancer cell lines were obtained from the American Type Culture Collection.

HG6 Monoclonal Antibody Generation

The HG6 hybridoma was maintained in DMEM supplemented with 10% FBS, 1mM sodium pyruvate, 1% pen/strep, 1% L-glutamine, and 0.1% 2-mercaptoethanol at 37C in a humidified incubator with 5% CO2. Prior to media conditioning, cells were slowly adapted to 5% IgG-stripped FBS followed by expansion of the culture to the desired volume. Media was then conditioned for 1wk prior to collection of supernatant, centrifugation to remove cell debris, and passed through a 0.2um filter. Supernatants were concentrated to less than a milliliter using Amicon Ultra-15 Centrifugal Filter Units (10k MWCO) (UFC903024) according to manufacturer's instructions. HG6-containing media was then incubated with Protein G Agarose (Pierce 20398), washed, and eluted according to manufacturer's recommendations. IgG positive fractions were tracked using absorbance at 280 nm. Pooled fractions were then dialyzed vs 1 L TBS (pH = 7.4) for 2 hours and 2 L TBS overnight at four degrees Celsius. Final protein concentration was determined using absorbance at 280 nm with a molar extinction coefficient of 150,000 $L\ mol^{-1}\ cm^{-1}$

PRX302 Sandwich ELISA Optimization

In order to develop the appropriate conditions for an accurate, robust, and reproducible sandwich ELISA, optimal detection and capture antibody conditions were evaluated. To

do this, we coated Nunc-Immuno micro well plates (Sigma M9410) with various concentrations of HG6 mouse monoclonal IgG in PBS pH = 7.4 and incubated this overnight, at room temperature, shaking, and protected from ambient light. The next day, all coating solution is removed and the plate is blocked with 300 uL of a 1% BSA solution in PBS incubated at RT for one hour shaking. All samples of PRX302 were diluted in blocking solution at least one hundred fold. Samples were incubated with coated plates for 2 hours at RT shaking. The plate was then washed three times with 300 uL of a solution of PBS containing 0.05% Tween20 and dried via dabbing. The MPC polyclonal rabbit antibody was then diluted at various concentrations in blocking solution and incubated in the same manner as the PRX samples. Prior to detection of the MPC antibody, the plate was washed three times and dried. A solution of anti-rabbit HRP-conjugated IgG (Cell Signaling 7074S) was then diluted 1:5000 in blocking buffer and incubated with the plate for one hour at RT shaking. The plate was then washed three times and incubated with a 1 mg/mL solution of ABTS substrate (Sigma 10102946001 ROCHE) in peroxide buffer (Sigma 11204530001 ROCHE). The reaction was then incubated 1 hour at RT while protected from ambient light. After incubation, the plate was read at both 410 and 570 nm with the final value being the difference between the two wavelengths.

Sandwich ELISA for Assay Validation and Release Studies

Based on the optimization studies, it was determined that the optimal concentrations for the capture and detection antibodies were 4 ug/mL and 5.5 ug/mL respectively. The protocol for all ELISA-based assays in this study is identical to the optimization work using these concentrations. For the parallelism and spike/recovery experiments, all samples were diluted in PBS (pH = 7.4) containing 1% BSA. To assess the effects of cell culture media (RPMI 1640 w/ 10% FBS) and human plasma (isolated from whole blood)

on the assay, PRX302 was diluted to 500 ng/mL in 100% whole media and plasma and further diluted 5 fold serially in sample buffer. Once the assay was completed, the respective points were superimposed on the standard curve based on their theoretical concentration and actual obtained A450-A570 value. For samples with unknown PRX values, we plotted the obtained A450-A570 and the theoretical concentration independent of the standard curve. To determine actual PRX302 concentration, we used a 4-parameteter non-linear regression and calculated the concentration using the same wavelength pair.

Hemolytic PRX302 Functional Assay

To characterize the functional parameters of PRX302 and validate the ELISA measurements independently, we used an erythrocyte-based hemoglobin release assay. Isolation of human erythrocytes (RBCs) from whole blood was done so by spinning down vials of donated blood at 800 x g for 15 minutes. The supernatant containing plasma was saved and the buffy coat was discarded. An aliquot of RBCs was taken and diluted to 4% in normal saline. This solution was spun to remove dead or damaged cells at 1000 x g for 5 minutes. RBCs were then washed once more in saline. Dilutions of PRX302 or unknown samples were made in PBS with BSA after being incubated with human PSA (Bio Rad 7820-0504) for two hours at 37 degrees Celsius. These solutions were then mixed with the washed 4% RBC solution and incubated for 2 hours at 37 degrees while rotating. Samples were then centrifuged at 1000 x g for 5 minutes in order remove intact RBCs. The supernatant was then transferred to a 96 well plate and read at 540 nm. The samples were then plotted as a function of percent hemolysis when compared to RBCs incubated with 2% Triton X100. The standard curve generated was then used to either show parallelism or determine the concentration of functional PRX from unknown

samples. For the most accurate calculations, samples were diluted so the A540 would correspond to the linear portion of the standard curve.

PRX302 PLGA Microparticle Generation

PRX302 MP generation was performed using a double immersion protocol. This was done via the same preparatory steps as the prostate-targeting pro-drug G114 in previous studies (15). Physical characteristics of these MPs were determined as previously described. Total protein loaded was determined by 280 UV spectroscopy.

PRX302 PLGA Release Assay

To accurately determine the release rates for various formulations of PRX302 MPs, we used the previously discussed PRX302 quantitative sandwich ELISA protocol. Lyophilized PRX microparticles were washed twice in saline containing 1% BSA for 5 minutes each and resuspended in this solution a concentration of 1 mg particles per mL of solution. The solution was sonicated on the lowest power for 10 seconds, three times, on ice and then incubated at 37 degrees shaking for various time points. To harvest the resulting supernatants and MP pellets, the suspension was centrifuged for 15 minutes at 800 x g with the resulting 0.5 mL supernatants and pellets being stored at -80 degrees Celsius until needed. Supernatants were diluted in ELISA sample buffer at several dilutions in order to obtain concentrations appropriate for the dynamic portion of the standard curve.

Tissue Culture Experiments & Cell Viability

PSA-expressing LNCaP cells and PSA-null DU145 cells were cultured in RPMI 1640 containing 10% FBS and supplemental L-glutamine. For incubations with PRX302 MP supernatant, LNCaPs were plated at 5000 cells per well and DU145 cells were plated at 1000 cells per well. PRX302 MP supernatant was then diluted serially directly into each

well and incubated for 48 hours. Cell morphology was monitored regularly using a light microscope. To directly measure cell viability, we performed the MTT assay. To do this, we removed 100 uL of media and supplemented each well with 15 uL of MTT dye directly. The cells were then incubated for 4 hours at 37 degrees. Cells were then lysed and the metabolized MTT dye was solubilized using 100 uL of stop solution. The plate was then incubated at room temperature for at least an hour and then read using A570-A650. A standard curve was used to determine the exact number of cells in each well as opposed to just reporting absorbance.

Results

To accurately determine how much PRX302 was released from the loaded PLGA MPs in terms of both concentration and as a percentage of total cargo loaded, it is essential that a sensitive, quantitative, and robust assay be used. To assess the viability of a sandwich ELISA using the HG6 and MPC antibodies as such an assay, we performed an optimization experiment using increasing concentrations of both. We also required this assay to have minimal background in biologically relevant samples to avoid issues related to the signal to noise ratio. Based on our optimization grid, higher concentrations of both HG6 and MPC increased the signal robustly while yielding very minute changes in the background (Figure 1A) suggesting that this antibody pair was appropriate for the development of this assay.

Quantitatively, we observed a robust and saturated increase signal in both capture and detection antibody (Figure 1B and 1C) as PRX302 concentrations increased. The capture antibody titration experiment (Figure 1B) showed an increase in the range of the assay in between 2 and 4 ug/mL and no change between 4 and 8 ug/mL. In order to determine the saturating concentration range for the detection antibody, we used at least

a 5 fold increase in concentration compared to the optimization grid. Similar to the capture antibody, we observed an increase in the range of the assay as concentrations

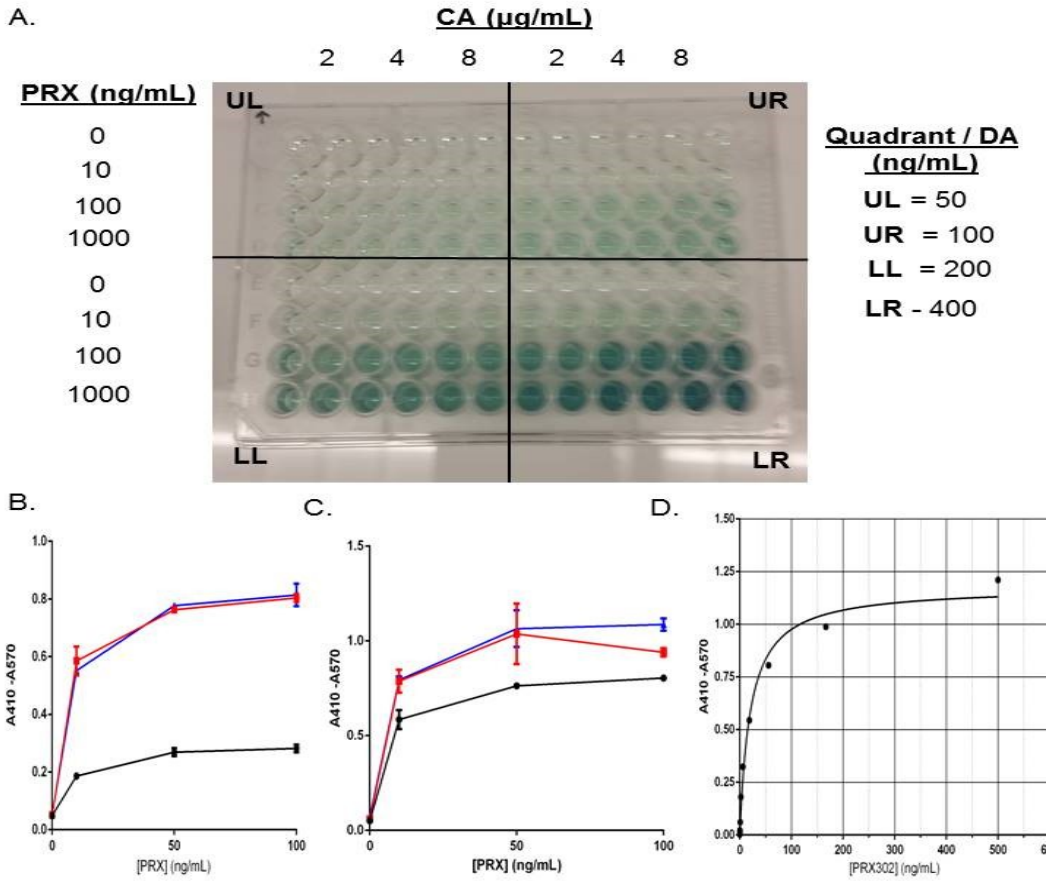

Figure 1: PRX302 Sandwich ELISA Development. Optimization plate for PRX302 ELISA. Concentrations of monoclonal HG6 (capture), polyclonal MPC (detection), and PRX302 standard at three concentrations (A). Effect of varying concentrations of capture antibody concentrations at 2 (black), 4 (red), and 8 (blue) ug/mL (B). Effect of varying concentrations of detection antibody concentrations at 2.7 (black), 5.5 (red), and 11.1 (blue) ug/mL (C). Comprehensive standard curve at concentrations ranging from 0.003 to 500 ng/mL (D). All values are represented as A410-A570.

increased until the signal saturated in between 5.5 ug/mL and 11.1 ug/mL. For both optimization experiments, we observed a linear increase in signal in between 0 and 10 ng/mL with the signal saturating in between 10 and 50 ng/mL and continuing to do so between 50 and 100 ug/mL. For the comprehensive standard curve, we used 4 ug/mL

capture antibody and 5.5 ug/mL detection antibody to maximize the dynamic range of the assay while minimizing the amount of each reagent used. The standard curve of this assay had a linear range typically in between 10 and 100 ng/mL and achieves saturating signal above 100 ng/mL (Figure 1D). Graphing the standard curve as a 4 parameter curve yields a sigmoidal curve that “flattens” below 10 ng/mL and above 100 ng/mL. The limit of detection for this assay, based on the standard curve, was approximately 1 ng/mL PRX302.

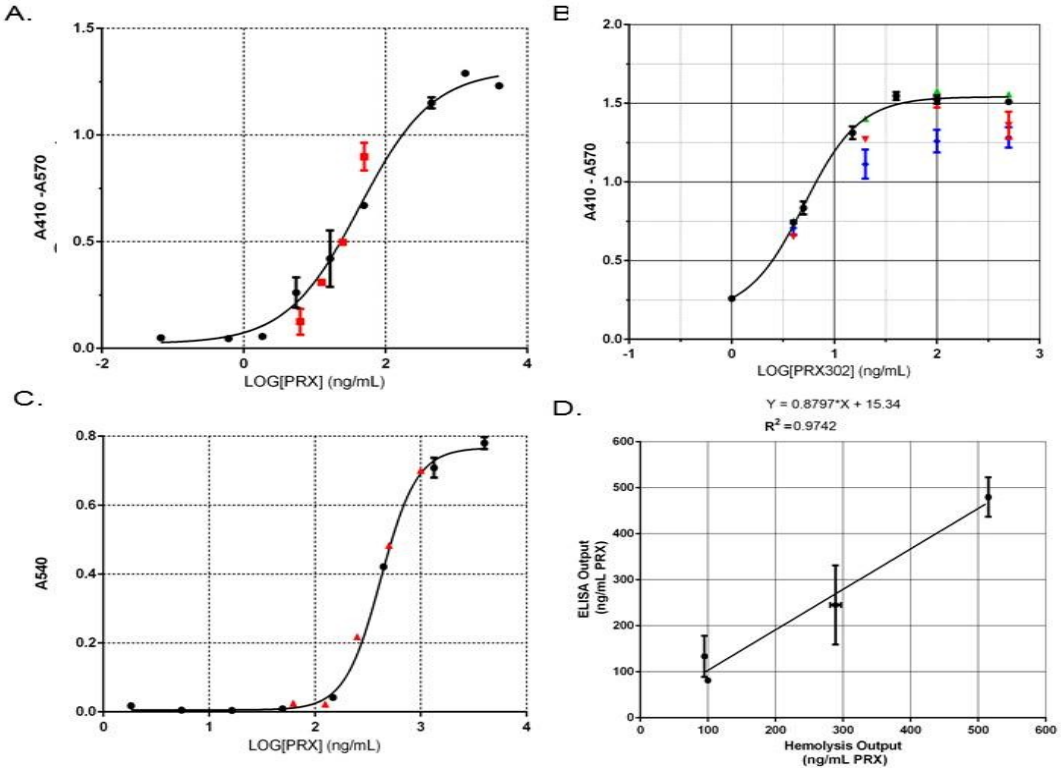

Figure 2: PRX302 Sandwich ELISA Validation. PRX302 standard curve (black) with independent parallel samples superimposed onto the curve (red) (A). PRX302 standard curve with independent parallel samples diluted in whole human plasma (blue) and serum-containing RMPI (B). Standard curve of a functional assay developed to independently validate PRX ELISA.. Independent points (red) were diluted and overlaid to show parallelism (C). Direct comparison of samples measured by PRX ELISA and functional hemolysis assay (D).

Typically, to validate an ELISA assay for a given analyte, independent samples of a known concentration are plotted on a standard curve generated on the same plate in order to show parallelism. We chose to dilute PRX302 1:2 from a starting concentration of 50 ng/mL, representing a large portion of the linear, and most dynamic range of our curve (Figure 2A). All points were superimposable on the curve with the exception of the 50 ng/mL dilution. In addition to assessing how independent samples in assay buffer behave, we performed a 'spike, recovery' assay in which PRX302 was diluted to a known concentration in either RPMI containing 10% FBS or 100% human plasma. This assay can be used to also determine if certain biological sample sources contain components that interfere with the assay's validity and at what concentration these effects can be mitigated. We observed almost no interference in the samples originally diluted in RPMI, as only the top 500 ng/mL point deviated from the standard curve (Figure 2B). All further dilutions (1:5 serially) were superimposable on the curve. For samples diluted in human plasma, there was a substantial decrease in signal observed in all dilutions above 1:125, as these samples had a dynamic range of approximately 80% of the standard curve.

Because our ELISA assay determines the concentration of total PRX302 in a solution and not functional drug, we used a hemolytic titer-based assay to calculate how much released pro-toxin was actually capable of killing cells. Briefly, this assay measures the release of hemoglobin from lysed erythrocytes in solution and, like the ELISA, is compared to a standard curve of known, fully functional PRX302. In this standard curve, we observe a 4 parameter sigmoidal relationship between the concentration of PRX302 in ng/mL and the percentage of total lysed erythrocytes compared to a detergent control (Figure 2C). The obtained standard curve had a limit of detection of approximately 100 ng/mL and was linear from 300 to 1000 ng/mL. Like the ELISA, we took independent

samples of known concentration and plotted it on our standard curve to show parallelism. All diluted samples were superimposable on the standard curve within the standard error. We then plotted samples which were diluted 1:2 from 500 ng/mL and calculated using the ELISA and hemolytic assays independently in order to compare them directly. When plotted, we observe a linear relationship between each sample set on each assay with a slope of 0.83. (Figure 2D). The hemolytic assay deviated from the trend at the lowest sample which had a concentration of 62.5 ng/mL.

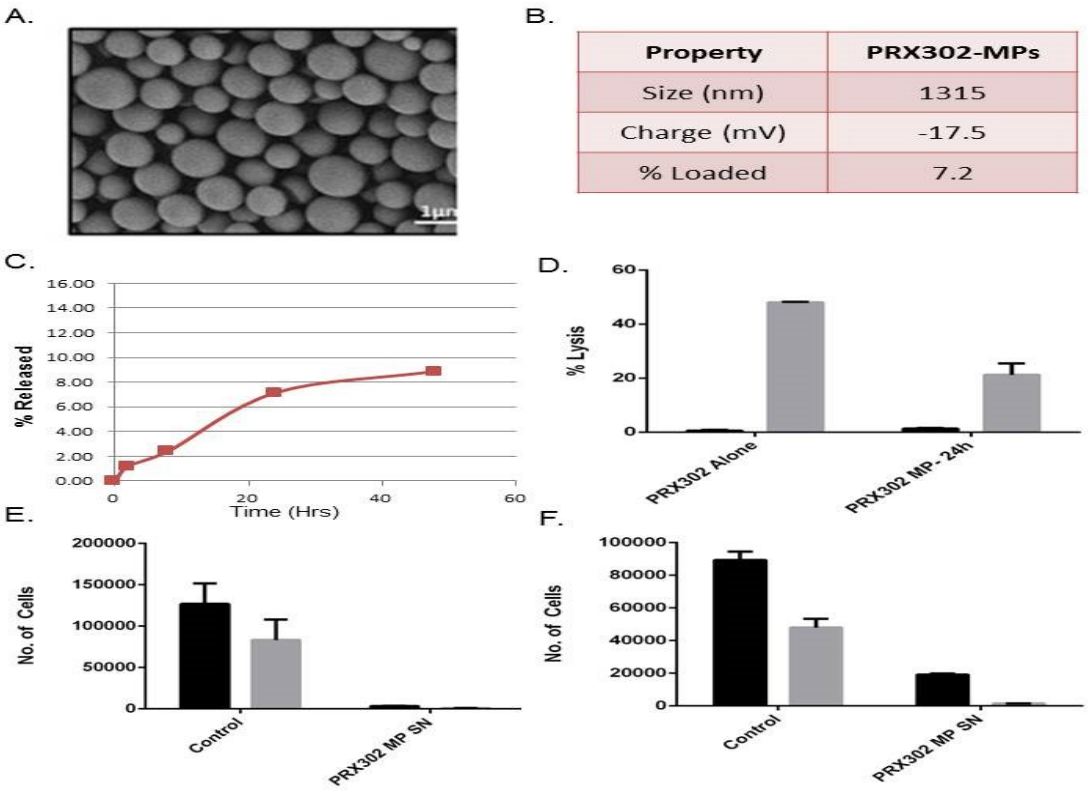

Figure 3: Characterization of PRX302 PLGA MPs. Electron micrograph of G114 loaded PLGA MPs from Levy et al. (A). Table depicting the properties of PRX302-loaded MPs (B). Release of PRX302 from 1 mg/mL MPs in solution over 2 days represented as % of total cargo released (D). Red blood cell lysis assay of either PRX302 alone or PRX302 MP supernatants with (grey) or without (black) PSA present (D). Viability of LNCaP (E) or DU145 (F) cells incubated for 48 hours with or without PRX302 MP supernatant and with (grey) or without (black) PSA.

We successfully encapsulated PRX302 into PLGA microspheres using the protocol as shown by Levy et al to encapsulate the pro-drug G114 in these polymers. Based off this study in which those MPs were of similar size, we expect the PRX302 loaded microspheres to physically resemble the G114 loaded material (Figure 3A). These MPs had an average size of roughly 1-2 microns and a loading efficiency of 7.1% (Figure 3B). Following two, five minute washes in saline, we observe roughly 10% of encapsulated PRX302 released over a period of 48 hours (Figure 3C) which seems to have plateaued as compared to the initial release kinetics over the first few hours. Released PRX302 MP supernatant lysed red blood cells to a similar degree as PRX302 diluted to the same concentration of 50 nM (concentration of supernatant determined from the ELISA) after 2 hours (Figure 3D). This supernatant, when diluted to a concentration of approximately 10 nM, killed LNCaP prostate cancer cells regardless of the presence of PSA (Figure 3E) while only affecting DU145 cells in the presence of PSA as measured by the MTT assay (Figure 3F).

Discussion

The major goal of this study is to develop a series of methods to assess the release of PRX302, a novel prostate targeted biologic pro-drug, from PLGA microspheres. In order to fully characterize the release and functionality of the molecule, we have developed two different bioassays to both determine the concentration of total and functional PRX302. The former assay, a homemade sandwich ELISA, utilized a monoclonal mouse antibody, deemed HG6, as a capture antibody and a rabbit polyclonal antibody, deemed MPC, as a detection antibody. We performed a series of optimization experiments in order to fully maximize the signal to noise ratio of this assay and to minimize reagent use. As the concentration of both antibody increased, we observed a robust increase in the dynamic range of the assay which eventually saturated. Based on these

experiments, we opted to use a concentration of 4 ug/mL HG6 and 5.5 ug/mL MPC. These concentrations were selected specifically due to the large dynamic range achieved while utilizing the smallest amount of material possible. The assay itself had a very robust signal to noise ratio with a linear range that spanned roughly an order of magnitude of PRX302 concentrations. All PRX302-containing samples in this study were diluted such that the concentration would fall in this range of the standard curve, thus ensuring for the most accurate determination of concentration possible. The other assay, a hemolytic functional assay, also allowed for the accurate determination of functional PRX302 in solution, however, this assay was much less sensitive and depended on the sample containing functional drug.

Before using our ELISA to determine the concentration of PRX302 released into solution, we validated this method via showing sample parallelism in a variety of biological samples. Specifically, samples were diluted to known concentrations in assay diluent, media with 10% FBS, and human plasma. Samples diluted in PBS with BSA and plotted onto the standard curve independently were mostly superimposable on the curve suggesting the assay is internally reproducible. Very little change in signal was observed in media with FBS suggesting the components of the solution are compatible with the assay and a dilution of 5 fold or more in assay buffer is suitable. We observed a substantial drop in signal when plasma was used. This is to be expected given the much higher concentration of total protein and other biological components that could interfere with the assay. We observe an accurate measurement of PRX302 in human plasma after a 125 fold dilution of the sample suggesting the responsible components that interfere with this assay are at a concentration compatible with accurate measurement of the pro-drug concentration at this concentration. We recommend that all samples that

are obtained from mammalian samples such as whole blood or plasma be diluted at least 125 fold in sample buffer in order for any measurements to be reliable.

We next validated our functional assay and compared it directly to the ELISA. This assay utilized the lysis of living, intact, human red blood cells and measured the release of soluble hemoglobin into the supernatant. By using a dose response curve of PRX302 vs total lysis, we can accurately and independently measure the concentration of this drug as a function of cell lysis and assess how much released PRX302 is functional. Red blood cells were selected for this assay as they are incapable of repairing aerolysin-induced plasma membrane damage and their release of a robust chromophore upon lysing. As we increased PRX302 concentration in this experiment, we observed a saturable dose-dependent increase in RBC lysis with an EC50 of approximately 500 ng/mL (10 nM) PRX302 after a 2 hour pre-incubation with PSA and a 2 hour exposure to the erythrocytes. This assay had a limit of detection of roughly 100 ng/mL PRX302 which, in comparison with the sandwich ELISA, is much less sensitive despite being simpler and more direct. When compared directly with the ELISA, we observed a linear relationship of samples above 100 ng/mL strongly suggesting that the hemolysis assay is capable of accurately measuring total protein assuming 100% of the protein is functional. This result also validates the hypothesis that the sandwich ELISA is capable of detecting all functional PRX302 in a sample. This side by side comparison will allow us to quantitate how much of the PRX302 protein is capable of killing PSA-expressing cells once released from the PLGA MPs.

We were pleased to trivially produce microspheres loaded with purified PRX302. These particles, being roughly 1-2 microns in diameter on average, are the desirable size for MSC internalization based on previously characterized properties of cell uptake (8, 17). The release of this material from these particles was then tracked over the course of 48

hours in which we observed roughly 10% of the protein cargo loaded was released into the supernatant. These rates are comparable to other proteins loaded in PLGA MPs and suggest that PRX302 can be used in this platform with relative ease. We were also pleased to observe that our assay was predictive of the concentration of PRX302, as our expected concentration of PRX302 determined by the ELISA was consistent with the published functional concentrations of this molecule on erythrocytes as well as LNCaP and DU145 prostate cancer cells. Released PRX302 also had no activity on RBCs until PSA was present strongly suggesting that the material released was completely intact, contained its C-terminal inhibitory piece, and would be non-toxic to cells not producing PSA *in vivo.* Because we did not observe the same amount of lysis as PRX302 at the same protein concentration, we expect that some portion of released material was not fully functional possibly due to aggregation or denaturing of the protein upon release. On LNCaP prostate cancer cells that produce some enzymatically active PSA *in vitro,* PRX302 MP supernatant grossly affected viability regardless or not if PSA was exogenously added suggesting that the PSA secreted by these cells activated the toxin enough to be functional. For the DU145 cells, we did observe some toxicity of the supernatant when no PSA was present. This suggests that, because DU145s do not produce any PSA, other proteases present on the cells were able to process the toxin and activate it to a degree. While surprising, PRX302 was shown to be functional at higher doses on non-PSA producing cells likely for this reason (13). Regardless, we were encouraged to see that PRX302, following release from these microspheres, was toxic to different cell lines in a PSA-specific manner and released from the microparticles at reasonable rates.

This work demonstrates two successful proofs of principles. The first is the development of a sensitive and robust biochemical assay to accurately detect the release of a novel

prostate-targeted biologic from PLGA microspheres. This tool will allow us to further develop other novel therapeutic platforms using this protein, study its pharmacokinetic properties further *in vivo*, and further improve on our loaded microparticle design and optimization. Second, we were able to show PRX302 being released from these particles at reasonable concentrations over a period of time consistent with their internalization into MSCs and that this pro-drug retained a majority of its activity and still required proteolytic processing and activation in order to be cytotoxic. Now that this system has been developed and the necessary assays optimized, we can further utilize this strategy to determine its potential as a novel and effective method to selectively deliver pro-drugs to prostate-derived tumors for therapeutic purposes. This work also demonstrates a methodical approach to developing a therapeutic platform and understanding the intricacies to novel technologies used to address human health-related challenges.

References

1. Antibody therapy of cancer. Nature Reviews Cancer. 2012;12(4):278.
2. Hines DJ, Kaplan DL. Poly(lactic-co-glycolic) acid-controlled-release systems: experimental and modeling insights. Crit Rev Ther Drug Carrier Syst. 2013;30(3):257-76.
3. Crotts G and Park TG (1998) Protein delivery from poly(lactic-coglycolic acid) biodegradable microspheres: Release kinetics and stability issues, Journal of Microencapsulation, 15:6, 699-713
4. Sanders LM, McRae GI, Vitale KM, Kell BK. Controlled delivery of an LHRH analogue from biodegradable injectable microspheres. Journal of Controlled Release. 2:187.
5. Jung Y, Kim JK, Shiozawa Y, et al. Recruitment of Mesenchymal Stem Cells Into Prostate Tumors Promotes Metastasis. Nature communications. 2013;4:1795.
6. Cheng J, Yang K, Zhang Q, et al. The role of mesenchymal stem cells in promoting the transformation of androgen-dependent human prostate cancer cells into androgen-independent manner. Scientific Reports. 2016;6:16993.
7. Mognetti B, Montagna GL, Perrelli MG, Pagliaro P, Penna C. Bone marrow mesenchymal stem cells increase motility of prostate cancer cells via production of stromal cell-derived factor-1α. Journal of Cellular and Molecular Medicine. 2013;17(2):287-292.
8. Ankrum JA, Miranda OR, Ng KS, Sarkar D, Xu C, Karp JM. Engineering cells with intracellular agent-loaded microparticles to control cell phenotype. Nat Protoc. 2014;9(2):233-45.
9. Buckley JT. The channel-forming toxin aerolysin. FEMS Microbiol Immunol. 1992;5(1-3):13-7.

10. Abrami L, Fivaz M, Decroly E, et al. The pore-forming toxin proaerolysin is activated by furin. J Biol Chem. 1998;273(49):32656-61.
11. Lebeau AM, Singh P, Isaacs JT, Denmeade SR. Prostate-specific antigen is a "chymotrypsin-like" serine protease with unique P1 substrate specificity. Biochemistry. 2009;48(15):3490-6.
12. Denmeade SR, Sokoll LJ, Chan DW, Khan SR, Isaacs JT. Concentration of enzymatically active prostate-specific antigen (PSA) in the extracellular fluid of primary human prostate cancers and human prostate cancer xenograft models. Prostate. 2001;48(1):1-6.
13. Williams SA, Merchant RF, Garrett-mayer E, Isaacs JT, Buckley JT, Denmeade SR. A prostate-specific antigen-activated channel-forming toxin as therapy for prostatic disease. J Natl Cancer Inst. 2007;99(5):376-85.
14. Abrami L, Fivaz M, Glauser P-E, Parton RG, van der Goot F. A Pore-forming Toxin Interacts with a GPI-anchored Protein and Causes Vacuolation of the Endoplasmic Reticulum. The Journal of Cell Biology. 1998;140(3):525-540.
15. Denmeade SR, Egerdie B, Steinhoff G, Merchant R, Abi-Habib R, Pommerville P. Phase 1 and 2 Studies Demonstrate the Safety and Efficacy of Intraprostatic Injection of PRX302 for the Targeted Treatment of Lower Urinary Tract Symptoms Secondary to Benign Prostatic Hyperplasia. European urology. 2011;59(5):747-754.
16. Levy O, Brennen WN, Han E, et al. A prodrug-doped cellular Trojan Horse for the potential treatment of prostate cancer. Biomaterials. 2016;91:140-50.
17. D. Sarkar, J.a. Ankrum, G.S.L. Teo, C.V. Carman, J.M. Karp. Cellular and extracellular programming of cell fate through engineered intracrine-, paracrine-, and endocrine-like mechanisms. Biomaterials, 32 (2011), pp. 3053–3061.

Chapter 3: PSA-Activated Serine Proteases as a Novel Therapeutic Strategy to Target Prostate Cancer

Abstract:

Prostate cancer is the most diagnosed malignancy in American men and the second leading cause of cancer-related death. Patients succumbing to the disease primarily suffer from metastatic cancers as opposed to localized disease. Currently, treatments for metastatic prostate cancer are largely palliative and fail to substantially improve patient lifespan. Thus, new innovative therapies are needed to target metastatic tumors. Prostate Specific Antigen (PSA) is a chymotrypsin-like serine protease secreted by both normal and cancerous prostate epithelial cells. Our lab has characterized PSA's enzymatic activity to be specific for the stroma of tumors despite reasonable concentrations in circulation. PSA is, therefore, an attractive target for cancer-selective cytotoxic therapy due to its localized activity and unique substrate profile. Because a vast majority of prostate cancer cells grow slowly and exist in the G0 stage of the cell cycle at any given point, a proliferation-independent cytotoxic payload is preferred in this strategy. Recently, it was shown that the human protease Granzyme B (GZMB), at low micromolar concentrations, can cleave an array of extracellular matrix (ECM) proteins thus perturbing cell growth, signaling, motility, and integrity. It is also well established that other human proteases such as trypsin can induce similar effects. Because both enzymes require N-terminal proteolytic activation to be functional, we propose to synthesize and characterize PSA-activated zymogen mutants capable of being selectively activated in the tumor stroma and targeting these effects to prostate-derived tumors. In this study, we examine the enzymatic and cell targeting parameters of these drugs, described as EK-PSA-TRP and EK-PSA-GZMB. These pro-enzymes were activated robustly by PSA and induced ECM damage to cancer cells *in vitro* thus

supporting the potential use of this strategy as means to target metastatic prostate cancers.

Introduction

Every year, more than 220,000 American men are diagnosed with prostate cancer. Despite notable success in managing patients with localized disease, 30,000 men will ultimately succumb to prostate cancer this year (1). A vast majority of these patients suffered from metastatic tumors as opposed to lesions located in the prostate exclusively. These tumors are usually resistant to most chemotherapeutic therapies and are able to evade the immune system following administration of therapy. Because metastatic prostate cancer (MPC) therapies only provide temporary relief from disease burden, it is vital that new, innovative therapeutic strategies are developed to combat this malignancy as stand-alone and adjuvant therapies.

Prostate-based malignancies are among the slowest growing of the solid tumors. Because a vast majority of tumor cells exist in the G0 phase of the cell cycle, traditional proliferation-dependent cytotoxic chemotherapy remains ineffective. Though docetaxel is currently approved to treat metastatic prostate cancer, it's mechanism of action depends on inhibiting localization of the Androgen Receptor via binding to microtubules (2). It is, therefore, essential that novel therapeutic strategies kill metastatic tumors in a proliferation-independent manner. Because most cytotoxic agents capable of killing non-proliferating cells are globally toxic to most tissue, converting these agents into therapeutics is dependent on the ability to regulate their activity to the tumor microenvironment.

Prostate-specific Antigen (PSA) is a secreted chymotrypsin-like serine protease expressed by both cancerous and non-cancerous prostate epithelial cells (3,4). PSA, most notably, has been characterized as a marker for prostate cancer progression due to its presence in the bloodstream in patients with viable tumors. Despite this, PSA is not

enzymatically active in the bloodstream of patients with localized or distal disease due to the presence of the serum protease inhibitors α-1-antichymotrypsin and α-2-macrglobulin which form covalent complexes with the enzyme (5, 6). Because of PSA's high expression and enzymatic activity in the stroma of prostate-derived tumors, including MPC, and the fact that it is rapidly inactivated in the bloodstream, PSA is an attractive target for a pro-drug based therapeutic strategy in which a proliferation-independent cytotoxin would be cleaved and activated selectively in the extracellular space of a tumor cell. One major benefit to this strategy is that not every cell in the microenvironment would need to express PSA in order to be targeted. This, so called, "field effect" is an interesting principle for MPC therapeutic strategies, as the pro-drug agent would target a highly heterogeneous tumor microenvironment and not only kill tumor cells but adjacent tumor-supporting stromal cells. In order to design efficient and selective protein and peptide sequences for PSA, our lab characterized PSA's ability to cleave various florescent substrates vs. other common proteases in circulation. This study showed that selective, efficiently-hydrolyzed substrates can be generated and that PSA prefers peptide substrates varying from four to seven amino acids in length that contain at least one serine upstream of the cleavage site (7). Given this substrate profile, our lab has generated several PSA-activated pro-drugs that kill cells only in the presence of enzymatically active PSA.

Granzyme B (GZMB), like PSA, is a secreted serine protease expressed by activated Cytotoxic T-Lymphocytes (CTLs) (8). When co-secreted into the immune synapse along with pore-forming proteins such as perforin, GZMB can translocate into the target cell cytoplasm, cleave and activate pro-apoptotic factors, and induce target cell death. Intracellular-substrates of GZMB include members of the caspase family, ICAD, BCL-2 and related proteins, and several pro-mitotic factors (9). Recently, GZMB was shown to

be able to degrade various components of the extracellular matrix (ECM) at high-nanomolar concentrations (10, 11, 12). This extra-cellular mechanism of GZMB was shown to induce anoikis of surrounding cells, decrease cell motility, and even potentially act as a pro-inflammatory cytokine. Interestingly, GZMB has been shown to be resistant to inhibition by protease inhibitors in serum suggesting it has long-acting effects *in vivo* (13). Upon trafficking to the secretory granule of the CTL, GZMB must be cleaved and activated on the N-terminus by Cathepsin C in order to be functional (14, 15). Another human protease, cationic trypsin (TRP), has been well characterized to cleave ECM components at similar doses as GZMB. TRP, also like GZMB, is expressed in an inactive confirmation with a N-terminal pro-piece, DDDDK, a substrate for the activating protease, enterokinase (EK) (16, 17). Because both GZMB and TRP have extracellular effects on human cells *in vitro* and have well characterized pro-forms activated by serine proteases, they are interesting candidates as potential prostate-targeting PSA-activated pro-drugs.

Recently, a method of mammalian-based expression system for human GZMB was established. Gerhmann et al. developed a rapid, efficient system in which GZMB can be expressed in milligram quantities by transiently transfecting HEK-293T cells. In order to minimize toxicity to cells expressing the protein, GZMB was expressed with a non-native enterokinase (EK) substrate (DDDDK) immediately upstream of Isoleucine 1 (the first AA of active GZMB) (18). This yielded an EK-activated GZMB mutant which was catalytically nonfunctional until incubation with active EK enzyme. Based on this work, we hypothesized that the insertion of a high-efficiency PSA substrate between I1 of GZMB and the EK peptide would yield an efficiently-cleaved PSA-activated mutant (EK-PSA-GZMB). Because human trypsinogen 1 (TRP) is non-specifically toxic to most cell types and is natively activated by EK on its N-terminus, we also postulated that using

this strategy would also yield an efficiently-cleaved PSA-activated mutant of trypsinogen (EK-PSA-TRP). In this study, we evaluate the enzymologic and pharmacologic properties of both PSA-activated proteins *in vitro*.

Materials and Methods

Design of PSA-activated GZMB and TRP proteins

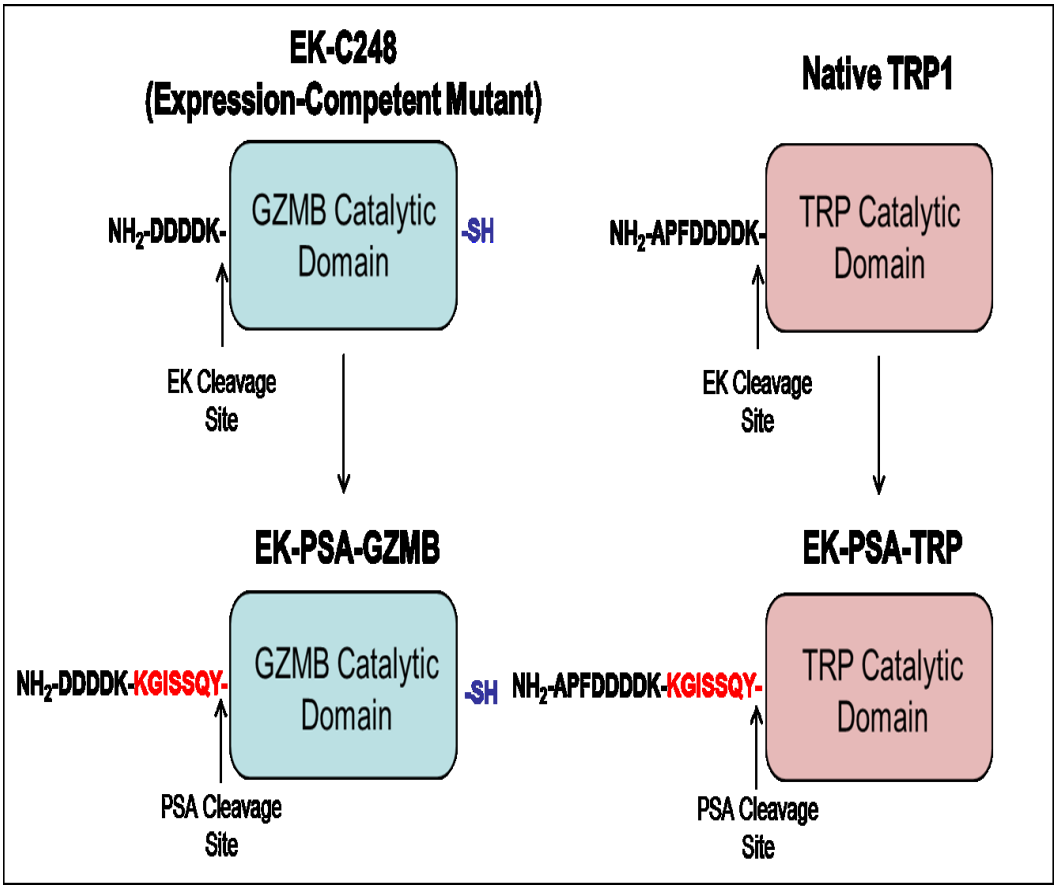

Figure 1: Schematic of EK-PSA-GZMB and EK-PSA-TRP pro-drugs. Mutations made to convert EK-activated GZMB into a PSA-activated zymogen (left) and WT Trypsin into a PSA-activated zymogen (right)

In order to synthesize constructs for both PSA-activated proteins, careful consideration should be made as to the locus of the PSA substrate and the substrate itself. Because serine protease perturbation of ECM proteins requires higher concentrations of active

enzyme, we chose the efficiently-cleaved, less specific PSA substrate KGISSQY. This peptide was inserted in between the inhibitory EK peptide DDDDK and the N-terminal Isoleucine residue of both proteins. Thus, hydrolysis by PSA of either EK-PSA-GZMB or EK-PSA-TRP by PSA would yield exclusively the active GZMB and TRP enzymes. For EK-PSA-GZMB a chemically conjugatable mutant containing a C-terminal reactive cysteine was used should a targeting moiety need to be added to enhance toxicity of the protein. This mutant had no effect on GZMB expression or catalytic activity (data not shown). Because EK natively activates TRP, we chose to leave the native APF tripeptide as the N-terminus of EK-PSA-TRP. Figure 1 depicts this strategy.

Cloning and mutagenesis of GZMB and TRP constructs

In order to express hGZMB in reasonable amounts using a mammalian expression system, the EK-C248 gene was first constructed. To do this, the WT GZMB gene (Origene Plasmid SC321693) was amplified out of the respective vector, altered to contain the C-terminal cysteine, and flanked with EcoR1 restriction site and upstream vector sequence with the primer set F: CAGTGTGGTGGAATTCATGCAACCAATCCTGCTTC R: GATATCTGCAGAATTCTTAGTAGCGTTTCATGGTTTT. PCR was run using Accuprime Pfx Supermix (Thermo 12344-040) enzyme mix and run according to manufacturer's instructions with a Tm of 53°C. PCR product was purified on a 1.5% agarose gel after running at 100V for 45 minutes, excised, and isolated using a NucleoSpin Gel and PCR clean up kit (Machery-Nagel 740609). For transient expression in HEK-293T cells, WT GZMB-C248 (Eco R1) was inserted into the vector pcDNA 3.1 (+) (Thermo V790-20) using an InFusion HD Cloning kit (CloneTech 638909). The resulting gene-containing plasmid insert was then transformed into Stellar Competent *E. Coli* (CloneTech 636763)

according to manufacturer's instructions. Colonies were picked, grown in 5mL LB containing 100 µg/mL Ampicillin for 8 hours, and expanded in 50mL LB containing 100 µg/mL. WT GZMB (pcDNA 3.1) was isolated using a PureLink® HiPure Plasmid Maxiprep Kit (K2100-06). DNA sequencing was performed using Sanger sequencing (T7 sequencing primer) via the Johns Hopkins Sequencing and Synthesis facility.

Because WT GZMB is toxic to HEK-293T cells, the protein must be expressed in an inactive conformation capable of being rapidly activated via proteolysis once expressed. For this reason, the native GE inhibitory di-peptide was replaced by an enterokinase cleavage site (as seen above). To mutate this cleavage site, GZMB-C248 (pcDNA3.1) was added to a Q5 Site Directed Mutagenesis (NEB E0554S) kit containing the primers F: CGACAAAATCATCGGGGGACATGAGG R: TCGTCGTCTGCATCTGCCCTGGGCAG. The reaction was run according to manufacturer's instructions with a Tm of 67°C and an extension time of 210 seconds. PCR product from this reaction was confirmed on a 1.5% agarose gel, ligated using the Q5 kit KLD enzyme mix, and transformed into NEB5α *E. Coli* according to manufacturer's instructions. EK-C248 (pcDNA3.1) was amplified, purified, and sequenced as described above. To convert this protein into a PSA-activated pro-drug, the PSA substrate KGISSQY was inserted between the DDDDK EK peptide and the active sequence of GZMB. Using the mutagenesis primers F: CTCTCAGTACATCATCGGGGGACATGAG R: GAGATTCCTTTTTTGTCGTCGTCGTCTGC, the plasmid EK-PSA-GZMB (pcDNA 3.1) was generated using the aforementioned mutagenesis protocol with a Tm of 64°C. The plasmid was amplified, harvested, and sequenced as mentioned above. In order to make a mutant lacking the DDDDK piece but with a PSA substrate on the N-terminus (PSA-GZMB), we utilized the above mutagenesis protocol (EK-C248 pcDNA3.1 as a template)

with the primer set F: AGGAATCTCCTCTCAGTACATCATCGGGGGACATGAGG R: TTATGATGATGATGATGATGTGCATCTGCCCTGGGCAG with a Tm of 67 degrees Celsius.

To generate a plasmid containing the human PRSS1 gene containing the KGISSQY PSA substrate and a hexa-histidine purification tag, we first cloned the PRSS1 gene into pcDNA3.1. Using the InFusion protocol described above, we inserted flanking Eco RI restriction sites on the ends of the human PRSS1 gene (human cationic trypsin) (Human PRSS1 natural ORF mammalian expression plasmid, Sino Biological, HG10816-CH) using the primer set F: CAGTGTGGTGGAATTCATGAATCCACTCCTGATCC R: GATATCTGCAGAATTCTTAGCTATTGGCAGCTATGG and a Tm of 52 degrees Celsius and an extension time of 210 seconds while following the recommended InFusion cloning protocol. Plasmid was transformed, grown, and harvested as described above. Next, we performed mutagenesis using the NEB method above in order to insert the KGISSQY sequence and a C-terminal Histidine tag. To insert the PSA sequence, the primer set F: CTCTCAGTACATCGTTGGGGGCTACAAC R: GAGATTCCTTTCTTGTCATCATCATCAAAGGG was used with a melting temperature of 61 degrees Celsius. For the mutagenesis respective to the Histidine tag, the set F: CACCACCATTAAGAATTCTGCAGATATCCAG R: GTGATGATGGCTATTGGCAGCTATGGTG and a Tm of 60 degrees Celsius was used. Lastly, to make a TRP mutant lacking the native EK piece but containing a PSA activation sequence (PSA-TRP) we mutagenized the EK-PSA-TRP pcDNA3.1 plasmid by deleting the DDDDK peptide. This was done using the primer set F: AAAGGAATCTCCTCTCAGTACATC R: AGCAAGAGCAGCTGCCAC with a Tm 64 degree Celsius. Like the GZMB constructs, all TRP mutants were sequenced using the Sanger method following isolation of the plasmid using a T7 promoter primer.

Expression of recombinant proteins in HEK293T cells

HEK293T cells (ATCC® CRL-3216) were grown in DMEM w/ high glucose, 10% Fetal Bovine Serum, and supplemental L-glutamine. For all constructs, 5 x 10^6 cells were plated in multiple T75 flasks and incubated for 48 hours at 37°C. To transiently transfect cultures, 25 µg of cDNA (per flask) was added to 1.2mL of OPTI-MEM low-serum media and mixed with 74 µL of FuGENE HD (Promega E2311). This mix was incubated for 10 minutes at room temperature, added to 20mL of DMEM media per T7, and incubated on cells overnight. To simplify the purification process, transfected cells were then washed once with 1X PBS (pH=7.4) and given serum-free, phenol-free DMEM w/ high glucose and L-glutamine. Cells were then incubated for at least 3 days. Supernatant was harvested before cell viability and attachment was compromised.

Purification of recombinant GZMB and TRP proteins

Once supernatant from transiently transfected HEK cells was collected, cell debris was removed from via centrifugation at 8000 x g for 10 minutes. The clarified media was then concentrated 20-fold using Amicon Ultra Centrifugation Filters (UFC901008) and mixed 1:1 with 1X PBS (pH = 7.4). For GZMB-based pro-drugs (including PSA-GZMB to keep impurities consistent), a cation exchange resin (Fractogel EMD SO_3^- Millipore 116882) was used to isolate the protein. Because GZMB has an unusually high pI of 9.5, the protein will bind a negatively charged column at a higher affinity at pH 7.4. For TRP based constructs, a Histidine binding Nickel resin was used (His-Select Ni Affinity Resin, Sigma P6611). The immobilized proteins were then washed with either 5mL of PBS or PBS containing 20mM Imidazole respectively three times. GZMB and TRP pro-drugs were then eluted using PBS containing either 1M NaCl or 300mM Imidazole respectively. Protein elution was tracked during this process using UV spectroscopy at

280 nm. Both constructs were then dialyzed to remove the components of the elution buffer and other small molecule contaminants. This was done by adding pooled fractions to a Slide-a-Lyzer Dialysis Cassette (MWCO 7K) (87722/87723) and dialyzing vs. PBS or PBS containing 1mM $CaCl_2$ respectively. Dialyses were done at 500 fold excess volume and 1000 fold excess volume for 4 hours and 24 hours respectively. Final protein concentrations were determined using A280.

PSA Activation and Protease assays

In order to assess PSA's ability to cleave, and activate both pro-drugs, both zymogen proteins were incubated with purified PSA (ABD Serotec 7820-0504). Specifically, PSA was added to a solution of EK-PSA-GZMB or EK-PSA-TRP in PBS to a final concentration of 0.01 mg/mL. This concentration was decided based upon the physiological concentrations of PSA in the prostate stroma determined by Denmeade et.al (5). All incubations were done at 37°C for the indicated time points. For Michaelis-Menten experiments, pre-incubations of EK-PSA-GZMB and EK-PSA-TRP with PSA were done overnight and 4 hours respectively.

In order to determine the enzymatic activity of GZMB and TRP-based constructs, specific peptide-based assays were used. For GZMB, a florescent based GZMB assay kit (Biovision K168-100) was used. The substrate, IETD-AFC, was diluted in assay buffer according to instructions and incubated with GZMB-containing samples for one hour at 37°C. Fluorescence was measured at 380 nm excitation and 500 nm emission wavelengths. Concentrations of AFC released were based off a standard curve of diluted AFC. For Michaelis-Menten kinetics of GZMB, a chromogenic substrate was used to measure catalytic activity of the protein. Specifically, Ac-IETD-pNA (AG Scientific G-

1085) was diluted in DMSO to a stock concentration of 25 mM and diluted to various concentrations. EK-PSA-GZMB solution was then added 1:1 and read at 405nm at various time points. For EK-PSA-TRP activity and kinetic experiments, z-GPR-pNA (Sigma C2276) was diluted in DMF to a concentration of 2 mM (for activity experiments) and mixed 1:1 with protein solutions or diluted several fold for Michaelis-Menten experiments. Solutions were read at 405nm after 15 min for activity assays and at various time points to determine kinetic parameters. For all assays, the extinction coefficient 13500 $M^{-1}cm^{-1}$ L was used to determine the concentration of released pNA. All readings were corrected to background florescence/absorbance. Activity readings are represented as amount of substrate process per minute per mg of enzyme added.

SDS PAGE and Western Blot Analysis

In order to confirm recombinant proteins were correctly sized, SDS PAGE was performed using a BioRad gel electrophoresis system. Samples containing recombinant EK-PSA-GZMB/TRP proteins were mixed 1:1 with 4X reducing SDS PAGE Sample Buffer and boiled for 5 minutes. Samples were then loaded and run at 150V until fully migrated. For protein staining, the gel was then washed 2-3 times with RO H_2O and stained for one hour with SimplyBlue Safe Stain solution (Thermo LC6060). To de-stain samples were washed in RO H_2O overnight. For Western Blotting, samples were run on a non-reducing gel and were transferred to PVDF Immuno-Blot membrane (BioRad 1620177) for 1 hour at 100V and incubated for one hour in TBST containing 5% milk. To monitor removal of the DDDDK peptide, an anti-DDDDK polyclonal antibody (Abcam 1162) was diluted to 1:5000 in TBST/milk and incubated with the membrane overnight at 4°C. The next day, the membrane was washed 5X with TBST and incubated with an anti-rabbit HRP-linked IgG (Cell Signaling #70762) diluted at 1:10000 in TBST/milk for one hour at 4°C. The blot was then washed 5X with TBST and incubated with

chemiluminescent substrate solution (Thermo 34077) diluted according to manufacturer's instructions. The blots were then developed at specified time points via an X-ray film processor.

Edman Degradation of EK-PSA-GZMB

In order to demonstrate site-specific cleavage and activation of EK-PSA-GZMB by PSA, EK-PSA-GZMB was treated with plus PSA or buffer as described above overnight at 37°C. Both samples were then run on an SDS PAGE gel and transferred to a PVDF membrane as described above. The blot was then dried at room temperature for an hour and stained with SimplyBlue stain to visualize proteins. Sample was then de-stained using a solution of methanol (40% v/v) and acetic acid (10% v/v). Bands corresponding to the molecular weight of EK-PSA-GZMB were cut and stored in 1.7mL microfuge tubes. Edman degradation was performed by the Johns Hopkins Sequencing and Synthesis facility. Analysis was done on the three most N-terminal amino acids for each sample.

Cell Culture, Viability, and Microscopy Experiments

All prostate cancer cells and stromal cell lines were grown in RPMI 1640 medium containing 10% FBS and supplemental L-glutamine. Because bovine serum protease inhibitors slow the activity of PSA and TRP *in vitro*, all experiments were done in serum-free conditions. In order to facilitate these conditions and maintain cell viability and growth, LNCaPs, and CWR22 Rv1 were plated on a 96 well plate pre-coated with FBS (100µL RPMI with 10% serum per well for 4 hours at 37°C) in phenol-free, serum-free RPMI 1640 with L-glutamine and B27 serum supplement (Thermo 17504). Cells were plated at 5000 cells per well unless stated otherwise. The next day, cells were treated with either 3000 or 500 nM of EK-PSA-GZMB and EK-PSA-TRP plus or minus PSA at a final concentration 0.005 mg/mL unless stated otherwise. Cells not treated with

recombinant protein were treated with the respective dialysis buffer. Cells were incubated until visual effects were prevalent or for 7 days at 37 degrees. For GZMB-attachment experiments, medium plus or minus 10% FBS and plus or minus 1μM GZMB. Solutions were then removed and cells were then plated in serum-free RPMI containing B27 and allowed to attach for 48 hours. To count the cells, the MTT assay was used. Specifically, 15μL of CellTiter 96 dye (Promega G4000) was added to each wells and incubated at 37°C for 4 hours. Stop solution was then added to each well at a volume of 100μL. Cells were then shaken for at least an hour at room temperature. The assay was read as the difference between absorbances at 570 and 650 nm. Cell number was calculated based off a standard curve for each cell line. To demonstrate altered cell morphology, cells were photographed using a Nikon TE200 fluorescence microscope with the Metamorph software package at indicated magnifications.

Results

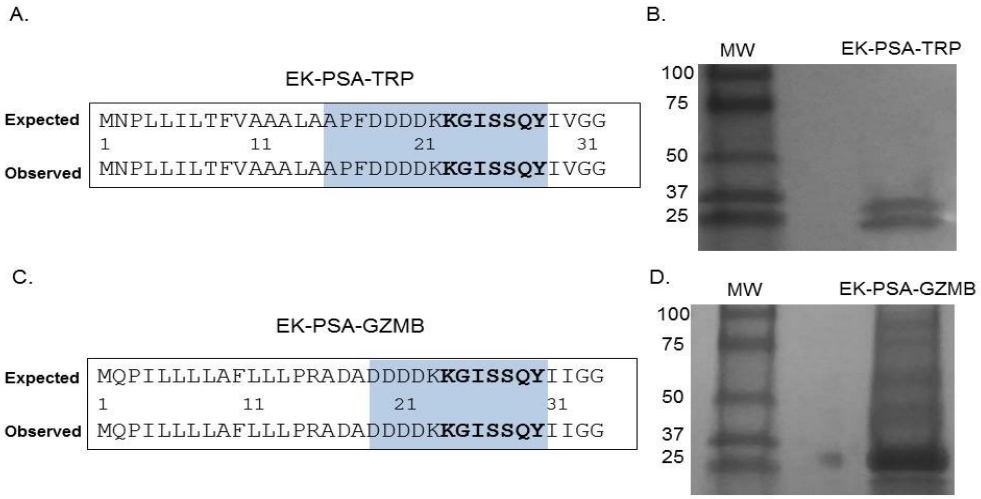

Figure 2 Cloning and Expression of PSA-Activated TRP and GZMB. Sanger DNA sequencing results of the mutated N-terminus of both EK-PSA-TRP (A) and EK-PSA-GZMB (C) genes. CBB-stained reducing SDS-PAGE gels with EK-PSA-TRP (B) and EK-PSA-GZMB (D).

To ensure all pro-drug enzymes were mutated correctly, we performed Sanger sequencing on both the PSA-activated TRP and GZMB genes. DNA sequencing analysis confirmed that both proteins contained an inserted KGISSQY PSA cut site immediately flanked by their respective catalytic domains and the inhibitory EK peptide (Figure 2A & 2C). For both mutants lacking their respective EK peptides, Sanger sequencing showed the successful removal of these residues thus yielding N-termini beginning with the KGISSQY substrate (data not shown). SDS PAGE analysis showed that both protein constructs were relatively pure following extraction from cell supernatant and further purification. EK-PSA-TRP protein when run under reducing conditions yielded two bands at 25 and 28 kDa (Figure 2B) while the GZMB mutant ran as a single band at 28 kDa (Figure 2D). Under non-reducing conditions EK-PSA-GZMB will run as both a monomer and a di-sulfide linked dimer (data not shown). Average yield was approximately 0.25 mg of EK-PSA-GZMB and 0.05 mg per flask of cells. It should also be noted that we obtained much lower expression yields for both PSA-activated protease mutants lacking the EK piece (referred to as PSA-TRP and PSA-GZMB). Yields did not improve when using NiNTA chromatography on PSA-GZMB despite it being cloned with a N-terminal His tag.

Following expression, harvesting, and NiNTA purification, we examined the enzymatic characteristics of the EK-PSA-TRP protein. Using a trypsin-specific chromogenic assay, we pre-incubated the drug plus or minus enzymatically active PSA. Both PSA and EK-PSA-TRP alone were unable to cleave the GPR-pNA substrate. Once pre-incubated together, we observed a steady increase in hydrolysis that stabilized after roughly 4 hours (Figure 3A). Western blotting of these mixtures using an antibody specific for the enterokinase substrate peptide on the N-terminus showed the uncleaved protein (running at both 25 and 28 kDa) with no PSA present. This signal was removed after a 4

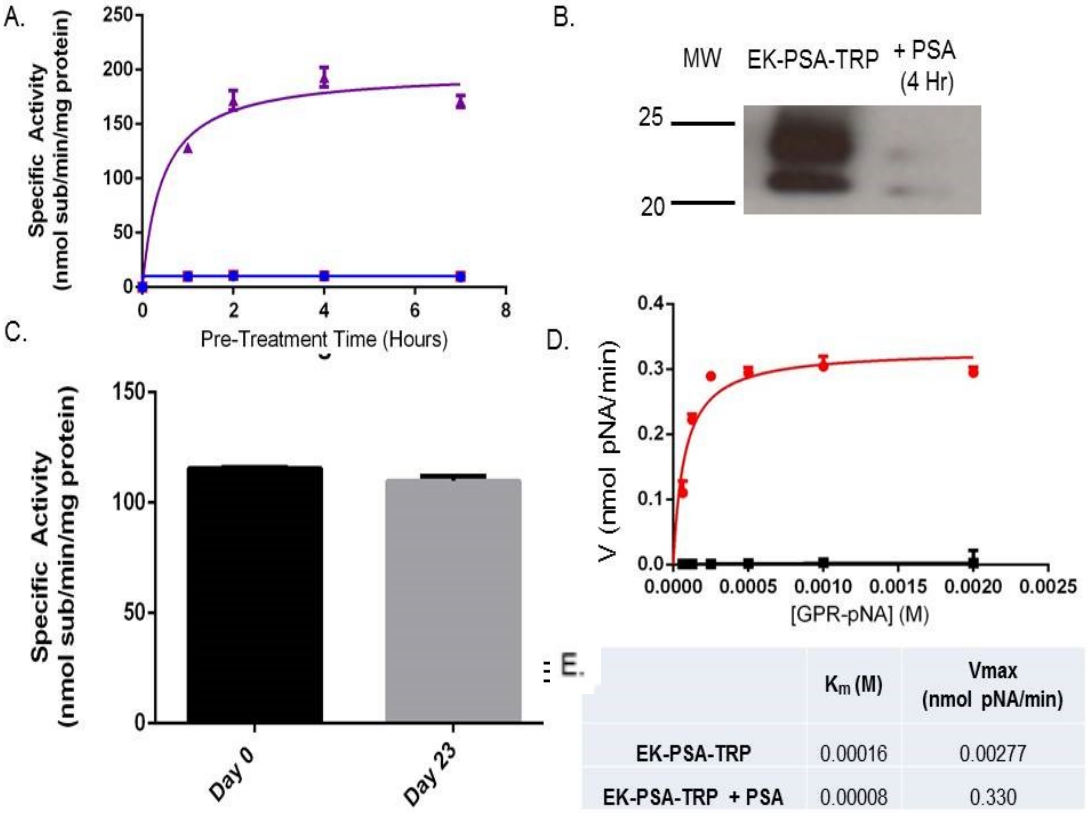

	K_m (M)	Vmax (nmol pNA/min)
EK-PSA-TRP	0.00016	0.00277
EK-PSA-TRP + PSA	0.00008	0.330

Figure 3: EK-PSA-TRP is a PSA-activated Trypsin mutant. Enzymatic hydrolysis of GPR-pNA by EK-PSA-TRP (red), PSA, (blue), and EK-PSA-TRP mixed with PSA (purple) pre-incubated for various times (A). Western blot analysis of EK-PSA-TRP +/- PSA probed with an anti-DDDDK rabbit polyclonal antibody (B). Enzymatic activity of EK-PSA-TRP incubated for 0 or 23 days at 37 degrees after being pre-exposed to PSA (C). Michaelis-Menten enzyme kinetics of EK-PSA-TRP (black) or EK-PSA-TRP with PSA (red) (D). Calculated enzymatic parameters of inactive and activated EK-PSA-TRP (E).

hour incubation with PSA (Figure 3B). Using the GPR-pNA release assay, we assessed the stability of this drug after a 4 hour pre-incubation with PSA. We observe no substantial loss of activity after a 23 day incubation at 37 degrees Celsius compared with Day 0 (Figure 3C). Velocity experiments confirmed that the active EK-PSA-TRP mutant displays classical Michaelis-Menten enzyme kinetics with linear changes in velocity below 500 uM substrate (Figure 3D). While there is some baseline activity of EK-PSA-TRP the Vmax between the PSA-treated and non-treated differ by almost 120-fold while the Km values were not notably different (Figure 3E).

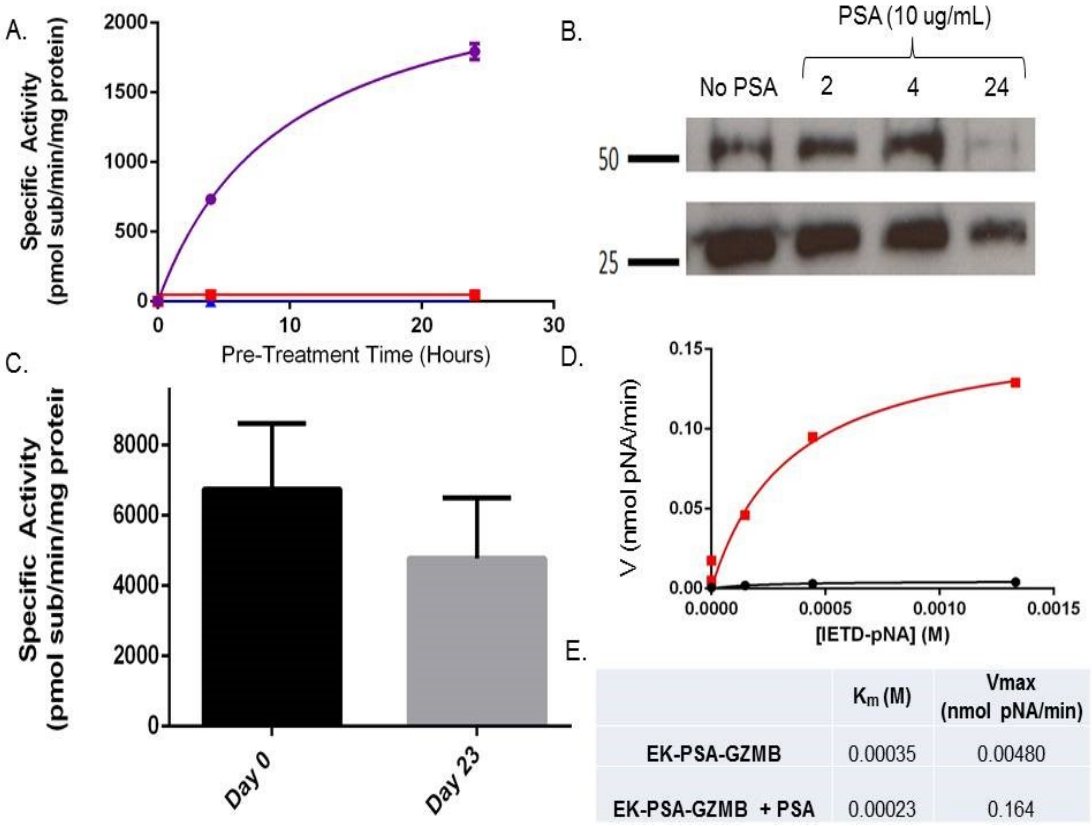

	K_m (M)	Vmax (nmol pNA/min)
EK-PSA-GZMB	0.00035	0.00480
EK-PSA-GZMB + PSA	0.00023	0.164

Figure 4: EK-GZMB-GZMB is a PSA-activated Granzyme B mutant. Enzymatic hydrolysis of IETD-AFC by EK-PSA-GZMB (red), PSA (blue), and EK-PSA-TRP mixed with PSA (purple) pre-incubated for various times (A). Western blot analysis of EK-PSA-GZMB +/- PSA probed with an anti-DDDDK rabbit polyclonal antibody (B). Enzymatic activity of EK-PSA-GZMB incubated for 23 days at 37 degrees after being pre-exposed to PSA (C). Michaelis-Menten enzyme kinetics of EK-PSA-GZMB (black) or EK-PSA-TRP with PSA (red) (D). Calculated enzymatic parameters of inactive and activated EK-PSA-GZMB (E).

Like the EK-PSA-TRP protein, we also aimed to evaluate the enzymatic activity of EK-PSA-GZMB in terms of activation kinetics, stability, and catalytic kinetics. Using a florescent substrate for GZMB, IETD-AFC, we assessed the activity of EK-PSA-GZMB with or without PSA pre-treatment following various pre-incubation times. Similar to the EK-PSA-TRP, the EK-PSA-GZMB had very low to no activity in this assay as well as the

sample containing PSA by itself (Figure 4A). However, PSA-treated EK-PSA-GZMB showed robust enzymatic processing of the substrate which seemed to plateau at 24 hours. Western Blotting the PSA treated EK-PSA-GZMB reactions using non-reducing conditions showed a decrease on both monomer and dimer bands of the protein with a vast majority of the signal removed after 24 hours (Figure 4B). Stability studies of activated EK-PSA-GZMB showed that like the EK-PSA-TRP protein, the enzyme retained most of its activity after 23 days at 37 degrees (Figure 4C). Following an overnight incubation with PSA, we observed an obvious difference in the baseline Vmax

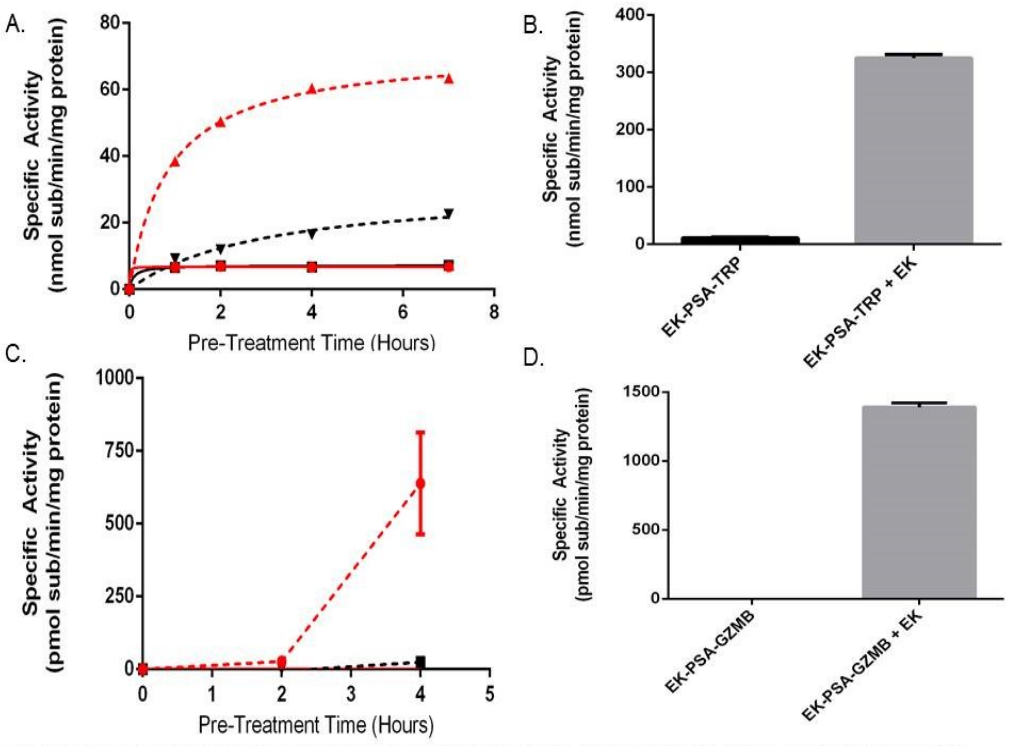

Figure 5: The N-terminal EK piece both stabilizes and inhibits EK-PSA-TRP and EK-PSA-GZMB. Enzymatic activity of pre-incubated EK-PSA-TRP + PSA (red dashed), PSA-TRP + PSA (black dashed), EK-PSA-TRP alone (red solid), and PSA-TRP alone (black solid) (A). Enzymatic activity of EK-PSA-TRP +/- a 4 hour EK treatment (B). Enzymatic activity of pre-incubated EK-PSA-GZMB + PSA (red dashed), PSA-GZMB + PSA (black dashed), EK-PSA-GZMB alone (red solid), and PSA-GZMB alone (black solid) (C). Enzymatic activity of EK-PSA-GZMB +/- a 4 hour EK treatment (D).

of the “inactive” EK-PSA-GZMB as opposed to the sample treated with PSA for the substrate IETD-pNA. Like EK-PSA-TRP, the enzyme’s linear change in velocity was observed at concentrations less than 0.5mM substrate. When comparing the baseline inactive species and the species that was incubated with PSA, we see a 30 fold increase in Vmax with relatively no difference in Km (Figure 4E). To confirm PSA cleavage was occurring at the desired locus on the protein, we isolated digested EK-PSA-GZMB and performed Edman degradation. N-terminal analysis of the protein confirmed that the residues I-I-G were the first three amino acids of the protein (data not shown) consistent with that of the active enzyme.

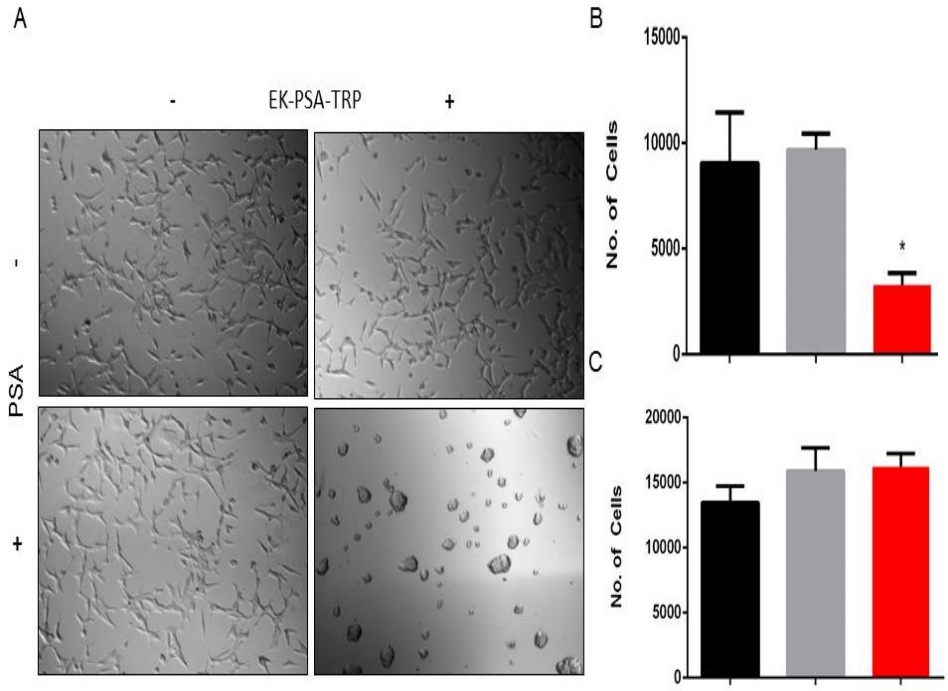

Figure 6: EK-PSA-TRP inhibits LNCaP cell growth selectively in the presence of PSA. Light microscopy images of LNCaP cells treated +/- 500 nM EK-PSA-TRP and +/- PSA at 10X magnification (A). MTT assay of LNCaP (B) or DU145 (C) cells treated with PSA (black), EK-PSA-TRP (grey) or both (red) for 7 days.

In order to more completely understand the mechanism behind the mutations made to modify the zymogen activation of TRP and GZMB, we removed the EK piece from each protein (native TRP and EK-GZMB) and inserted the PSA-activated substrate KGISSQY yielding mutants deemed PSA-TRP and PSA-GZMB. Activation kinetic assays with PSA-TRP and EK-PSA-TRP showed activation of both proteins following a four hour PSA incubation, however, EK-PSA-TRP was approximately 4 fold more active when comparing the specific activity (Figure 5A). For EK-PSA-GZMB and PSA-GZMB we observed a similar trend, in that the mutant containing the EK piece was robustly more active than the mutant lacking it (Figure 5A & 5C). In the case of GZMB, the PSA-GZMB species had no detectable activity compared to the somewhat active PSA-TRP. Both

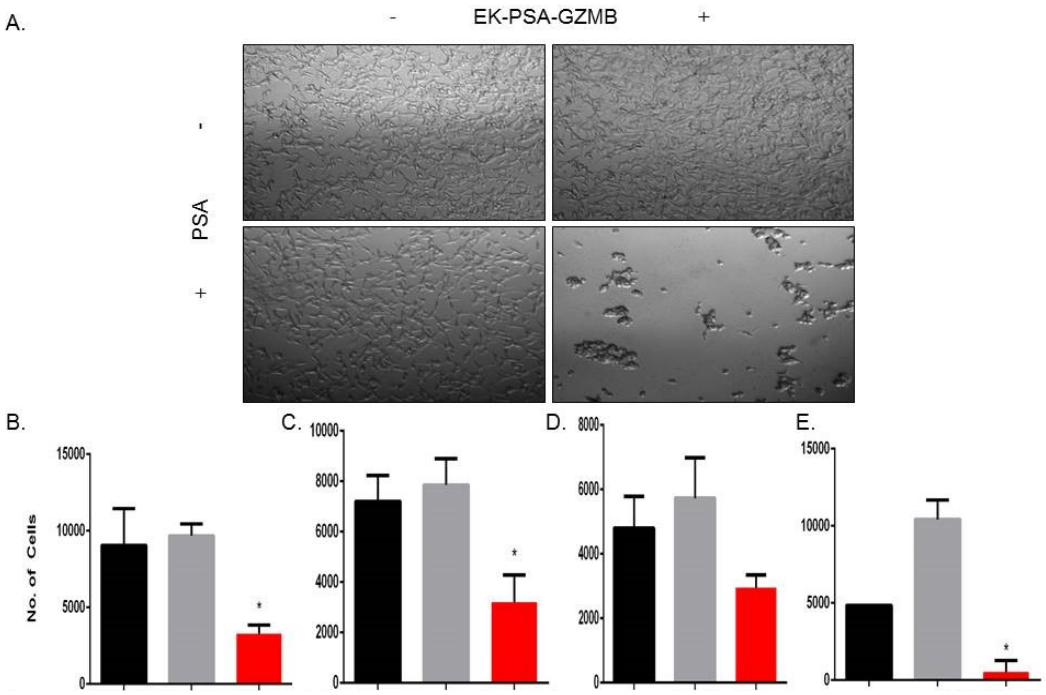

Figure 7: EK-PSA-GZMB inhibits cell growth selectively in the presence of PSA. Light microscopy images of LNCaP cells treated +/- 3 uM EK-PSA-GZMB and +/- PSA at 10X magnification (A). MTT assay of LNCaP (B), DU145 (C), CWR22 Rv1 (D), or human prostate stromal cells (E) treated with either PSA (black bars), EK-PSA-GZMB (grey bars), or both (red bars) for 7 or 9 days.

EK-PSA-TRP and EK-PSA-GZMB proteins, when treated with porcine EK at 5 EU/mL were both robustly active after a four hour incubation (Figure 5B & 5D). Both active enzymes had a higher specific activity following incubation with EK than with PSA.

In order to accurately mimic the prostate cancer microenvironment and evaluate any effect these proteins have on cell growth, we plated various cell types on plastic tissue culture plates pre-treated with media containing 10% serum. The cells were then allowed to attach to the dish and remain viable in media lacking serum protease inhibitors that would otherwise disrupt PSA's ability to activate these drugs. EK-PSA-TRP at 0.5 uM was treated on LNCaP cells plus or minus exogenously added PSA. Cells treated with the vehicle alone grew slower than under normal conditions but were otherwise healthy and viable (Figure 6A). LNCaP cells exposed to either PSA alone or EK-PSA-TRP alone were unaffected. However, when both were co-incubated on cells, we observe gross morphology and violent aggregation consistent with how LNCaPs grow with no ECM present (Figure 6A). Using the MTT assay and a LNCaP standard curve, we were able to quantitate the cell number for each treated group. Over the period of 5 days, we observe that both groups treated with EK-PSA-TRP or PSA alone doubled in cell count which was not substantially different from the control cells. LNCaP cells affected by activated TRP digestion of the ECM did not grow at all, as number of cells plated and counted cells were identical. This difference in cell number was found to be statistically significant ($p < 0.05$). This experiment was repeated on DU145 (Figure 6C) but no notable differences in morphology or cell growth between treated and untreated cells was observed.

We performed the same set of experiments to assess EK-PSA-GZMB's ability to inhibit the growth of prostate cancer cells and if the toxicity was limited to just LNCaP cells. For

the light microscopy experiment, we observed, again, no effect of the cells treated with EK-PSA-GZMB or PSA alone. In combination, 3 uM EK-PSA-GZMB activated by PSA induced obvious morphology changes and clumping of affected cells (Figure 7A). To further understand these effects kinetically, we used time lapse microscopy and observed that a majority of the clumping occurs within 24 hours of treatment with the activated GZMB protein (data not shown). Like the EK-PSA-TRP drug, these effects correlated with a significantly significant difference in growth, with cells treated with PSA and EK-PSA-GZMB not appearing to grow when compared to controls and the starting number of cells plated on Day 0 (Figure 7B). Unlike the EK-PSA-TRP protein, however, we did observe both a morphological and anti-proliferative effect on DU145, CWR22 Rv1, and stromal cells. When treated with PSA or EK-PSA-GZMB alone, no morphological differences were observed on any of these cells. PSA-treated EK-PSA-GZMB induced cell aggregation, morphological changes and differences in cell adhesion to the plate (data not shown). Like the LNCaPs treated with EK-PSA-GZMB, we observe a growth inhibitory effect on each cell line when compared with the respective controls on DU145, CWR22 Rv1, and human prostate stromal cells(Figure 7C, 7D and 7E) with statistically significant differences being observed in the DU145s and stromal cells. Interestingly, GZMB at this dose induced morphological effects on PC3 and LAPC4 cells but no changes in cell count was seen (data not shown).

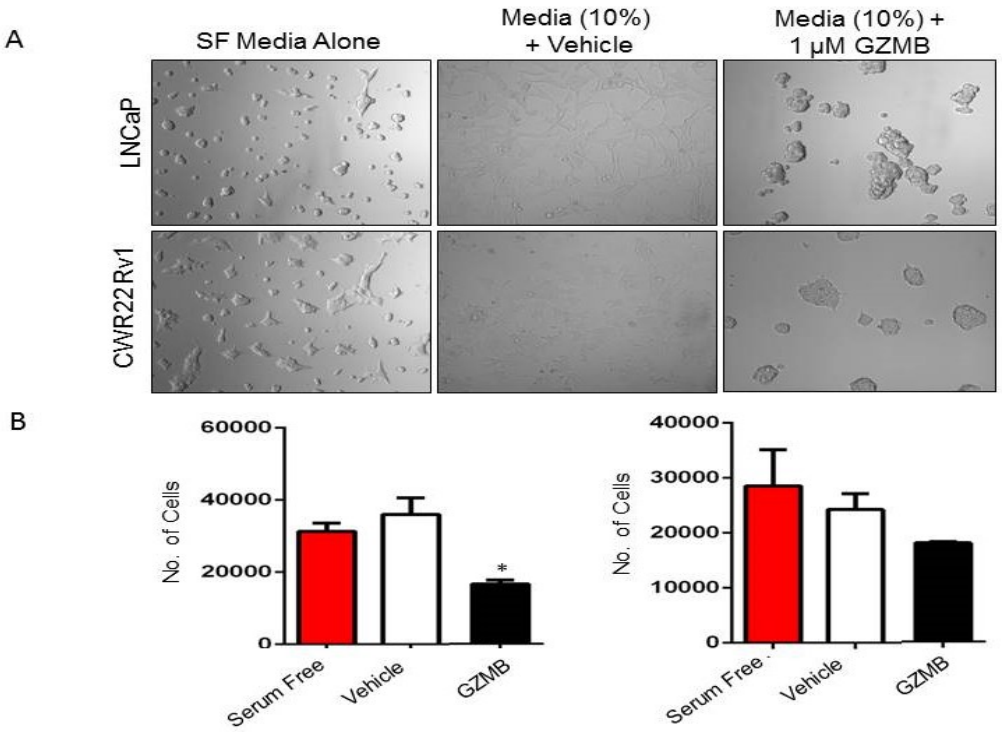

Figure 8: GZMB induces prostate cancer cell growth inhibition via damage to the ECM. Light microscopy images of LNCaP (top) and CWR22 Rv1 (bottom) were plated in serum free RPMI (B27 supplemented). in wells treated with buffer (left), media-containing serum (middle) or media with serum and 1 uM GZMB (right) and incubated for 48 hours at 37 degrees. Magnification is 10X (A). Quantitation of plated LNCaP (left) and CWR22 Rv1 (right) 48 hours after plating (B).

Because we observed notable effects on cell morphology and growth which strongly correlated with enzymatic activity of these drugs, we aimed to examine whether these effects were driven by protease-induced ECM damage. To do this, we pre-coated a plate with serum free media, media containing 10% serum, or media with serum and 1 uM GZMB. We then removed the solutions and plated LNCaPs and CWR22 Rv1 cells in serum free media and incubated them for 48 hours. Cells plated on surfaces coated with media attached well, had normal morphology, and proliferated (Figure 8A). Cells plated in serum free wells did not attach but appeared to grow at rates comparable to the control. Both LNCaPs and CWR22 Rv1 cells plated on wells treated with serum and

GZMB displayed morphology similar to those treated with activated EK-PSA-GZMB and did not grow as well when quantitated with the MTT assay (Figure 8B). Only the growth of the LNCaP cells were significantly affected by the GZMB treated matrix while the CWR22 Rv1 cells were not despite the obvious visual effects.

Discussion

It has been reported in the literature that human cancer cells *in vitro* can be targeted via disruption of their interactions with the ECM. This is an attractive mode of therapeutic targeting as it affects the entire tumor and not just cells expressing a specific marker. Because our lab has examined the potential role of proteases in cancer chemotherapy, we opted to explore the idea of using human proteases as an agent capable of damaging the tumor ECM. In order to hone this potential route of toxicity to the tumor microenvironment and limit the effects on normal tissue, we sought to engineer these proteases into zymogen mutants capable of being activated selectively by PSA. To achieve this, we chose to modulate the zymogen activation of human TRP, as it has been well established to digest components of the ECM and has a well characterized zymogen activation. Our mutant, EK-PSA-TRP, contained a robustly cleaved PSA substrate, KGISSQY flanked by the inhibitory EK substrate and the rest of the enzyme. This protein was successfully expressed in mammalian tissues, albeit at rather low levels due to toxic effects observed on the HEK293T cells. Following purification, SDS PAGE showed that this species runs as two bands, likely a post translational modification, as both were cleaved by PSA and were isolated using NiNTA agarose and, therefore, not a proteolytic fragment on either terminus. We also chose human GZMB as a second candidate due to its published ability to digest the ECM, to be expressed as a zymogen with an EK piece on the N-terminus, and to resist inhibition via serum protease

inhibitors. This protein was easily expressed in mammalian cells and ran as a single band on a protein gel.

We have successfully engineered both human TRP and GZMB to be activated by PSA. Incubation experiments with PSA using a TRP and GZMB specific substrate has shown that both mutants, EK-PSA-TRP and EK-PSA-GZMB, remain inactive until incubated with PSA. Interestingly, we observe very different activation kinetics of both drugs based on the plateau of the enzymatic assay and the immunoblots probing with an anti-DDDDK antibody. Because the TRP zymogen was activated at least 5 times faster than the GZMB, it suggests the PSA substrate was presented in a more favorable conformation on the TRP pro-drug possibly due to the EK piece already being in a more native orientation. Both pro-drugs showed less activity per mg enzyme than their EK-activated counterparts suggesting that the PSA substrate peptide affects the folding of the enzymes negatively. We were, however, pleased to see that both enzymes retained a majority of their initial activity following a 23 day incubation at 37 degrees Celsius suggesting their stability would not be a limitation for use as an *in vivo* therapy. We were also pleased to see the robust difference in Vmax values for both enzymes compared to their zymogen counterparts while seeing very little change in Km suggesting that PSA activation and removal of the EK inhibitory piece induced a conformational change in the zymogen that increased enzymatic turnover as opposed to changing substrate binding. Edman degradation analysis also strongly suggests that the PSA cleavage occurred specifically in between the C-terminal tyrosine residue of the PSA substrate and the N-terminal isoleucine of GZMB, as intended.

The simple insertion of the KGISSQY PSA substrate into the native TRP and EK-GZMB proteins to yield a PSA-activated mutant was unprecedentedly simple. We chose to further delve into the role of both peptides (DDDDK and KGISSQY) in yielding such a

mutant given that EK-GZMB and WT TRP have already been established as EK activated zymogens. To do this, we designed two more mutants containing only the KGISSQY substrate on the N-termini of TRP and GZMB deemed PSA-TRP and PSA-GZMB respectively. We then expressed these mutants in mammalian tissues and used the same chromatography methods as the EK-containing proteins. It should be noted that, in terms of expression, both PSA-GZMB and PSA-TRP expressed at much lower levels than the EK-containing PSA-activated variants suggesting that the EK piece promotes proper folding and expression of these enzymes. Furthermore, PSA-TRP and PSA-GZMB had substantially less activity when incubated with PSA at the same length as EK-PSA-TRP and EK-PSA-GZMB with PSA-GZMB having no detectable activity after a 4 hour incubation with PSA. This also indicates that the EK piece plays a role in the proper folding of the inactive zymogen so the functional enzyme can be released once the EK peptide is proteolytically removed. Because EK also activated EK-PSA-TRP and EK-PSA-GZMB robustly, it also strongly suggests that the DDDDK peptide also plays a major role in inhibiting the enzymes and retaining the inactive conformation, possibly due to the very strong ionic charge and secondary structure formed by the piece. It is interesting that the PSA-TRP protein retained some activity once activated by PSA as opposed to the PSA-GZMB protein suggesting the TRP is more tolerant about which peptides reside on its N-terminus for proper expression and folding. Because the DDDDK EK piece seems to promote folding, proper presentation of the KGISSQY peptide activation substrate, and direct inhibition of the enzymes when attached, we highly recommend it's use as a pro-piece for any further mutant serine proteases that require activation by a target protease.

In order fully characterize both EK-PSA-GZMB and EK-PSA-TRP's ability to target cells in culture. We assessed this by incubating both drugs in serum free media (to facilitate

PSA activation) on cells plated on a bed of matrix proteins derived from FBS. On LNCaP prostate cancer cells, we observed obvious morphological and proliferative effects from both drugs only when PSA and the pro-drug were co-incubated. While EK-PSA-GZMB had these effects on various other prostate cancer cell lines to a varying degree, we did not observe these effects on any other cell line when using EK-PSA-TRP including DU145. This may be due to the fact that many cancer lines secrete anti-trypsin protease inhibitors as a mechanism to prevent extracellular damage via trypsin and trypsin like proteases. GZMB, on the other hand, has been shown to be inherently resistant to inhibition via serum protease inhibitors which would explain the discrepancy between these two drugs (13). Regardless, we were pleased to see our GZMB pro-drug to have these effects on several lines in the presence of PSA as well as human prostate stromal cells which suggests that GZMB could have the capacity to disrupt the tissue architecture in a tumor which would yield a more comprehensive response. It is also worth noting that some cell lines (PC3 and LAPC4) were affected morphologically but not in terms of growth suggesting that these ECM interactions and their role in cell biology differs wildly between tumors.

To ensure whether GZMB's effects were solely due to ECM damage, we treated plates coated with ECM proteins from FBS with GZMB in a cell free context and then plated cells in serum free media once the GZMB was removed. We observed very similar effects on both cell lines which were sensitive to GZMB in co-culture experiments. Because GZMB was removed from the plate once the cells were added and that the cell morphology was very similar to that of the cells incubated on an empty plate with no ECM, it is reasonable to conclude that a majority the effects seen were due to ECM damage caused by GZMB proteolysis. It is possible; however, that the anti-proliferative

effects seen on the cells were due to factors other than ECM damage, as it appears the cells grew slightly better than when incubated with GZMB directly.

Despite observing robust *in vitro* effects of these PSA-activated proteases, we observed no obvious antitumor effects of the drugs when injected IV or IT into LNCaP-bearing nude mice at any dose. While disappointing, this lack of efficacy may be due to not enough enzymatically active PSA being expressed by the tumors themselves as LNCaP xenografts, though PSA positive, do not produce near the levels of enzymatic PSA as human tumors. Because we used physiologically relevant concentrations of active PSA in our tissue culture experiments, we would expect these pro-drugs to be functional in the context of the prostate cancer microenvironment in a human. It is also possible that these drugs may not be able to generate anti-tumor effects by themselves and may need other means of chemotherapy to synergize with. While speculative, it is evident based on the observed *in vitro* effects that prostate cancer cells under duress will aggregate together in order to avoid undergoing anoikis or other negative effects. It is possible that combing our GZMB pro-drug with an agent that blocks these interactions, such as an E-cadherin antibody, may facilitate a synergistic anti-tumor effect. Given that GZMB extracellular effects seems to be pro-inflammatory, it is possible that a GZMB pro drug could be used to recruit local immune cells to the tumor and help facilitate an anti-tumor immune response. Our GZMB pro drug may be best used with immune check point inhibitors or other types of clinically approved cancer immunotherapy.

We successfully engineered two human enzymes to be activated by cancer-specific proteases not active in the bloodstream. These pro-drugs had favorable enzymatic activity characteristics while having some interesting anti-cancer activity *in vitro.* We are encouraged by this work as it elucidates a novel mechanism to regulate and engineer human proteases, one of the largest and most diverse classes of enzyme, to be

activated by other proteases of interest. We postulate that the use of the EK inhibitory peptide and a known protease site could be used to modulate the activity of a number of proteases via proteolytic activation of a number of other target proteases. We are also encouraged by the idea of using therapeutic agents to generate a field effect that prevents tumor cells from thriving. Virtually all currently approved therapeutics directly, in one way or another, interact with the cancer cells. We have demonstrated a strategy to selectively modify a microenvironment so that it changes tumor biology and generate an anti-tumor response. Should similar means be used successfully in *in vivo* models, these therapies may have the capacity to minimize recurrence of resistant cancer cells and combat the problem of tumor heterogeneity which has limited the efficacy of therapeutic strategies in extending and improving the quality of lives in patients.

References

1. Howlader N, Noone AM, Krapcho M, Miller D, Bishop K, Altekruse SF, Kosary CL, Yu M, Ruhl J, Tatalovich Z, Mariotto A, Lewis DR, Chen HS, Feuer EJ, Cronin KA (eds). SEER Cancer Statistics Review, 1975-2013, National Cancer Institute. Bethesda, MD,
2. Zhu ML, Horbinski CM, Garzotto M, Qian DZ, Beer TM, Kyprianou N. Tubulin-targeting chemotherapy impairs androgen receptor activity in prostate cancer. Cancer Res. 2010;70(20):7992-8002.
3. Lebeau AM, Singh P, Isaacs JT, Denmeade SR. Prostate-specific antigen is a "chymotrypsin-like" serine protease with unique P1 substrate specificity. Biochemistry. 2009;48(15):3490-6.
4. Balk SP, Ko YJ, Bubley GJ. Biology of prostate-specific antigen. J Clin Oncol. 2003;21(2):383-91.
5. Denmeade SR, Sokoll LJ, Chan DW, Khan SR, Isaacs JT. Concentration of enzymatically active prostate-specific antigen (PSA) in the extracellular fluid of primary human prostate cancers and human prostate cancer xenograft models. Prostate. 2001;48(1):1-6.
6. Stenman UH, Leinonen J, Alfthan H, Rannikko S, Tuhkanen K, Alfthan O. A complex between prostate-specific antigen and alpha 1-antichymotrypsin is the major form of prostate-specific antigen in serum of patients with prostatic cancer: assay of the complex improves clinical sensitivity for cancer. Cancer Res. 1991;51(1):222-6.
7. Denmeade SR, Lou W, Lövgren J, Malm J, Lilja H, Isaacs JT. Specific and efficient peptide substrates for assaying the proteolytic activity of prostate-specific antigen. Cancer Res. 1997;57(21):4924-30.

8. Hoves S, Trapani JA, Voskoboinik I. The battlefield of perforin/granzyme cell death pathways. J Leukoc Biol. 2010;87(2):237-43.
9. Cullen SP, Adrain C, Lüthi AU, Duriez PJ, Martin SJ. Human and murine granzyme B exhibit divergent substrate preferences. The Journal of Cell Biology. 2007;176(4):435-444.
10. Buzza MS, Zamurs L, Sun J, et al. Extracellular matrix remodeling by human granzyme B via cleavage of vitronectin, fibronectin, and laminin. J Biol Chem. 2005;280(25):23549-58.
11. Parkinson LG, Toro A, Zhao H, Brown K, Tebbutt SJ, Granville DJ. Granzyme B mediates both direct and indirect cleavage of extracellular matrix in skin after chronic low-dose ultraviolet light irradiation. Aging Cell. 2015;14(1):67-77.
12. Boivin WA, Cooper DM, Hiebert PR, Granville DJ.Intracellular versus extracellular granzyme B in immunity and disease: challenging the dogma. Laboratory Investigation. 2009;89(11):1195.
13. Kurschus FC, Kleinschmidt M, Fellows E, et al. Killing of target cells by redirected granzyme B in the absence of perforin. FEBS Lett. 2004;562(1-3):87-92.
14. D'angelo ME, Bird PI, Peters C, Reinheckel T, Trapani JA, Sutton VR. Cathepsin H is an additional convertase of pro-granzyme B. J Biol Chem. 2010;285(27):20514-9.
15. Pham CT, Ley TJ. Dipeptidyl peptidase I is required for the processing and activation of granzymes A and B in vivo. Proc Natl Acad Sci USA. 1999;96(15):8627-32.
16. Bates WB, Koch FC. Studies on the trypsinogen, enterokinase, and trypsin system. Journal of Biological Chemistry. The Journal of Biological Chemistry. 1935. 111, 197-215.
17. Grant DA, Hermon-taylor J. Hydrolysis of artificial substrates by enterokinase and trypsin and the development of a sensitive specific assay for enterokinase in serum. Biochim Biophys Acta. 1979;567(1):207-15.

18. Gehrmann M, Doss BT, Wagner M, et al. A novel expression and purification system for the production of enzymatic and biologically active human granzyme B. J Immunol Methods. 2011;371(1-2):8-17.

Chapter 4: Targeted Delivery of Cytotoxic Proteins via Small Molecule Peptidase Inhibitors

Abstract

Prostate cancer is the leading cause of cancer death in American men. This is despite countless advancements in understanding the biochemical and physiological properties that drives lethal disease. Currently, there are no approved curative therapies for metastatic prostate cancer. Protein-based targeted agents offer a unique advantage to treating metastatic tumors due to their natural tendency to accumulate in the tumor micro-environment. In order to further improve selectivity and minimize systemic toxicity of such an agent, our lab has previously explored and evaluated novel ways to regulate cytotoxic proteins for therapeutic purposes. Prostate Specific Membrane Antigen (PSMA) is an extracellular carboxy-peptidase-like enzyme expressed in both benign and cancerous prostate epithelium. PSMA has been classically shown to be aggressively upregulated by metastatic prostate cancer cells and is a reliable predictor of recurrent and more aggressive disease. Recently, a small class of urea-linked dipeptide inhibitors has been developed against PSMA in order to selectively deliver imaging agents to tumor cells. We hypothesize that conjugation of protein cytotoxins with these PSMA-binding ureas would yield a novel and potent agent capable of selectively binding PSMA and entering the tumor cell and induce subsequent cell death. To evaluate this, we synthesized two protein-urea cytotoxins using the apoptosis-inducing protease Granzyme B and the potent bacterial protein toxin fragment, PE35. In this study, we demonstrate the synthesis and biochemical properties of these agents and compare their ability to target PSMA-expressing cells in culture. Furthermore, we also characterize the anti-tumor effects of the PE35-urea conjugate in xenograft-based animal models. This study demonstrates the properties of these molecules and

correlates these properties with their efficacy as well as describes effective methods to evaluate future, related agents.

Introduction

Every year, hundreds of thousands of American men are diagnosed with prostate cancer (1). Fortunately, a majority of these men go on to survive years after their initial diagnosis. Despite the disease's high survival rate relative to other solid malignancies, a subset of patients will succumb to their cancer. Most of these patients, at time of diagnosis, presented with metastatic prostate cancer (MPC) as opposed to disease localized in the prostate. It is clear that the focus in treating prostate cancer should be on metastatic, therapy resistant tumors that ultimately contribute to the mortality of this disease. Currently, there is no approved cure for metastatic prostate cancer. While therapeutic options have expanded in recent years, these treatments usually expand life marginally and are usually palliative. One major challenge associated with treating MPC is that these tumor cells grow much more slowly than other cancers. While this likely plays a role in the longevity associated with prostate cancer, it renders most tumors insensitive to traditional chemotherapeutic approaches. It is, therefore, essential that novel chemical approaches to targeting these tumors work independently of cell proliferation, as most cells within a patient are in the G0 stage of the cell cycle at any given point. Because of this, our lab has become intrigued by the idea of re-targeting highly potent and robust environmental toxins to MPC cells via biochemical engineering techniques.

Of all the potential markers selective to MPC cells, few are as enticing as the Prostate Specific Membrane Antigen (PSMA). PSMA is a membrane-bound extracellular carboxypeptidase enzyme expressed by prostate epithelial cells (2). Its function in both normal and malignant biology has not been fully characterized despite the discovery of a panel of specific of diverse substrates. One such substrate is the neurotransmitter N-acetyl-aspartyl-glutamate (NAAG). PSMA processes this dipeptide into N-acetyl-

aspartate and free glutamate (3). In the context of prostate cancer, PSMA has been shown to be over-expressed in neoplastic tissue as it transitions from normal to malignant and has increased activity in prostate cancer cells compared to normal (4,5). It has also been proposed in the literature that PSMA is an accurate predictive marker of recurrent, more aggressive prostate cancer as tumors over-expressing the gene were more likely to suffer future relapse and relapsed faster than patients who did not at time of diagnosis (4). Because of PSMA's strong association with aggressive, more resistant prostate cancer, it's unique extracellular catalytic activity, it's expression in neo-vasculature in non-prostate cancer tumors (6) and its rapid recycling in cells (7), it is an excellent choice as a target for delivering cytotoxic payloads to MPC cells, as a number of PSMA-targeted antibodies have been in development for the treatment and diagnosis of prostate cancer (8)

Recently, a class of urea-linked dipeptides was developed as imaging agents for MPC. These agents (deemed 'ureas' or PSMA-binding 'ureas' in this work) contain a glutamate and lysine residue linked by a urea group rather than an amide (9). PSMA-ureas bind remarkably well to the catalytic pocket of PSMA and inhibit its enzymatic activity. It has also been shown that these compounds are capable of delivering low molecular weight cargo to PSMA-expressing cells with remarkable selectivity given the simple molecular structure of the urea backbone. One such molecule was developed by Chen et al in which the infrared-fluorescent dye IR800CW was covalently coupled to the PSMA-binding urea scaffold. This compound selectively concentrated into a PSMA-expressing PC3 xenograft and was barely detectable in a PSMA-null control xenograft in IR-based imaging experiments demonstrating the impressive ability to selectively deliver cargo molecules to PSMA-producing tumors (10). Because of this, we hypothesize that PSMA-binding ureas can serve as effective and specific 'Trojan horse' molecules to facilitate

the delivery of cytotoxic protein payloads which have been shown to naturally accumulate into tumors via the Enhanced Permeability and Retention effect (11).

In order to evaluate the potential of developing a ligand-targeted cytotoxic protein conjugate via a PSMA-binding urea, we chose to conjugate two diverse yet well understood proteins capable of inducing rapid and comprehensive cell death and compare their biochemical and pharmacological properties. The first protein we selected, human Granzyme B (GZMB), is a caspase-like serine protease secreted by activated cytotoxic T lymphocytes upon stimulation by a neoplastic or virally infected cell (12). GZMB, when co-secreted with the pore-forming protein perforin, is translocated into the target cell cytoplasm where it is able to cleave a myriad of pro-apoptotic and anti-survival substrates thus inducing cell death (13). While GZMB is a well-studied and effective killer of mammalian cells, its function is dependent on perforin facilitated endocytosis and translocation from the target cell endosome to the cytoplasm (14,15). Because PSMA-ureas concentrate in the perinuclear endosome space due to PSMA"s recycling pathway, we postulated that GZMB-urea conjugates may not induce cell death at relevant concentrations. We also selected a cysteine-containing fragment of the pseudomonas exotoxin A gene (PE35), a bacterial toxin enzyme which disrupts target cell translation via ADP-ribosylation of the crucial diphthamide residue on Elongation Factor 2 (16). PE35 is an engineered cytotoxin whose ability to bind and internalize into cells has been perturbed via deletion of the cell targeting domain Ia structure (17). Currently, there are several immunotoxins containing PE fragments in the clinical setting (18), with one, moxetumumab, in Phase III studies for the treatment of Hairy Cell Leukemia (19). Because PE35 has been shown to be able to escape cell endosomes upon delivery via antibodies or growth factors, we rationalized that PE35 would still be functional despite endosome localization via PSMA's recycling pathway.

In this study we design, synthesize, and evaluate two protein-urea conjugates using the GZMB and PE35 proteins as cargo. To accomplish this, briefly, we used mutants of these proteins that contain reactive cysteine residues capable of reacting with maleimide moieties. PSMA-binding urea compounds were synthesized with a reactive maleimide functional group linked by 2 PEG units (compound referred to as MU2). Once synthesized and purified, these conjugates were evaluated for their ability to bind and inhibit PSMA, internalize into PSMA-expressing cells, and their ability to target MPC cell lines *in vitro* and *in vivo* in a PSMA-specific manner.

Materials and Methods

Materials

For synthesis of the MU2 compound, Preparative reverse phase chromatography was performed on a Biotage Isolera One Purification system using a SiliCycle 25g C18 column (SiliCycle Inc., Quebec, Canada) (230-400 mesh, 40-63 micron column) and a gradient elution of 95% solvent A, 5% solvent B to 60% solvent A, 40% solvent B over 20 minutes where solvent A is 100% water + 0.1% TFA and solvent B is 100% acetonitrile + 0.1% TFA and flow rate is 25mL/min. HPLC analysis was performed on an Agilent 1260 Infinity HPLC system (Santa Clara, CA, USA) using a 10 X 250 mm Luna C18, 10 micron column (Phenomenex, Torrance CA, USA) and a gradient elution of 90% solvent A, 10% solvent B to 10% solvent A, 90% solvent B over 30 minutes where solvent A is 100% water + 0.1% TFA and solvent B is 100% acetonitrile + 0.1% TFA at a flow rate of 5mL/m. 1H-NMR spectra was measured on a Bruker Avance 400 MHz spectrometer. Mal-PEG2-NHS was purchased from BroadPharm (San Diego, CA, USA).

For protein and biological studies, all reagents were purchased from Sigma Aldrich unless stated otherwise.

Synthesis of maleimide-linked PSMA-binding ureas for conjugation

(3S,7S)-22-(2,5-dioxo-2,5-dihydro-1H-pyrrol-1-yl)-5,13,20-trioxo-16-oxa-4,6,12,19-tetraazadocosane-1,3,7-tricarboxylic acid, 3.

To a solution of the Lys-Glu urea amine formate salt (20) (100 mg, 0.19 mmol) and DIPEA (131 µL, 0.75 mmol) in anhydrous DMF (1.5 mL), was added Mal-PEG2-NHS (104 mg, 0.24 mmol) in one portion and allowed to stir at ambient temperature. After 1 h, DMF was evaporated off and crude 2 was dissolved in 1.5 mL of TFA/methylene chloride (2:1) and allowed to stir overnight. The solvent was then concentrated under reduced pressure, and the crude mixture purified by reversed phase chromatography using a C18 column and eluting with a gradient of 95:5 water (0.1% TFA)/acetonitrile (0.1% TFA) to 60:40 water (0.1% TFA)/acetonitrile (0.1% TFA) over 20 mins. After lyophilization, the product was obtained as a white flaky solid. The isolated yield is 75 mg (64%). Purity as measured by HPLC was 95%. 1H-NMR (400MHz, DMSO-d6): 8.01 (br, 1H), 7.80 (br, 1H), 6.99 (s, 2H), 6.29 (br, 2H), 4.16−3.93 (comp, 2H), 3.67−3.51 (comp, 5H), 3.50−3.40 (comp, 5H), 3.38−3.27 (comp, 2H), 3.19−3.07 (comp, 2H), 3.05−2.94 (m, 1H), 2.46−2.38 (m, 1H), 2.37−2.15 (comp, 5H), 1.98−1.82 (m, 1H), 1.78−1.56 (comp, 2H), 1.55−1.43 (m, 1H), 1.43−1.17 (comp, 3H); MS: calculated for [C26H40N5O13]+, 630.6 [M + H]+; found 630.4.

Cloning of GZMB gene and cysteine 248 mutagenesis

We chose to design a GZMB expression construct as was done by Gehrmann et al (21). Briefly, GZMB was cloned with two modifications for rapid and efficient expression and urea conjugation. First, we removed the native two amino acids on the N-terminus of GZMB and replaced them with an enterokinase substrate, DDDDK. This was shown to improve expression yields and minimize toxicity on HEK-293T cells. Second, we inserted

a C-terminal reactive cysteine due to previous works in which GZMB immunotoxins were synthesized with the targeting moiety on the C-terminus. To clone the gene into a mammalian expression vector, we amplified the GZMB gene (Origene plasmid SC3231693) with the primers F: CAGTGTGGTGGAATTCATGCAACCAATCCTGCTTC R: GATATCTGCAGAATTCTTAGTAGCGTTTCATGGTTTT using an Accuprime Pfx PCR mix (Thermo 12344024) according to manufacturer's instructions with a melting temperature of 53 degrees Celsius. PCR product containing the GZMB gene with a C-terminal cysteine (C248) was then purified on a 1.5% agarose gel and cloned into the mammalian expression vector pcDNA3.1 using an In-Fusion HD cloning kit (Clonetech 638909) according to manufacturer's instructions. Plasmid was then grown up and isolated using Stellar Competent E Coli (CloneTech 636763) according to manufacturer's instructions. The correct product was harvested and isolated using a PureLink® HiPure Plasmid Filter Maxiprep Kit (Thermo K210017) out of 50 mL of cell suspension and sequenced using the Sanger method via the Johns Hopkins Sequencing and Synthesis core facility.

The DDDDK EK piece was inserted using a Q5 Site Directed Mutagenesis Kit (E0554S) and the primer set F: CGACAAAATCATCGGGGGACATGAGG R: TCGTCGTCTGCATCTGCCCTGGGCAG using a melting temperature of 67 degrees Celsius. Product was transformed, grown, harvested, and sequenced as described above. For all work with pcDNA3.1-transformed E Coli, a solution of 100 ug/mL Ampicillin was used in LB. All cells were plated on 1.5% agar plates containing 100 ug/mL Ampicillin.

Expression and harvesting of GZMB and PE35 proteins

Based on the work done by Gehrmann et al, we expressed EK-C248 GZMB in HEK-293T cells. HEK cells were grown in T75 flasks in 20 mL DMEM containing 10% FBS

and supplemental L-glutamine (5mM) at a seeding density of 5 x 10^6 cells per flask. Twenty four hours following seeding, cells were transiently transfected with 25 ug of plasmid mixed with 1.1 mL of OPTI-MEM media and 74 uL of FuGene HD lipofectamine reagent (Promega E2311) per T75 which was incubated for 10 minutes at room temperature. The mix was then added to cell culture and incubated overnight at 37 degrees. The next day, cells were washed one time with 1X PBS solution and cultured in 10 mL serum-free DMEM containing glutamine and incubated for 3 days or longer. To harvest, cell supernatant was collected and centrifuged for 10 minutes at 8000 x g in order to remove insoluble debris. The solution was then concentrated to less than a mL using Amicon Ultra-15 Centrifugal Filter Units (Millipore UFC901024) and stored until needed at 4 degrees.

The plasmid containing PE35 with a reactive cysteine near the N-terminus of the protein pCT11 (21) was generously donated to us by the laboratory of Dr. Ira Pastan. This plasmid was transformed into BL21 DE3 E Coli according to manufacturer's instructions and grown on plates containing 50 ug/mL Ampicillin. Colonies were picked and grown up in 500 mL TB containing Amp until the optical density reached 0.4. The culture was then induced using 500 uM IPTG and incubated overnight at room temperature, shaking at 250 RPM. The next day, the culture was pelleted via a 5000 x g spin for 20 minutes and the periplasmic fractions were harvested. To do this, the pellet was then resuspended in a solution of 15 mL 30 mM Tris pH =8, with 150 mM NaCl, 20% sucrose, 0.5 mM EDTA and cOmplete protease inhibitor cocktail in order to osmotically shock the cells. Cells were incubated for 15 minutes on ice and re-pelleted using a 5000 x g spin for 20 minutes. Supernatant was saved and shock protocol was repeated using reverse osmosis water. The supernatant was combined with the first fraction and spun at 10,000 x g for 10 minutes to remove any insoluble debris. The resulting supernatant was then

concentrated using Amicon filters to less than a mL and then diluted in 20 mL of PBS with a pH = of 6.5. To clean up this solution, we then added 1 mL of washed Q Sepharose Fast Flow anion exchange resin (GE Healthcare 17-0510-10) and incubated for 20 minutes at room temperature. The beads were loaded into a disposable column and washed twice with 10 mL of PBS. PE35 was then eluted from the column using 4 fractions of 0.5 mL PBS pH = 6.5 containing 1 M NaCl. Fractions were then pooled and dialyzed vs 1 L PBS pH = 7.4 in a Slide-a-Lyzer Dialysis Cassette (MWCO 7K) (87722) for 2 hours at 4 degrees and then overnight vs 2 L of buffer in order to remove the excess salt. Dialysate was then stored at 4 degrees until needed. Protein concentrations were determined by A280. Content of each prep was validated with reducing SDS PAGE.

Protein-MU2 conjugations and chromatography

In order to maximize the efficiency of protein-urea coupling, proteins were gently reduced prior to coupling. Because contaminating thiol groups can compete with the protein cysteine thiols, we used the non-sulfur containing reducing agent TCEP to disrupt inter-protein disulfide dimer formation. This was done by incubating TCEP in water and diluting to a concentration of 0.5 mM (at least 5-fold excess of protein) at room temperature for at least an hour. We then diluted 1-2 mg of MU2 (compound 3) in water and adjusted the pH of this solution to 6-7 as the initial solution has a pH of approximately 2 and cysteine-maleimide coupling reactions are very pH sensitive. The solution of MU2 was diluted to 1 mM in the reduced protein solution and incubated at room temperature for an hour and then at four degrees overnight. For BSA conjugation, because Ellman's assay was used to characterize the coupling, no reducing agent was added, as it reacts rapidly with Ellman's reagent.

Prior to conjugation, GZMB-MU2 was activated using EK to release the fully functional enzyme. Purified EK from porcine intestine was diluted in a solution of 10 mM TrisHCl and 10 mM $CaCl_2$ and diluted to a solution of 5 EU/mL and digested for 30 minutes at 37 degrees. To purify the GZMB-MU2 conjugate (and remove the excess MU2 and EK), we performed cation exchange chromatography using a negatively-charged $SO3^-$ resin (Fractogel EMD SO3- Millipore 116882). Coupling reaction and 1 mL washed resin was diluted in 10mL PBS pH= 7.4 and incubated at room temperature for 20 minutes shaking. This solution was then loaded into a disposable column and washed with 20 mL of PBS. Protein was then eluted using PBS containing 1M NaCl in 0.3mL fractions. Protein containing fractions were dialyzed as described above to remove the excess salt.

For PE35-MU2, we used gel filtration chromatography on a Fast Protein Liquid Chromatography apparatus. Briefly, the conjugation reaction was spun at 18,000 x g for 10 minutes and loaded into an AKTAprime Plus FPLC System (GE 11001313) using a washed HiLoad Superdex 200 PG (GE 28989335) column. One milliliter fractions were collected and monitored using A280 spec. Fractions containing protein were then run on SDS PAGE. All fractions containing primarily the band specific for PE35 were pooled and concentrated to less than 1 mL. This method was also used to purify Fluorescein-labeled PE35-MU2.

Fluorescein Conjugation of protein-ureas

To create fluorescent probes whose uptake can be monitored using a confocal microscopy-based assay, we synthesized fluorescein-labeled protein-MU2 constructs. This was done by using NHS-fluorescein (Thermo 46410). Free amines on each protein were labeled by incubating NHS-Fluorescein (dissolved in DMSO) with the crude

reaction (prior to purification) for one to two hours at room temperature in the dark. Free NHS-Fluorescein was removed using either Pierce™ Dye Removal Columns (Thermo 22858) according to manufacturer's recommendations or via FPLC. Conjugation efficiency was determined using the ratio between A280 and A495 using the respective molar extinction coefficient for each protein, and the fluorescein conjugate.

Validation of Protein-urea Conjugation

To assess whether or not each protein-drug conjugate was synthesized successfully, we used either the thiol-reactive chromogenic reagent DNTB (Ellman's reagent), the fluorescent substrate ABDF, or a non-reducing SDS PAGE gel based assay. For the DNTB assay, thiol concentrations must be above 50 uM. BSA solutions plus or minus MU2 were mixed 1:1 with a 2mM solution of DNTB in DMSO. The reaction was then incubated at room temperature for 10 minutes shaking and read at 412 nm. Concentration of thiol was determined using the molar extinction coefficient of DNTB. For the gel-based assay, GZMB solutions plus or minus conjugate were purified and dialyzed as described above which allowed any free thiol to form disulfides. The reactions were then run on a non-reducing SDS PAGE gel using a BioRad Mini-Protean gelcast system (BioRad 1658005) with Mini-Protean 4-15% pre-cast gels. Gels were run at 150V for 45 minutes, washed once with water, stained with SimplyBlue (Thermo LC6060) protein stain, and de-stained in water. The ABDF assay was performed using a Sensolyte ABDF Assay Kit (Anaspec AS-72137) according to manufacturer's recommendations. The plate was read at 389/513 ex/em. Free thiol concentrations of PE35 plus or minus MU2 were determined using a GSH standard curve.

PSMA enzymatic assay

To confirm successful protein-drug coupling and that the MU2 compound is capable of binding PSMA, we performed an enzymatic assay specific for PSMA activity and correlated inhibition of substrate hydrolysis with protein-urea binding. Lysate from LNCaP cells (robustly PSMA positive) was generated by pelleting cells from culture, lysing them in a solution of 50 mM Tris HCl pH=7.5, 140 mM NaCl, and 1 % Triton X-100 to a concentration of 1 x 10^7 per mL of solution. Cells were then incubated on ice for 15 minutes and then spun at 18,000 x g for 15 minutes. Supernatant was then harvested and stored at -80 degrees Celsius or used immediately. The lysate was then diluted 1:10 in PBS and incubated with the PSMA specific substrate N-acetyl-aspartyl-glutamate (diluted to a final concentration of 4 uM) (NAAG) and either buffer, a protein-urea conjugate solution, a naked protein solution, or a control urea molecule, ZJ43 to validate the assay. This mix was incubated at 37 degrees Celsius for 4 hours. To determine the amount of NAAG converted to N-acetyl-aspartate and free glutamate by PSMA in each sample, we then added a fluorescent enzyme-coupled Amplex Red Glutamic Acid/Glutamate Oxidase Assay Kit (Thermo A-12221) mix according to the protocol provided. This reaction was done in Costar™ 96-Well Half-Area Plates (Fischer Corning 3694) in 100 uL total volume and was incubated for one hour at 37 degrees Celsius in the dark. The plate was then read at 530/590 nm ex/em. Activity was measured in raw RFUs and inhibition curves were based off a variable 4 parameter nonlinear regression. Naked and conjugated protein activity was measured in terms of % untreated controls.

GZMB Functional Assay

Once GZMB and MU2 had been successfully conjugated, we aimed to ensure that the MU2 coupling had no effect on the actual function of the enzyme. To evaluate GZMB activity, we used a GZMB-specific enzymatic assay (Biovision K168-100) that measures the cleavage of the peptide IETD and release of the fluorophore amino-methyl-coumarin

(AMC). Assay conditions were run according to manufacturer's suggestions. The plate was read at 380/500 ex/em following incubation. This reaction with GZMB or GZMB-MU2 was compared to a standard curve of free AMC to calculate the amount of substrate released.

In Vitro Characterization of Protein-Urea Conjugates

All cell lines were grown in RPMI containing 10% FBS with supplemental L-glutamine at 5mM and were passaged weekly. All experiments using PIP and Flu-PC3 cells were performed in the presence of 2 ug/mL puromycin in order to maintain PSMA/control plasmid expression respectively. At day -1, all cells were passaged and plated at the following densities based on their growth. PIP/Flu-PC3 were plated at 500 cells per well, DU145 at 1000 cells per well, CWR22 Rv1 at 2000 cells per well, and LNCaP/LAPC4 (grown in IMDM with serum and glutamine) at 5000 cells per well. Twenty four hours later, cells were treated with either vehicle (PBS pH=7.4) or the protein drug conjugate of interest at doses up to 250 nM. For GZMB-MU2, doses of 100 nM were not exceeded due to GZMB's ability to affect cell growth via extracellular matrix remodeling. All drug dilutions were made at 2x and diluted 1:1 in media to their final concentration in the dish. On day 5, 100 uL of media was removed from each well and 15uL of MTT dye (Promega G3582) was added. Plates were incubated at 37 degrees for 4 hours and stopped using the provided Stop solution. The assay was then incubated at room temperature shaking for up to 24 hours and read vs wells containing no cells at A570-A650. A standard curve was then used to calculate the number of cells in each well. Figures represented as a percentage of vehicle-treated cells. To assess the potency of each drug, we used a non-linear, 4 parameter, normalized inhibition curve to determine the IC50. For the pulse-soak PE35 experiments, we incubated cells for 24 hours with the drug, removed the media, and supplemented the cells with fresh media and compared the efficacy to cells

soaked in the drug for 5 days. Cells were photographed using a Nikon TE200 fluorescence microscope with the Metamorph software package at indicated magnifications.

Flor-Protein-Urea Confocal Uptake Assay

To assess the ability for PSMA-producing cells to internalize Fluorescein-labeled GZMB-MU2 or PE35-MU2, we treated PIP-PC3 and Flu-PC3 cells with both conjugates and used fluorescein uptake as a read out when visualized via confocal microscopy. This assay also allowed us to visualize where the constructs were being compartmentalized. We plated PIP and Flu cells at confluency on 12-well glass microscope plates (MatTek P12G-1.5-10-F) and incubated overnight. The next morning, cells were treated with 100 nM of the protein-drug conjugate for 2 hours at 37 degrees Celsius. We also added 10 uM 2-PMPA, another competitive inhibitor of PSMA to assess the specificity of the uptake for PSMA. The media was then removed and cells were washed three times with PBS. The cells were then incubated with 0.5 mL of Methanol for 30 seconds in order to fix and permeabilize them. Next, we added ProLong DAPI-containing mountant (Thermo P36962) and allowed the plates to dry for 10 minutes at room temperate in the dark. To visualize the cells we used a Nikon C1si True Spectral Imaging Confocal Laser Scanning Microscope System. All images were analyzed using ImageJ software. All images are at 20X magnification unless stated otherwise.

In vivo characterization of PE35-MU2

We grew LNCaP cells (passage 30), PIP, and Flu cells in culture in order to inoculate mice for xenograft studies. Cells were cultured, trypsinized, and resuspended in a 90% matrigel suspension for inoculation. Either one million PIP/Flu cells or 2 million LNCaP cells were injected subcutaneously into nude male mice. Animals were then monitored

until tumors reached at least 0.1 (PIP/Flu) or 0.3 (LNCaP) cubic centimeters in volume. We then injected 20 ug of PE35-MU2 or naked PE35 intratumorly consecutively for two days and then measured tumor volume and animal weight every three days. For IV efficacy studies, animals were dosed with 50 ug (2 mg per kg) drug via tail vain injection. Once tumors grew larger than 1 cc, animals were sacrificed via CO2 asphyxiation. Tumors were then excised, weighed, and fixed in formalin solutions. Tumor histology was then performed by the Johns Hopkins Histology core facility. For the LNCaP models, we also determined circulating PSA via ELISA by collecting blood retro-orbitally and submitting the sample to the Johns Hopkins clinical chemistry core facility.

Results

Using the PSMA-binding scaffold, we opted to synthesize a readily conjugatable, thiol reactive species linked together by 2 PEG units. This was done by reacting the scaffold's free amine (from the lysine side chain) with a maleimide-containing a linker with a reactive N-Hydroxysuccinimidyl ester (Figure 1A). These two were linked by 2 polyethylene glycol subunits and yielded a maleimide linked, PSMA-binding urea deemed MU2. Mass spectrometry of the compound showed a single major peak with a m/z value of 629, the expected molecular weight of MU2. The lack of other peaks suggests the compound is relatively pure (Figure 1B). Using simple amino acid mutagenesis, we designed two protein-drug conjugates by introducing cysteine residues capable of covalently reacting with the maleimide group on MU2. This reaction can be robustly done at pH 7-8 in aqueous buffered solutions favoring the protein's stability and structure (Figure 1C).

Once the MU2 compound was validated and cysteine-containing mutants were generated of GZMB and PE35, we performed covalent couplings in the presence of the thiol-free reducing agent TCEP. Because Bovine Serum Albumin already contains a readily reactive, external cysteine, we opted to assess the ease and feasibility of MU2-protein coupling. Ellman's assay analysis showed that approximately 40% of cysteine 34 in BSA is reactive at pH 7.4 in aqueous solution under non-reducing conditions. Once MU2 was mixed with the protein overnight, we detected zero free thiols in solution (Figure 1D). To confirm successful coupling with EK-activated C248 GZMB, we ran both naked and coupled protein through ion exchanged, dialyzed overnight, and ran on a

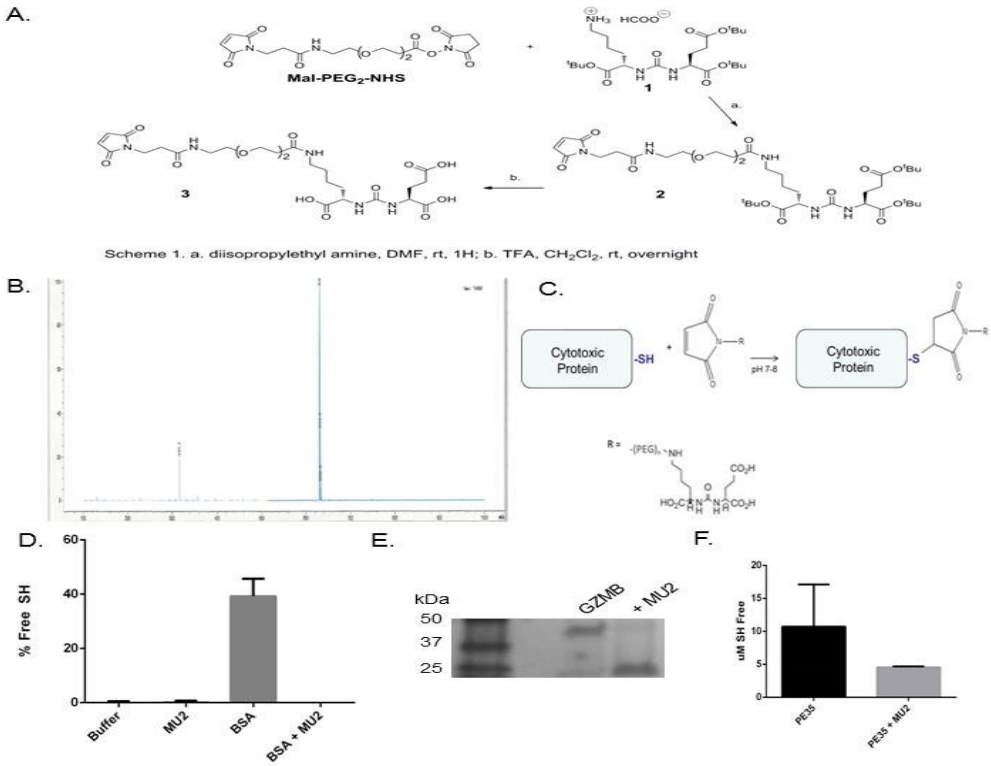

Figure 1: Synthesis and production of protein-urea drug conjugates. Chemical synthesis scheme taken to make a thiol-reactive maleimide-linked urea separated by two PEG units (MU2) (A). Mass spectrometry plot of MU2 product (B). Diagram depicting the protein-MU2 conjugation reaction (C). Ellman's reagent assay of BSA +/- MU2 under non-reducing conditions (D). Non-reducing SDS PAGE gel of C-terminal reactive GZMB +/- MU2 following dialysis (E). ABD-F fluorescent assay of PE35 +/- MU2 (F).

non-reducing SDS PAGE gel. Once stained, gel analysis showed that dialyzed C248 exists in both dimeric and monomeric states with the majority of the material being linked via disulfides. GZMB mixed with MU2, conversely, existed in primarily the monomeric state at the expected molecular weight of 28 kDa (Figure 1E). Lastly, we used the thiol-reactive, fluorescent ABD-F assay to confirm coupling between MU2 and a mutant of PE containing a cysteine, PE35. This assay showed that uncoupled PE35, under reducing conditions, a 0.5 mg/mL solution of protein (14 uM) had a free sulfhydryl content of 10 uM while the couple material had a free sulfhydryl content of 4 uM (Figure 1F).

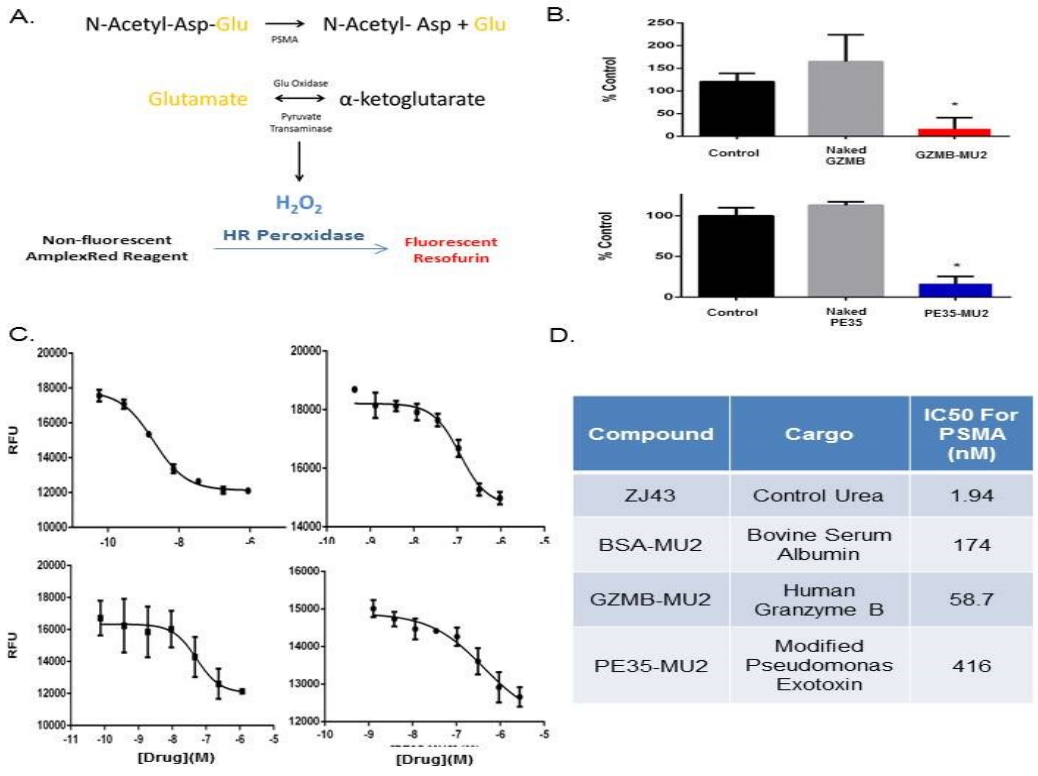

Compound	Cargo	IC50 For PSMA (nM)
ZJ43	Control Urea	1.94
BSA-MU2	Bovine Serum Albumin	174
GZMB-MU2	Human Granzyme B	58.7
PE35-MU2	Modified Pseudomonas Exotoxin	416

Figure 2: Protein-urea conjugates bind and inhibit PSMA. Scheme of the enzyme-coupled PSMA enzymatic assay utilized to detect urea-conjugate binding (A). Inhibition of PSMA by coupled or naked cytotoxic proteins represented as a percentage of the control reaction (B). Dose response curves of ZJ43 (top left), BSA-MU2 (top right), GZMB-MU2 (bottom left), and PE35-MU2 (bottom right) (C). Table describing the IC50 values for PSMA obtained for each compound (D).

Because PSMA is both expensive and difficult to express at reasonable quantities, we opted to use a cell lysate-based coupled enzyme assay to measure our protein-drug conjugates' ability to bind to the protein. Briefly, PSMA from LNCaP cell lysate, cleaves the substrate NAAG to NAA and free glutamate. We then added a reaction mix that converts glutamate to alpha-ketoglutarate via glutamate oxidase generating hydrogen peroxide in aqueous solution. Horseradish peroxidase can then catalyze the conversion of a non-fluorescent probe to a fluorescent species easily detected at 530/590 excitation/emission (Figure 2B). When compared to buffer-treated controls, both GZMB and PE35 proteins have no effect on this assay. However, conjugated GZMB and PE35 proteins both inhibited PSMA enzymolysis at 1 uM (Figure 2B). For all three protein-urea conjugates (including BSA), we observe a dose dependent, 4 parameter inhibition of PSMA in this assay with increasing inhibition upon increasing conjugate concentrations (Figure 2C). We observe IC50 values within the same range for all three protein conjugates while the control urea compound, ZJ43, has an IC50 of 1.9 nM, consistent with that published by Zhou et al (Figure 2D).

PSMA-binding assays confirmed that the urea portion of the conjugate was still functional following conjugation, however, it was unclear whether protein functionality was affected by this modification. We assessed this using a Granzyme B specific proteolysis assay with both naked and coupled expressed GZMB. We observe no change in specific activity per mg protein between naked and conjugated GZMB (Figure 3A). When tested at doses up to 300 nM, we observed no effect on proliferation, cell morphology, or viability on any cell lines regardless if PSMA was expressed or not (Figure 3B). For LNCaP cells, we do observe toxicity at doses above 300 nM that affects morphology and cell proliferation but this was not enhanced when the urea moiety was present (data not shown). To assess whether or not the lack of toxicity was due to lack

of internalization or whether GZMB was not functional in this intracellular context, fluorescein-tagged GZMB-MU2 was dosed on cells at 100 nM for two hours. We also stained these cells with DAPI in order to contextualize any observed uptake. After a 1 hour incubation, we observe positive staining on the PIP-PC3 cells in the fluorescein channel but not on the Flu-PC3 cells. The staining on the PIP-PC3 cells appears most punctate and associated with the DAPI stain with some association to the membrane (Figure 3C). When the magnification of the PIP cells is increased to 60x, we observe

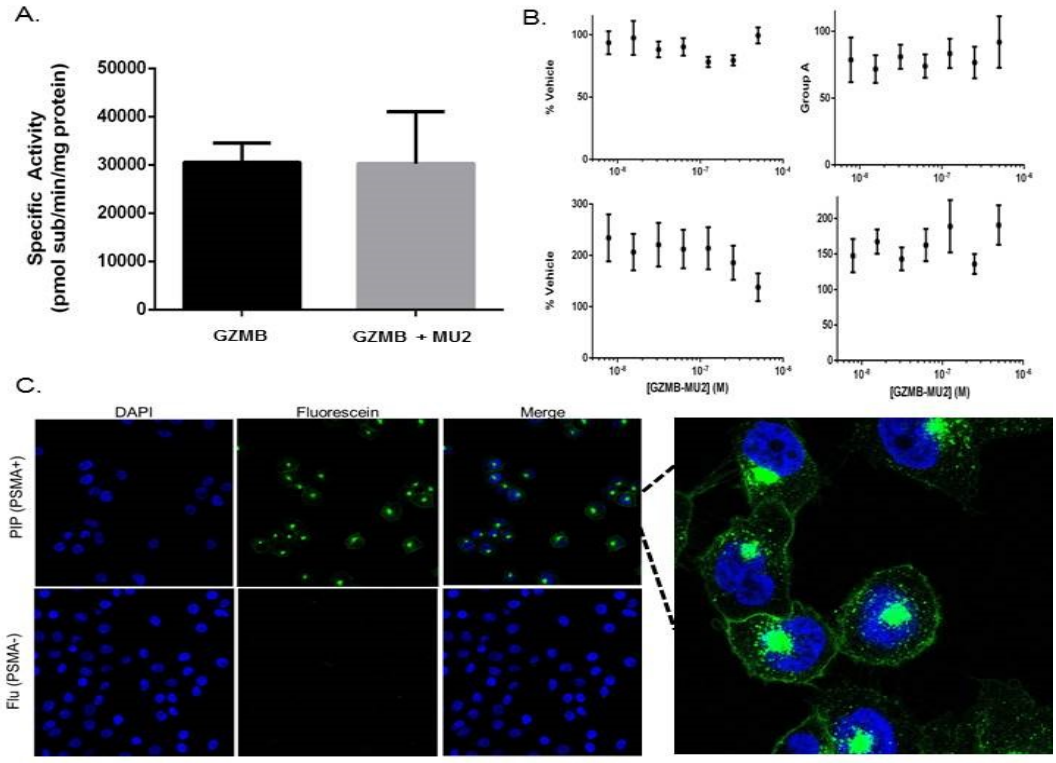

Figure 3: GZMB-MU2 internalizes into PIP cells but does not induce cell death. Enzymatic activity of GZMB or GZMB-MU2 using a GZMB-specific fluorescent substrate (A). Cytotoxicity of purified GZMB-MU2 on PIP-PC3 (top left), Flu-PC3 (top right), LAPC4 (bottom left), or CWR22 Rv1 (bottom right) (B). Confocal microscopy of PIP or Flu-PC3 cells treated with Flor-GZMB-MU2 for 1 hour at 20X magnification (left) or 60X (right) (C).

compartmentalization of the signal both a large foci near the nuclear space of the cell and in smaller foci distributed throughout the cytoplasm of the cell.

To determine the ability of PE35-MU2 to kill cells in a PSMA specific manner, we first treated PIP and Flu-PC3 with both conjugated and naked PE35. Somewhat surprisingly, we observed a cytotoxic effect of the unconjugated material on both PIP and Flu-PC3 cells with little difference in IC50. Conjugation of PE35 to a PSMA-binding urea improved

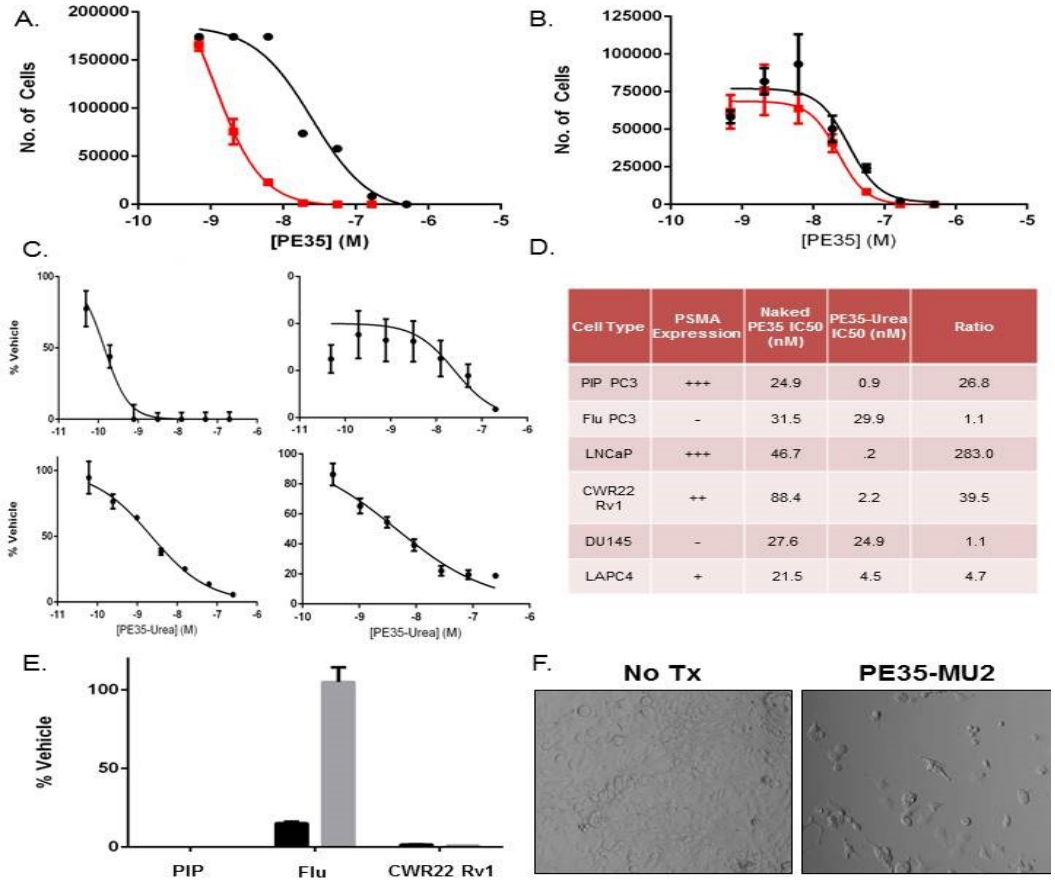

Cell Type	PSMA Expression	Naked PE35 IC50 (nM)	PE35-Urea IC50 (nM)	Ratio
PIP PC3	+++	24.9	0.9	26.8
Flu PC3	-	31.5	29.9	1.1
LNCaP	+++	46.7	.2	283.0
CWR22 Rv1	++	88.4	2.2	39.5
DU145	-	27.6	24.9	1.1
LAPC4	+	21.5	4.5	4.7

Figure 4: PE35-MU2 is selectively toxic to PSMA producing cells. Viability of PIP-PC3 (A) or Flu-PC3 (B) cells treated with naked PE35 (black) or PE35-MU2 (red). Dose response curve LNCaP (top left), DU145 (top right), CWR22 Rv1 (bottom left) or LAPC4 (bottom right) (C). Table depicting the IC50 values obtained on various cell lines with naked or conjugated PE35 (D). Pulse-soak experiment in which PIP-PC3, Flu-PC3, or CWR22 Rv1 were dosed with 250 nM PE35-MU2 for 5 days (black bars) or pulsed for 24 hours (grey bars) (E). Light microscopy images of CWR22 Rv1 cells treated with 3 nM PE35-MU2 for 5 days at 10x magnification (F).

the potency on this drug on PIP-PC3 but not Flu-PC3, with the coupled-protein toxin having an IC50 of 0.9 nM against PIP cells (Figure 4A and 4B). We observed similar effects of the toxin on LNCaP, CWR22 Rv1, LAPC4, and DU145 cells in that both coupled and uncoupled material had a dose dependent cytotoxic effect on cell viability with IC50s consistent with the PIP and Flu cell data (Figure 4C). To assess the effect of urea conjugation on the ability of the toxin to kill cells we calculated the ratio of the IC50s of the naked and coupled protein with the higher ratios indicating that the conjugation improved the targeting of the toxin. We observe that all PSMA producing cell lines have a ratio above 1 and all PSMA negative lines have a ratio of approximately one (Figure 4D). We also asked whether or not pulsing cells with the conjugate further enhanced

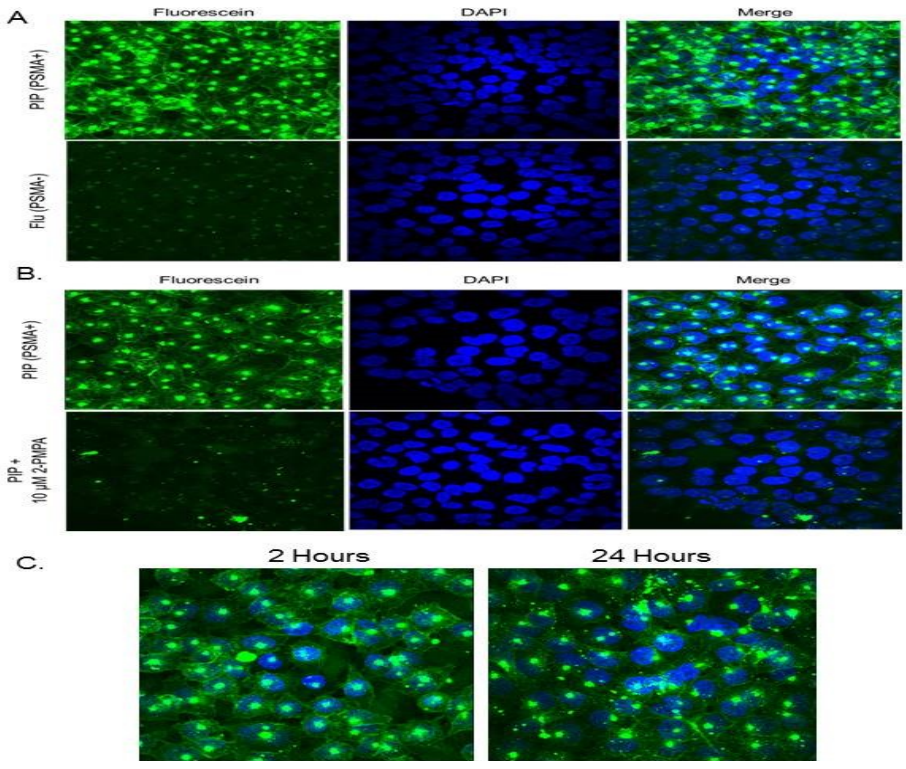

Figure 5: PE35-MU2 is selectively internalized by PSMA expressing cells. Confocal microscopy images of PIP-PC3 or Flu-PC3 treated with Flor-PE35-MU2 for one hour (A). PIP-PC3 cells treated with Flor-PE35-MU2 plus or minus 10 uM 2PMPA (B). Time course of Flor-PE35-MU2-treated PIP-PC3 cells (C).

selectivity at high doses on PSMA producing cell lines. At a dose of 250 nM, the PSMA producing cell lines PIP and CWR22 Rv1 were killed regardless if they were exposed for 24 hours or 5 days. Flu cells, however, were rescued from PE35-MU2 toxicity when pulsed with the drug for 24 hours (Figure 4E). Lastly, we visualized CWR22 Rv1 cells treated with the toxin at lethal doses at Day 5. While we clearly see a substantially decreased number of cells, we also see structural morphology consistent with apoptosis such as blebbing and shattering (Figure 4F).

Like the GZMB, we assessed the uptake of Flor-PE35-MU2 using a confocal microscopy assay. Like the GZMB conjugate probe, we see vibrant labeling of the PIP-PC3 cells after a two hour treatment with 100 nM of the compound. We also observe some baseline uptake of the compound after exposure to Flu-PC3 cells for the same treatment conditions. Also like the GZMB-MU2 treatment, we observe a punctate staining pattern that appears to stain both the plasma membrane and the endosomal trafficking system. (Figure 5A). To ensure this effect was PSMA specific and not a result of a differential in uptake between PIP and Flu-PC3 cells, we treated PIP cells with either the PE35-MU2 probe alone or the probe with 10 uM of the compound 2-PMPA, a potent competitive inhibitor of PSMA that has been shown to out compete the urea class of compounds for PSMA binding. When treated with this drug, we see ablation of fluorescein labeling on these cells (Figure 5B). Lastly, we aimed to observe if there was a change in signal over a time period of 24 hours. Compared to the 2 hour time point, we see no obvious differences in the intensity of the staining of the cells nor do we see a change in the pattern in terms of both dissemination and compartmentalization of the signal (Figure 5C).

Nude mice inoculated with PIP, Flu, and LNCaP xenografts were administered IV and IT injections of PE35-MU2 in order to assess the toxicity and efficacy of the construct. PIP

tumors injected IT with the protein-drug conjugate showed no change in tumor volume while control cells quadrupled in size. Flu xenografts, however, did not respond when injected with the compound and seemed to grow at a comparable rate to their control-dosed counterparts (Figure 6A and 6B). To ensure that the toxin itself had little to no effect on these tumors, we injected LNCaP xenografts with 20 ug of both conjugated and unconjugated toxin. While the unconjugated grew roughly the same as the controls, we

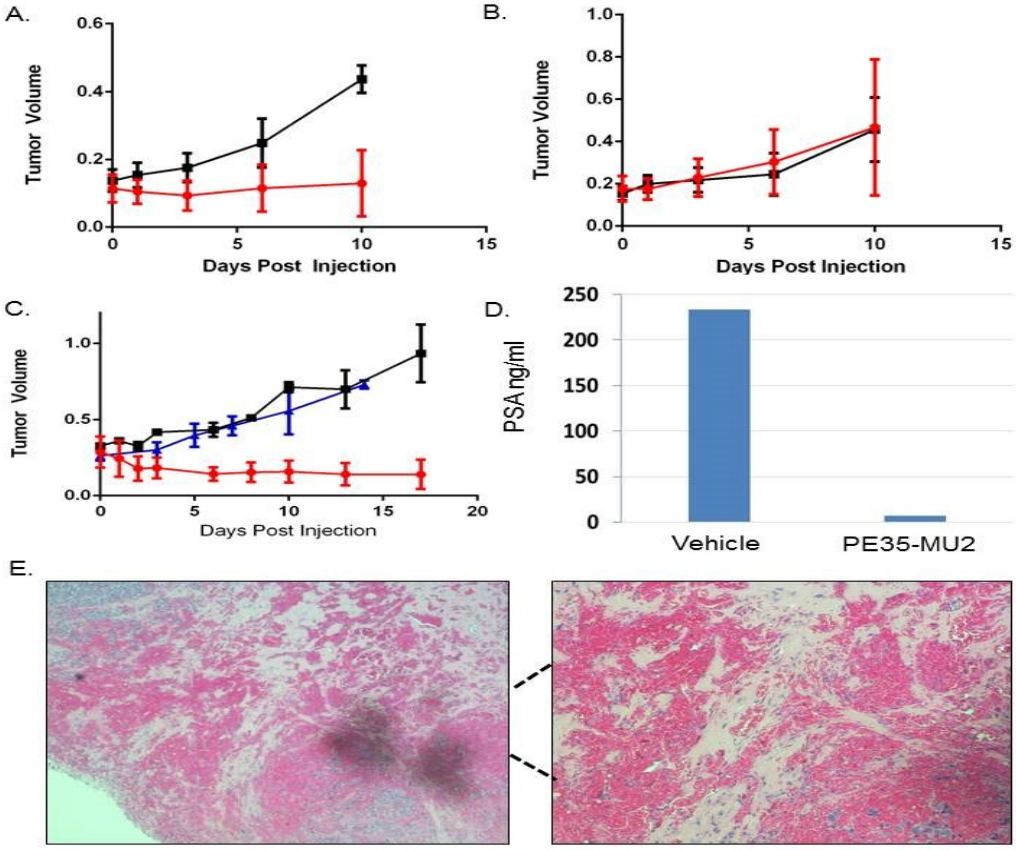

Figure 6: PE35-MU2 regresses PSMA expressing xenografts when injected intratumorly. Growth of PIP-PC3 (A) and Flu-PC3 (B) following two injections of vehicle (black) or 20 ug PE35-MU2 (red). LNCaP xenograft growth following two injections of either vehicle (black), 20 ug uncoupled PE35 (blue) or 20 ug PE35-MU2 (red) (C). PSA levels determined via ELISA of LNCaP-bearing nude mice after 3 weeks of treatment (D). H & E staining of a PE35-MU2- injected LNCaP tumor after 3 weeks treatment at 4x (left or 10x (right) (E).

saw no change in tumor size of the conjugate-dosed xenografts after 2 weeks (Figure 6D). Mice treated for an equal amount of time were measured for circulating PSA. We observed almost no detectable PSA in IT-injected PE35-MU2 mice compared to control animals (Figure 6D). To observe the tissue architecture of these tumors, we performed H & E staining on larger tumors dosed with the drug that responded via shrinkage. The remaining tissue was mostly composed of dead, necrotic with viable cells visible at low abundance (Figure 6E). IV dosing of nude mice with two different doses of PE35-MU2 (2 and 6 mpk) showed substantial body weight loss in the higher dose but less so in the lower dose with no animals perishing (data not shown). The 2 mpk dose was then selected for IV efficacy studies. We saw no major changes in tumor volume in either PIP or Flu mice injected with PE35-MU2 at this dose after 4 consecutive administrations of the drug (data not shown). Of the ten animals injected, two experienced lethal toxicity during this course of treatment suggesting that the 4 daily doses approached the maximum tolerated concentration of this drug in these animals.

Discussion

In this work, we have successfully shown that PSMA-binding ureas have the capacity to selectively, rapidly, and efficiently deliver cytotoxic protein payloads to cells producing the gene. These conjugates were synthesized fairly simply using cysteine-containing mutants of the protein toxins GZMB and PE35 and a maleimide-linked PSMA-binding urea. We chose these two agents due to their diverse mechanisms of action, need to be delivered into cells in order to be functional, and previous successes when fused to other targeting moieties such as antibodies. Using fluorescent and gel-based assays, we confirmed that coupling of our synthesized PSMA-binding urea compounds was simple, effective, and mostly quantitative. For the GZMB coupling, we observed complete ablation of disulfide dimer formation under non-reducing conditions using SDS PAGE

suggesting strongly that most of the cysteines on the protein were occupied by reacted ureas and unable to form these oligomers. The thiol selective fluorophore ABD-F showed a reduction of free thiols in solution once the MU2 molecule was coupled to PE35 under reducing conditions. We did observe some residual thiol present in the PE35-MU2 sample suggesting that some of this material had not fully coupled. At any rate, the ease of this chemistry suggests that the formation of similar conjugates is trivial and that other similar strategies can be employed for a diverse profile of therapeutic protein agents.

Using an enzyme-coupled PSMA activity assay, we observed inhibition of PSMA by three different purified protein-urea conjugates. This assay traced the conversion of NAAG, a physiologically relevant and specific PSMA dipeptide substrate, to NAA and free glutamate and correlated PSMA inhibition with urea binding. None of the naked protein agents tested had any effect on this assay at any concentration tested. BSA-MU2, GZMB-MU2, and PE35-MU2 all inhibited PSMA with IC50 values ranging from roughly 50 to 500 nM. We were somewhat surprised to see such a large range of potencies given that the linked urea did not change between the three. We interpret this result with two hypotheses. The first is that incomplete coupling (as what was possibly seen in the PE35-MU2 reaction) yielded naked protein in the sample threw off the calculation of the concentration of conjugated material present (A280 was used to determine protein-urea concentration). The other is that the urea molecule has different properties depending on what it's linked to and that certain protein motifs can interact with the urea moiety and affect its ability to occupy the PSMA active site. We were encouraged, however, to see the PE35-MU2 construct internalize and kill cells very efficiently despite having the supposedly weakest binding to PSMA suggesting that this

assay alone cannot be used to predict the efficacy of a protein-urea conjugate with respect to cell internalization or function.

We are disappointed to report that despite binding PSMA and being enzymatically active, GZMB-MU2 had no effect on cell viability at concentrations below 100 nM. As stated earlier, we did see toxicity on cells of GZMB-MU2 at concentrations higher than 500 nM on DU145, CWR22 Rv1, and LNCaP. There did not seem to be a difference in this effect between conjugated and unconjugated protein suggesting that the mechanism was independent of PSMA uptake. It has been reported in the literature that GZMB can cleave and remodel members of the extracellular matrix and disrupt cell growth (22) which could explain why this effect is present in a system in which the protein does not seem to be entering the cells. Regardless, we were surprised to see rapid and specific uptake of the protein conjugate by PSMA-expressing PIP-PC3 cells despite no toxicity being observed. This and the punctate and non-diffuse staining pattern on the confocal images strongly suggests that GZMB-MU2 is being sequestered in the endosome of the cell and reaching its final destination in the perinuclear endosomal space. Localization of GZMB is crucial for its function and because the primary substrates of the protease are specific to the cell cytoplasm. It is likely then that this localization in the endosome is a limiting factor for this agent as a cytotoxic therapy. This result is consistent with GZMB's function in the immune system, as its ability to induce cell death is dependent upon endosomal escape via perforin pores. This result, while not desired, elucidates the critical characteristics for a toxic payload must have when delivered by PSMA-urea molecules or other tumor-selective targeting molecules.

Because the GZMB-MU2 molecule was unable to escape the endosomal compartmentalization following internalization via PSMA binding, we opted to utilize other means of targeting. We envision two solutions to overcome endosomal

entrapment. The first is to deliver a radio-isotope capable of inducing chromatin damage via proximity emission of radiation such as 177-Lu PSMA-617 (23) which does not need to exit the endosome. The other is to use a toxin that can efficiently exit this space once delivered. PE35 has been well characterized to access cytoplasmic its substrates following intracellular delivery despite the mechanism being somewhat unclear. We were pleased to see that where the GZMB compound failed, we observed success with the PE35-MU2. The conjugate selectively and potently targeted PSMA-expressing prostate cancer lines at concentrations up to two orders of magnitude lower than PSMA non-expressing cells. We were also pleased to observe that naked PE35, while somewhat toxic to these cell lines, had IC50 values that were nearly identical to the urea conjugate on cells not expressing PSMA strongly suggesting that, again, this targeting is driven solely by PSMA expression. We also, using a fluorescent PE35-MU2 probe, observed specific uptake in PIP-PC3 cells but not in Flu PC3 cells whose only biological difference is production of the PSMA protein. To further confirm that this uptake was PSMA-driven and not an artifact of the cell lines, we showed disruption of PE35-MU2 internalization using a PSMA inhibitor, known as 2-PMPA, which binds to the active site of the enzyme and can out-compete the urea. Kinetic experiments showed that a majority of the net uptake of this drug occurs within the first two hours of exposure and is maintained for at least 24 hours, likely due to PSMA's constant shuttling between the endosomal space and the plasma membrane. We rationalized that pulsing cells with this drug at high concentrations should minimize the non-specific toxicity of this protein on PSMA negative cells. When pulsed with PE-MU2, both PIP and CWR22 Rv1 cells were still killed rapidly but Flu-PC3 cells were not affected suggesting that non-specific toxicity of this protein is a slow, transient process that can be overcome by brief, high dose, pulses of the drug as opposed to constant exposure. Lastly, we were somewhat surprised to see no difference in staining pattern between the 2 and 24 hour time point, suggesting

that a majority of the PE35 cargo does not escape the endosome and that only a relatively small number of PE35 molecules are responsible for cell killing, as we begin to see cytotoxic effects of this drug on PSMA-producing cells at 24 hour time points. Based on the confocal time lapse experiment of PE35-MU2, it is possible that GZMB, at low levels is able to escape the endosome by itself at low levels but requires a much higher concentration of functional cytoplasmic enzyme to catalyze the activation of cell death pathways.

We were encouraged to see that, when injected straight into the tumor, PE35-MU2 had an anti-tumor effect on PIP and LNCaP xenografts in nude mice but not Flu over the course of two to three weeks. These tumors did not change in volume compared to their size at the time of injection suggesting that the overall number of viable tumor tissue had decreased due to cell death matching our *in vitro* tissue culture experiments using this model. We were also pleased to see that the unconjugated protein had little to no effect on LNCaP xenografts. The lack of observable toxicity on Flu cells or with the uncouple protein suggests that a majority of the IT efficacy observed was PSMA specific and not due to non-specific uptake of the toxin or due to varied retention times of these constructs. PSA measurements in the LNCaP bearing mice also confirmed that the decrease in size observed was consistent with tumor burden. Histology of injected tumors also showed that a majority of the tissue had undergone cell death and that there was only a small portion of the remaining tumor that was viable. Unfortunately, despite having nice anti-tumor effects when injected IT and safe when administered IV at reasonable does, we did not observe any noticeable effect on PIP and Flu xenograft mice when injected with 2 MPK PE35-MU2 suggesting that the toxin does not have a preferable pharmacokinetic profile, consistent with some of the observed limitations of other anti-body drug conjugates containing PE-based payloads. Conjugation of this

construct to HSA, an Fc domain, or using more PEGylated linkers may improve the systemic availability of this targeted toxin thus making it a better pharmacophore (24).

A vast majority of cytotoxic proteins and small molecules used for cancer chemotherapy have been targeted to tumors using protein-based Trojan horse strategies. Usually, these strategies employ the use of monoclonal antibodies, growth factors, or single chain variable fragments. In this work, we show the delivery of cytotoxic protein payloads to tumor cells using a small molecule inhibitor Trojan horse. This method has some advantages over protein targeted strategies, as these agents may have longer half-lives and are less susceptible to immunological responses that limit therapeutic application. This work introduces a novel PSMA-selective therapeutic agent containing a potent bacterial toxin. This agent was very impressive in *in vitro* and some *in vivo* models but was not particularly efficacious in IV dosing experiments. Other biochemical engineering approaches may be able to improve the half-life of these conjugates. Because some toxicity was observed *in vivo*, reducing off-target toxicity via disruption of cell uptake mechanisms or using toxins with a larger therapeutic index could also improve the IV efficacy of these agents. Regardless, these results display a novel method to deliver cytotoxic proteins to cancer cells and may lay the groundwork for other ligand-targeted cytotoxic therapies to be developed. Another potential problem could be that the thiol-ester linkage formed by the cysteine-maleimide linkage may be disrupted via a sulfhydryl replacement reaction with free albumin *in vivo* (25). Recently developed, more-stable linker technology may help to remedy this problem (26). Ultimately, these PSMA-ureas offer an exciting new method to concentrate pharmaceutic agents into cells in a selective manner via trivial, gentle, and cheap chemical means and are an interesting addition to the arsenal of therapeutic strategies to treat human cancers.

References

1. Howlader N, Noone AM, Krapcho M, Miller D, Bishop K, Altekruse SF, Kosary CL, Yu M, Ruhl J, Tatalovich Z, Mariotto A, Lewis DR, Chen HS, Feuer EJ, Cronin KA (eds). SEER Cancer Statistics Review, 1975-2013, National Cancer Institute. Bethesda, MD.
2. Chang SS. Overview of Prostate-Specific Membrane Antigen. Reviews in Urology. 2004;6 (Suppl 10):S13-S18.
3. Carter RE, Feldman AR, Coyle JT. Prostate-specific membrane antigen is a hydrolase with substrate and pharmacologic characteristics of a neuropeptidase. Proc Natl Acad Sci USA. 1996;93(2):749-53.
4. Sweat SD, Pacelli A, Murphy GP, Bostwick DG. Prostate-specific membrane antigen expression is greatest in prostate adenocarcinoma and lymph node metastases. Urology. 1998;52(4):637-40.
5. Lapidus RG, Tiffany CW, Isaacs JT, Slusher BS. Prostate-specific membrane antigen (PSMA) enzyme activity is elevated in prostate cancer cells. Prostate. 2000;45(4):350-4.
6. Haffner MC, Kronberger IE, Ross JS, et al. Prostate-specific membrane antigen expression in the neovasculature of gastric and colorectal cancers. Hum Pathol. 2009;40(12):1754-61.
7. Liu H, Rajasekaran AK, Moy P, Xia Y, Kim S, Navarro V, Rahmati R, Bander NH. 1998. Constitutive and antibody-induced internalization of prostate-specific membrane antigen. *Cancer Res* **58**: 4055–4060.

8. Naveed H. Akhtar, Orrin Pail, Ankeeta Saran, Lauren Tyrell, and Scott T. Tagawa, “Prostate-Specific Membrane Antigen-Based Therapeutics,” Advances in Urology, vol. 2012, Article ID 973820, 9 pages, 2012.
9. Will L, Sonni I, Kopka K, Kratochwil C, Giesel FL, Haberkorn U. Radiolabelled PSMA small molecule inhibitors. Q J Nucl Med Mol Imaging. 2017;48(supplement 2):25P.
10. Chen Y, Dhara S, Banerjee SR, et al. A Low Molecular Weight PSMA-Based Fluorescent Imaging Agent for Cancer. Biochemical and biophysical research communications. 2009;390(3):624-629.
11. Greish K. Enhanced permeability and retention (EPR) effect for anticancer nanomedicine drug targeting. Methods Mol Biol. 2010;624:25-37.
12. Hoves S, Trapani JA, Voskoboinik I. The battlefield of perforin/granzyme cell death pathways. J Leukoc Biol. 2010;87(2):237-43.
13. Cullen SP, Adrain C, Lüthi AU, Duriez PJ, Martin SJ. Human and murine granzyme B exhibit divergent substrate preferences. The Journal of Cell Biology. 2007;176(4):435-444.
14. Keefe D, Shi L, Feske S, et al. Perforin triggers a plasma membrane-repair response that facilitates CTL induction of apoptosis. Immunity. 2005;23(3):249-62.
15. Thiery J, Keefe D, Boulant S, et al. Perforin pores in the endosomal membrane trigger release of endocytosed granzyme B to the cytosol of target cells. Nature immunology. 2011;12(8):770-777.
16. Wolf P, Elsässer-beile U. Pseudomonas exotoxin A: from virulence factor to anti-cancer agent. Int J Med Microbiol. 2009;299(3):161-76.

17. Chaudhary VK, FitzGerald DJ, Adhya S, Pastan I. Activity of a recombinant fusion protein between transforming growth factor type alpha and *Pseudomonas* toxin. Proc Natl Acad Sci USA. 1987;84:4538–4542.
18. Wolf P, Elsässer-beile U. Pseudomonas exotoxin A: from virulence factor to anti-cancer agent. Int J Med Microbiol. 2009;299(3):161-76.
19. Kreitman RJ, Tallman MS, Robak T, et al. Phase I Trial of Anti-CD22 Recombinant Immunotoxin Moxetumomab Pasudotox (CAT-8015 or HA22) in Patients With Hairy Cell Leukemia. Journal of Clinical Oncology. 2012;30(15):1822-1828.
20. Marasca KP, Hillier SM, Femia FJ. Barone D, Joyal JL, Zimmerman CN, Kozikowski AP, Barrett JA, Eckelman WC, Babich JW. A series of halogenated heterodimeric inhibitors of prostate specific membrane antigen (PSMA) as radiolabeled probes for targeting prostate cancer. J. Med. Chem. 52: 347-357 (2009).
21. Gehrmann M, Doss BT, Wagner M, et al. A novel expression and purification system for the production of enzymatic and biologically active human granzyme B. J Immunol Methods. 2011;371(1-2):8-17.
22. Buzza MS, Zamurs L, Sun J, et al. Extracellular matrix remodeling by human granzyme B via cleavage of vitronectin, fibronectin, and laminin. J Biol Chem. 2005;280(25):23549-58.
23. Kratochwil C, Giesel FL, Stefanova M, et al. PSMA-Targeted Radionuclide Therapy of Metastatic Castration-Resistant Prostate Cancer with 177Lu-Labeled PSMA-617. J Nucl Med. 2016;57(8):1170-6.
24. Strohl WR. Fusion Proteins for Half-Life Extension of Biologics as a Strategy to Make Biobetters. *Biodrugs*. 2015;29(4):215-239.

25. Shen BQ, Xu K, Liu L, et al. Conjugation site modulates the in vivo stability and therapeutic activity of antibody-drug conjugates. Nat Biotechnol. 2012;30(2):184-9.
26. Lyon RP, Setter JR, Bovee TD, et al. Self-hydrolyzing maleimides improve the stability and pharmacological properties of antibody-drug conjugates. Nat Biotechnol. 2014;32(10):1059-62.

Oliver C Rogers, BS

PhD Candidate- Johns Hopkins University

E-mail: orogers18@gmail.com

Born

September 26, 1989

Columbus, Ohio

Education

August 2012- March 2017: PhD, Pharmacology & Molecular Sciences

Johns Hopkins Medical Institutions, Baltimore MD, 21287

Thesis Advisor: Dr. Samuel R. Denmeade, M.D.

Thesis: “Novel Methods of Targeting Protein Cytotoxins to Metastatic Prostate Tumors”

Sept 2008- June 2012: Bachelor of Science, Biology

Minor, Chemistry

University of Cincinnati, Cincinnati, OH 45219

GPA: 3.515

Research Interests

- Protein Engineering
- Pharmacology
- Cancer Biology & Oncology
- Enzymology

Research Positions Held

Position	Start	End	Institution	Supervisor
Staff Scientist	Apr-17	Present	Revolve Biotech	Elad Firnberg, PhD
Graduate Student	Aug-12	Mar-17	Johns Hopkins University	Sam Denmeade, MD
Research Assistant	Aug-11	Jun-12	University of Cincinnati	Terence Kirley, PhD
Undergraduate Fellow	Jun-11	Aug-11	University of Cincinnati	Terence Kirley, PhD
Student Assistant	Jan-10	May-11	University of Cincinnati	Nira Ben-Jonathan, PhD

Academic and Professional Honors

Scheinberg Travel Award- Johns Hopkins Medical Institutions- Fall 2015

Voted “Best Scientific Contribution” Univ. of Cincinnati SURF Research Presentations- Summer 2011

ASPET Summer Undergraduate Research Fellowship (SURF) (Univ. of Cincinnati)- Summer 2011

University of Cincinnati Dean’s List: Fall 2008, Winter 2009, Spring 2009, Fall 2010, Spring 2011, Fall 2011, Winter 2012

Named University of Cincinnati FYE Peer Mentor-Fall 2009

University of Cincinnati Cincinnatus Century Scholarship- Fall 2008

Memberships in Professional Societies

American Association for the Advancement of Science (Graduate)

American Society for Pharmacology and Experimental Therapeutics (Undergraduate)

Publications

Rogers OC, Anthony L, Rosen DM, Therres JA, Das D, Yang X, Minn I, Mease R, Pomper M, Denmeade SR2Targeted Delivery of Cytotoxic Proteins via Small Molecule Peptidase Inhibitors. 2017. In preparation.

Rogers OC, Antony L, Brennen WN, Denmeade SR, PSA-Activated Serine Proteases as a Novel Therapeutic Strategy to Target Prostate Cancer. 2017. In Preparation.

Rogers OC, Pruitt F, Antony L, Kizewski A, Kisteman LN, Karp JM, Howard P, Denmeade SR, Isaacs, JI, Brennen WN. PLGA Microparticle Encapsulation of a Novel Prostate-Targeted Biologic For Tumor Delivery: Characterization of Release and Functionality. 2017 In preparation.

Rogers OC, Yen HR, Solomon A, Abi-Habib R, Buckley JT, Drake CG, Denmeade SR. A Potent IL-2R Targeting Pro-drug as a Novel Anti-tumor Vaccine Adjuvant. 2017. In preparation.

Oral Presentations

Engineering Human Granzyme B to Target Prostate Cancer Cells. 3rd Annual Proteins and Antibodies Therapeutics, October 2015, Boston, MA.

Abstracts

Rogers O, Antony L, Brennen W, Denmeade SR: Engineered Serine Proteases as Novel Prostate Cancer Therapeutics. Multi-Institutional Prostate Cancer Program Retreat. March 2016. Ft. Lauderdale, FL.

Rogers O, Antony L, Brennen W, Denmeade SR, Engineering Human Granzyme B to Target Prostate Cancer Cells. 3rd Annual Proteins and Antibodies Therapeutics, October 2015, Boston, MA.

Rogers O, Antony L, Brennen W, Denmeade S, Proaerolysin Based Chimeric Protoxins: A Novel Therapy for Metastatic Prostate Cancer. Multi-Institutional Prostate Cancer Program Retreat. March 2014. Ft. Lauderdale, FL.

Teaching/Mentoring

Johns Hopkins Medical Institutions- MERIT/SHARP- Student Mentor- July 2015- July 2016

University of Cincinnati Center For First Year Education- Peer Leader and Mentor- September 2009- June 2011